UNIVERSITÀ DEGLI STUDI DI BOLOGNA

UNIVERSITY OF BOLOGNA

TESI DI DOTTORATO DI RICERCA

PhD THESIS

FINITE VOLUME SPECTRUM

OF SINE-GORDON MODEL

AND ITS RESTRICTIONS

Dr. Giovanni FEVERATI [1]

JANUARY 2000

---

[1] e-mail: feverati@bo.infn.it

Contents

Chapter 1

SOME GENERAL FACTS

After a short introduction, the most important known facts about sine-Gordon and massive Thirring models are exposed. It is also explained their connection with the $c = 1$ free boson.

1.1   Introduction

As a very large number of papers in literature, this thesis principally deals with the sine-Gordon model, which has been well known at the classical level for the late fifty years and plays also an important role in quantum theory, thanks to its particular properties of non-linearity and integrability. It has been successfully applied in very different sectors of Mathematics and Physics, from partial differential equation theory to particle physics or solid state physics. Recent applications of the classical model are related to nonlinear optics (resonant dielectric media) and optical fibers, magnetic properties of polymers, propagation of waves in crystals and so on. Interesting applications of the quantum model are related to Kondo effect and to the thermodynamics of some chemical compound, as can be found in [45] (see also section 4.10). At the same time, the quantum theory shows a phenomenology that is similar to the Skyrme model used before QCD era to describe barions and strong interactions.

The most relevant properties of the model are

- at a classical level, all the solutions of the equations of motion are known (exact integrability via inverse scattering method)

- the classical solutions describe solitons, antisolitons and bound states (breathers)[1] ; in a scattering process this solutions are transparent (it is the mathematical meaning of "soliton")

- it admits, both at a classical and at the quantum level, a countable infinite set of conserved charges

- the quantization of the theory describes an interacting particle with its antiparticle and, in a certain (attractive) regime, bound states

- the S matrix has been exactly determined; only elastic scattering processes can take place (i.e. no particle production), that is the quantum analog of the classical transparency of solitons

---

[1] The so called mesonic solutions are excluded in this analysis.

Finite size effects

Finite size effects are widely recognized to play an important role in modern statistical mechanics and quantum field theory. From a statistical point of view, it is known that no phase transitions take place in a finite volume system. For example, specific heat $c(T)$, that is divergent at the critical point, if the system has finite size looses it divergence; one observes only a rounded peak, in the plot $c(T)$ versus T. Moreover, there is only an interval around critical temperature T_c where the finite size effects are relevant. Out of this interval, they are negligible (because only near T_c the correlation length can be comparable with the size of the system). The interesting fact is that specific heat (and other critical quantities) have a scaling behaviour (i.e. varying the size L) that is fixed by the (infinite size) critical exponents (see [12]). This is a general fact: as argued in [24], the UV behaviour of the scaling functions (see later) is fixed by the conformal dimensions of the operators that belong to the universality class of the critical point (i.e. the CFT describing the critical point of the statistical system).

Also in quantum field theory interesting phenomena appear. If the space-time geometry is a cylinder of circumference L, Casimir effects change the energy of a two body interaction, because particles interact in the two possible directions, as shown in figure 1.1 (looking forward one can see his own back). Also new radiative corrections to a propagating particle may appear because of the closed geometry. A system on a finite volume has discrete energy and momentum spectra.
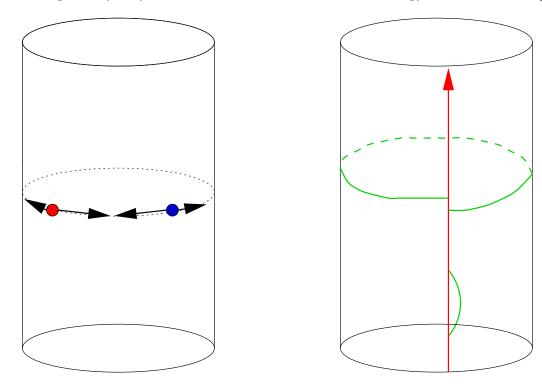
Figure 1.1: Finite size effects

Lüscher [13, 14] has show that the corrections to the free system eigenvalues of E, P depends on the scattering amplitudes (i.e. on the S matrix). This general fact can be used to extract informations on an infinite space QFT from a numerical simulation, that obviously is affected by finite size effects.

Notice that a cylinder geometry can also be interpreted as a finite temperature field theory (temperature is L^{-1}). Such a theory is related to the phase transition between confined and deconfined phase in QCD.

In general, a physical quantity (for example the free energy) that depends on the renormalization scale L (it parameterizes the renormalization flow) is a *scaling function*. The energy and momentum computed in (3.58, 3.59) are scaling functions, because in the NLIE the scale L appears.

There are many methods of investigation of the finite size effects. One of them, that has been very fruitful even for theories which are not integrable, is the *truncated conformal space approach* (see [15] and section 1.4), which is an intrinsically non-perturbative approximation method. It has problems of principal nature, coming from the fact that one does not have an analytic control of the spectrum, and of practical nature, because to reach a certain precision in the resulting energy levels one has sometimes to resort to very high truncation levels and introduce enormous matrices to diagonalize.

For integrable QFT, there also exist *exact analytic* methods to compute the finite size effects, like e.g. the *Thermodynamic Bethe Ansatz* (TBA), which was used to calculate the vacuum (Casimir) energy [16]. The method was later extended to include ground states of charged sectors [36]. More recently, using analytic properties of the TBA equations extended for complex values of the volume parameter, an approach to get excited states was proposed in [18]. Their method to get excited states sheds light on the analytic structure of the dependence of scaling functions on the spatial volume and up to now was the only method developed to deal with excited states in perturbations of minimal models. Its main drawback is that to obtain the equation for a given excited state one has to do analytic continuation for each case separately, and a major part of this continuation can only be carried out numerically. Because of the complications of the analytic continuation, this method is limited at present to simple cases of integrable perturbations of Virasoro minimal models and some other perturbed conformal field theories. Similar results were obtained in [19, 41].

This thesis reports on a novel approach to the excited states of IQFTs in finite volume, based on the *nonlinear integral equation* (NLIE) method, which has its origin in the so-called *light-cone lattice Bethe Ansatz* approach to regularize integrable QFTs. It was argued in [4] that sine-Gordon theory can be regularized using an inhomogeneous 6-vertex model (or equivalently, an inhomogeneous XXZ chain). The NLIE was originally developed in this framework to describe the ground state scaling function (Casimir energy) in sine-Gordon theory in [7] and it was shown that in the ultraviolet limit it reproduces the correct value of the central charge $c = 1$. Similar methods were independently introduced in Condensed Matter Physics by other authors [17].

The NLIE was first extended to excited states in [32] where the spectrum of states containing only solitons (and no antisolitons/breathers) has been described. Using an idea by Zamolodchikov [30] they also showed that a twisted version of the equation was able to describe ground states of unitary Virasoro minimal models perturbed by the operator $\Phi_{(1,3)}$. A framework for generic excited states of even topological charge in sine-Gordon theory was outlined by Destri and de Vega in [8]. However, there has been a contradiction between the results of the two papers, which was resolved in [27, 9] where it was shown that it was related to the locality and the operator content of limiting ultraviolet conformal field theory (CFT). Besides that, strong evidence for the correctness of the predicted spectrum was given by comparing it to predictions coming from the truncated conformal space (TCS) method, pioneered by Yurov and Zamolodchikov in [15] and extended to $c = 1$ theories in [27, 9]. Later a modification of the NLIE to describe the states of sine-Gordon/massive Thirring theory with odd topological charge was conjectured [28].

The NLIE for sine-Gordon theory was generalized to models built on general simply-laced algebras of ADE type in [42] for the case of the vacuum. More recently, in [43] P. Zinn-Justin extended the method to the spectrum of excited states for these models and he also made a first attempt to describe perturbations of minimal models of CFT. A general framework for describing general excited states of minimal models perturbed by $\Phi_{(1,3)}$ (only massive case) can be found

in [34], where is stated the correct form of NLIE equation to deal with this case, and also the simplest examples of the resulting excited states are checked (see chapter 4).

In the following chapters, the general setup of NLIE will be presented, with the most relevant examples.

Chapter 1 is devoted to summarize some well known facts that will be used in the following.

In Chapter 2 the light-cone lattice is introduced and the Bethe equations for the 6 vertex model are written.

Chapter 3 is devoted to obtain an integral equation equivalent to Bethe Ansatz, but that allows a continuum limit procedure. The analysis of the so obtained continuum theory is in Chapter 4.

1.2   c=1 CFT: free boson

To fix some conventions and to define certain objects which are used later, a brief summary is given of the $c = 1$ free boson with a target space of a circle of radius R. The Lagrangian of this CFT is taken to be

$$\mathcal{L} = \frac{1}{8\pi} \int_0^L \partial_\mu \varphi(x,\,t) \partial^\mu \varphi(x,\,t) dx \,,\; x \in [0,L] \,, \tag{1.1}$$

where L is the spatial volume (i.e. the theory is defined on a cylindrical spacetime with circumference L). In the sequel often the complex Euclidean coordinates will be used $z = e^{2\pi(t-ix)/L}$, $\bar{z} = e^{2\pi(t+ix)/L}$. The superselection sectors are classified by the $\widehat{U(1)}_L \times \widehat{U(1)}_R$ Kac-Moody symmetry algebra, generated by the currents

$$J(z) = i\partial_z \varphi \,, \quad \bar{J}(\bar{z}) = i\partial_{\bar{z}} \varphi \,.$$

The left/right moving energy-momentum tensor is given by

$$T(z) = \frac{1}{8\pi} \partial_z \varphi \partial_z \varphi = \sum_{k=-\infty}^{\infty} L_k z^{-k-2} \quad,\quad \bar{T}(\bar{z}) = \frac{1}{8\pi} \partial_{\bar{z}} \varphi \partial_{\bar{z}} \varphi = \sum_{k=-\infty}^{\infty} \bar{L}_k \bar{z}^{-k-2}$$

The coefficients L_n and $\bar{L}_n$ of the Laurent expansion of these fields generate two mutually commuting Virasoro algebras. If the (quasi)periodic boundary conditions are required

$$\varphi(x+L,\,t) = \varphi(x,\,t) + 2\pi mR \,, \quad m \in \mathbb{Z} \,,$$

then the sectors are labelled by a pair of numbers $(n,\,m)$, where $\frac{n}{R}$ (n is half integer because of the locality, see later) is the eigenvalue of the total field momentum π_0

$$\pi_0 = \int_0^L \pi(x,\,t)dx \,, \quad \pi(x,\,t) = \frac{1}{4\pi}\partial_t \varphi(x,\,t) \,,$$

and m is the winding number, i.e. the eigenvalue of the topological charge Q defined by

$$Q = \frac{1}{2\pi R} \int_0^L \partial_x \varphi(x,\,t)dx \,.$$

In the sector with quantum numbers (n, m), the scalar field is expanded in modes as follows:

$$\begin{aligned}
\varphi(x, t) &= \phi(z) + \bar{\phi}(\bar{z}) \,, \\
\phi(z) &= \frac{1}{2}\varphi_0 - ip_+ \log z + i \sum_{k \neq 0} \frac{1}{k} a_k z^{-k} \,, \\
\bar{\phi}(\bar{z}) &= \frac{1}{2}\varphi_0 - ip_- \log \bar{z} + i \sum_{k \neq 0} \frac{1}{k} \bar{a}_k \bar{z}^{-k} \,,
\end{aligned}$$

where the left and right moving field momenta $p_\pm$ (which are in fact the two $U(1)$ Kac-Moody charges) are given by

$$p_\pm = \frac{n}{R} \pm \frac{1}{2} mR \,. \tag{1.2}$$

The Virasoro generators take the form

$$L_n = \frac{1}{2} \sum_{k=-\infty}^{\infty} : a_{n-k} a_k : \,, \quad \bar{L}_n = \frac{1}{2} \sum_{k=-\infty}^{\infty} : \bar{a}_{n-k} \bar{a}_k : \,,$$

where the colons denote the usual normal ordering, according to which the oscillator with the larger index is put to the right.

The ground states of the different sectors (n, m) are created from the vacuum by the (Kac-Moody) primary fields, which are vertex operators of the form

$$V_{(n,m)}(z, \bar{z}) =: \exp i(p_+ \phi(z) + p_- \bar{\phi}(\bar{z})) : \,. \tag{1.3}$$

The left and right conformal weights of the field $V_{(n,m)}$ (i.e. the eigenvalues of L_0 and $\bar{L}_0$) are given by the formulae

$$\Delta^\pm = \frac{p_\pm^2}{2}. \tag{1.4}$$

The Hilbert space of the theory is given by the direct sum of the Fock modules built over the states

$$|n, m\rangle = V_{(n,m)}(0, 0) |vac\rangle \,, \tag{1.5}$$

with the help of the creation operators a_{-k}, $\bar{a}_{-k}$ $k > 0$:

$$\mathcal{H} = \bigoplus_{(n,m)} \{a_{-k_1} \dots a_{-k_p} \bar{a}_{-l_1} \dots \bar{a}_{-l_q} |n, m\rangle, \, k_1, \dots k_p, \, l_1, \dots l_q \in \mathbb{Z}_+\}$$

The boson Hamiltonian on the cylinder is expressed in terms of the Virasoro operators as

$$H_{CFT} = \frac{2\pi}{L} \left(L_0 + \overline{L}_0 - \frac{c}{12} \right) \,, \tag{1.6}$$

where the central charge is $c = 1$. The generator of spatial translations is given by

$$P = \frac{2\pi}{L} \left(L_0 - \bar{L}_0 \right) \ . \tag{1.7}$$

The operator $L_0 - \bar{L}_0$ is the conformal spin which has eigenvalue nm on the primary field $V_{(n, m)}$.

One can also introduce twisted sectors using the operator $\mathcal{T}$ that performs spatial translations by L: $x \to x + L$. The primary fields $V_{(n, m)}$ as defined above satisfy the periodicity condition $\mathcal{T} V_{(n, m)} = V_{(n, m)}$. If the more general twisted boundary condition labelled by a real parameter ν is required

$$\mathcal{T} V_{(n, m)} = \exp \left(i\nu Q \right) V_{(n, m)} \, ,$$

then it is possible to generate superselection sectors for which $n \in \mathbb{Z} + \frac{\nu}{2\pi}$.

It is important to stress that a particular $c = 1$ CFT is specified by giving the spectrum of the quantum numbers (n, m) (and the compactification radius R) such that the corresponding set of vertex operators (and their descendants) forms a *closed and local* operator algebra. The locality requirement is equivalent to the fact that the operator product expansions of any two such local operators is single valued in the complex plane of z. This condition, which is weaker than the modular invariance of the CFT, is the adequate one since the theory is considered on a space-time cylinder and do not wish to define it on higher genus surfaces.

By this requirement of locality, it was proved in [20] that there are only two maximal local subalgebras of vertex operators: $\mathcal{A}_b$ generated by the vertex operators

$$\{ V_{(n, m)} : \ n, \, m \in \mathbb{Z} \} \, ,$$

and $\mathcal{A}_f$ generated by

$$\{ V_{(n, m)} : \ n \in \mathbb{Z}, \, m \in 2\mathbb{Z} \ or \ n \in \mathbb{Z} + \frac{1}{2}, \, m \in 2\mathbb{Z} + 1 \} \, .$$

Other sets of vertex operators can be built, but the product of two of them gives a nonlocal expression.

1.3   Sine-Gordon/massive Thirring field theory

The minkowskian lagrangian of sine-Gordon theory is given by[2]

$$\mathcal{L}_{sG} = \int \left(\frac{1}{2} \partial_\nu \Phi \partial^\nu \Phi + \frac{\mu^2}{\beta^2} : \cos \left(\beta \Phi \right) : \right) dx \, , \tag{1.8}$$

where Φ denotes a real scalar field, while that of the massive Thirring theory is of the following form:

$$\mathcal{L}_{mTh} = \int \left(\bar{\Psi} (i\gamma_\nu \partial^\nu + m_0) \Psi - \frac{g}{2} \bar{\Psi} \gamma^\nu \Psi \bar{\Psi} \gamma_\nu \Psi \right) dx \, , \tag{1.9}$$

---

[2] Integration sign without any specification means integration on the whole real axis.
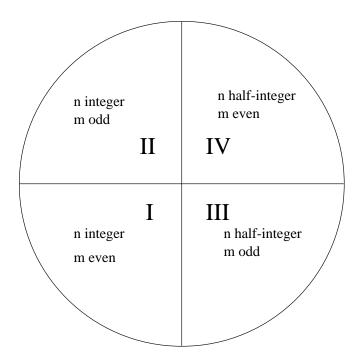
Figure 1.2: The family of vertex operators $V_{(n,m)}$ with $n \in \mathbb{Z}/2$ and $m \in \mathbb{Z}$. Sector **I** is the common subspace. **I** and **III** are $\mathcal{A}_f$, that defines the UV behaviour of massive Thirring; **I** and **II** are $\mathcal{A}_b$ that is the UV of sine-Gordon, **IV** is a sector of non mutually local vertex operators.

describing a current-current selfinteraction of a Dirac fermion Ψ. It is known that the two theories are deeply related provided their coupling constants satisfy

$$\frac{\beta^2}{4\pi} = \frac{1}{1 + g/\pi} \,.$$

For comparison with the Destri-de Vega nonlinear integral equation, it is important to deal with cylindrical sine-Gordon and massive Thirring, i.e. the integrals in (1.8, 1.9) must be taken in the interval $[0, L]$.

The cos term in (1.8) can be considered as a perturbation of the $c = 1$ free boson compactified on a cylinder, as described in section 1.2. Similarly the massless ($m_0 = 0$) Thirring model is a $c = 1$ conformal field theory and the mass term plays the role of a perturbation. From Coleman's paper [21] it is known that correlation functions of the perturbing fields $\bar{\Psi}\Psi$ and $: \cos \beta \Phi :$ are identical, then both models can be considered as the perturbations of a $c = 1$ compactified boson by a potential V :

$$H_{sG/mTh} = H_{CFT} + V \quad , \quad V = \lambda \int_0^L \left(V_{(1,0)}(z, \overline{z}) + V_{(-1,0)}(z, \overline{z}) \right) dx \,, \tag{1.10}$$

which is related to the bosonic lagrangian (1.8) by the following redefinitions of the field and the parameters:

$$\varphi = \sqrt{4\pi}\Phi \,, \quad R = \frac{\sqrt{4\pi}}{\beta} \,, \quad \lambda = \frac{\mu^2}{2\beta^2} \,. \tag{1.11}$$

For later convenience, a new parameter p can be defined by

$$p = \frac{\beta^2}{8\pi - \beta^2} = \frac{1}{2R^2 - 1} \ . \tag{1.12}$$

The point $p = 1$ (i.e. $g = 0$) is the free fermion point, corresponding to a massive Dirac free fermion. The particle spectrum of sG for $p > 1$ is composed by the soliton (s) and its antiparticle, the antisoliton ($\bar{s}$). It is known as repulsive regime because no bound states can take place. $p < 1$ is the attractive regime, because s and $\bar{s}$ can form bound states that are known as breathers. The values $p = \frac{1}{k}$, $k = 1, 2, \dots$ are the thresholds where a new bound state appears. The potential term becomes marginal when $\beta^2 = 8\pi$ which corresponds to $p = \infty$. The perturbation conserves the topological charge Q, which can be identified with the usual topological charge of the sG theory and with the fermion number of the mTh model.

Mandelstam [22] showed that a fermion operator satisfying the massive Thirring equation of motion can be constructed as a nonlocal functional of a pseudoscalar field (boson) satisfying the sine-Gordon equation. But the fermion and the boson are not relatively local and then do not create the same particle (the two theories are not equivalent).

The difference between them is that they correspond to the perturbation by the same operator of the two *different local* c=1 CFTs $\mathcal{A}_b$ and $\mathcal{A}_f$ as in 1.2. The short distance behaviour of the sG theory is described by the local operator algebra $\mathcal{A}_b$, while the primary fields of the UV limit of mTh theory are $\mathcal{A}_f$.

Note that the two algebras share a common subspace with even values of the topological charge, generated by $\{V_{(n,m)} : n \in \mathbb{Z}, m \in 2\mathbb{Z}\}$, where the massive theories described by the lagrangians (1.8) and (1.9) are identical. Exactly in this subspace holds the well known proof by Coleman about the equivalence of the two theories [21]. The figure 1.2 shows the four sectors where all the vertex operators live.

1.4   Truncated Conformal space at $c = 1$

In this section is given a brief description of Truncated Conformal Space (TCS) method for $c = 1$ theories. It will be usefull, in chapter 4 to have a comparison of the data obtained from the non-linear integral equation that will be introduced.

The TCS method was originally created to describe perturbations of Virasoro minimal models in finite spatial volume [15]. Here is presented an extension of the method to study perturbations of a $c = 1$ compactified boson, more closely the perturbation corresponding to sine-Gordon theory.

The Hilbert space of the $c = 1$ theory (on a cylinder) can be split into sectors labelled by the values of P and Q, which are quantised by integers. The numerical computations shall be restricted to the $P = 0$ sector (it is not expected that any relevant new information would come from considering $P \neq 0$). The TCS method consists of retaining only those states in such a sector for which the eigenvalue of H_{CFT} is less than a certain upper value E_{cut}, so the truncated space is defined as

$$\mathcal{H}_{TCS}(s, m, E_{cut}) = \{|\Psi\rangle : \ P|\Psi\rangle = s|\Psi\rangle, Q|\Psi\rangle = m|\Psi\rangle, H_{CFT}|\Psi\rangle \leq E_{cut}|\Psi\rangle\} \ . \tag{1.13}$$

For a given value of s, m and E_{cut} this space is always finite dimensional. In this space, the Hamiltonian, represented on the basis of the eigenstates of the unperturbed $c = 1$ Hamiltonian (i.e. eigenstates of $\widehat{L_0} + \widehat{\overline{L}_0})^3$, is a finite size matrix whose eigenvalues can be computed using a numerical diagonalization method. The explicit form of this matrix is the following:

---

[3] In this section, an hat on a letter means matrix

$$\widehat{H} = \frac{2\pi}{L} \left(\widehat{L_0} + \widehat{\overline{L}_0} - \frac{c}{12}\widehat{I} + \lambda \frac{L^{2-h}}{(2\pi)^{1-h}}\widehat{B} \right) ,\tag{1.14}$$

where $\widehat{L_0}$ and $\widehat{\overline{L}_0}$ are diagonal matrices with their diagonal elements being the left and right conformal weights, $\widehat{I}$ is the identity matrix,

$$h = \Delta_V^+ + \Delta_V^- = \frac{\beta^2}{4\pi} = \frac{2p}{p+1}\tag{1.15}$$

is the scaling dimension of the perturbing potential V and the matrix elements of $\widehat{B}$ are

$$\widehat{B}_{\Phi,\Psi} = \frac{1}{2} \langle \Phi | V_{(1,0)}(1,1) + V_{(0,1)}(1,1) | \Psi \rangle .\tag{1.16}$$

The units are chosen in terms of the soliton mass $\mathcal{M}$ which is related to the coupling constant λ by the mass gap formula[4] obtained from TBA in [25]:

$$\lambda = \kappa \mathcal{M}^{2-h},\tag{1.17}$$

where

$$\kappa = \frac{2\Gamma(h/2)}{\pi\Gamma(1-h/2)} \left(\frac{\sqrt{\pi}\Gamma\left(\frac{1}{2-h}\right)}{2\Gamma\left(\frac{h}{4-2h}\right)} \right)^{2-h} .\tag{1.18}$$

In what follows the energy scale is normalized by taking $\mathcal{M} = 1$; the dimensionless volume $\mathcal{M}L$ is denoted by l. For numerical computations, the dimensionless Hamiltonian

$$\widehat{h} = \frac{\widehat{H}}{\mathcal{M}} = \frac{2\pi}{l} \left(\widehat{L_0} + \widehat{\overline{L}_0} - \frac{c}{12}\widehat{I} + \kappa \frac{l^{2-h}}{(2\pi)^{1-h}}\widehat{B} \right)\tag{1.19}$$

will be used. The usefulness of the TCS method lies in the fact that it provides a nonperturbative method of numerically obtaining the spectrum (the mass gap, the mass ratios and the scattering amplitudes) of the theory. Therefore it can serve as a tool to check the exact results obtained for integrable field theories and get a picture of the physical behaviour even for the nonintegrable case. The systematic error introduced by the truncation procedure is called the *truncation error*; it increases with the volume L and can be made smaller by increasing the truncation level (at the price of increasing the size of the matrices, which is bound from above by machine memory and computation time).

Let us make some general remarks on how the TCS method applies to $c = 1$ theories. First note that the Hilbert space (even after specifying the sector by the eigenvalues of P and Q) consists of infinitely many Verma modules labelled by the quantum number n. At any finite value of E_{cut} only finitely many of such Verma modules contribute, but their number increases with E_{cut}. As a result one has to deal with many more states than in the case of minimal models. The results of TCS are supposed to approach the exact results in the limit $E_{cut} \to \infty$. The convergence

---

[4] Notice the analogy with both s-G/mTh that are obtained perturbing the free boson theory by a "mass term".

can be very slow, while the number of states rises faster than exponentially with the truncation level. The perturbing operator has scaling dimension which ranges between 0 and 2, becoming more relevant in the attractive regime, while the number of states corresponding to a given value of E_{cut} becomes larger as moving towards $p = 0$, which affects the convergence just the other way around.

Generally, the energy of any state goes with the volume L as

$$\frac{E_\Psi(L)}{\mathcal{M}} = -\frac{\pi\left(c - 12\left(\Delta_\Psi + \overline{\Delta}_\Psi\right)\right)}{6l} + Bl + \sum_{k=1}^\infty C_k\left(\Psi\right)l^{k(2-h)}, \qquad (1.20)$$

where Δ_Ψ $(\overline{\Delta}_\Psi)$ are the left (right) conformal dimensions of the state in the ultraviolet limit, B is the universal bulk energy constant (the vacuum energy density) and the infinite sum represents the perturbative contributions from the potential V.

The bulk energy constant has also been predicted from TBA and reads [25]

$$B = -\frac{1}{4}\tan\left(\frac{p\pi}{2}\right) \qquad (1.21)$$

(the same result was obtained from the NLIE approach in [7]). This is a highly nonanalytic function of p and it becomes infinite at the points where p is an odd integer. In fact, at these points there is a value of k for which $k(2 - h) = 1$, and $C_k\left(\Psi\right) \to \infty$. The infinite parts of B and $C_k\left(\Psi\right)$ exactly cancel, leaving a logarithmic (proportional to $l \log l$) and a finite linear contribution to the energy, by a sort of a resonance mechanism. All of these "logarithmic points" are in the repulsive regime. However, due to UV problems in the repulsive regime we are not able to check numerically the logarithmic corrections to the bulk energy.

The origin of UV divergences can be understood from *conformal perturbation theory* (CPT). It is known that when the scaling dimension h of the perturbing potential exceeds 1, CPT suffers from ultraviolet divergences which should be removed by some renormalization procedure. The TCS method is something very similar to CPT: it operates in the basis of the UV wave functions as well, but computes the energy levels using the variational approach and therefore could be called "*conformal variation theory*" (CVT). As a result, it is expected that there could be UV divergences for the range of couplings where $h > 1$ which is exactly the repulsive regime $p > 1$ [26]. The numerical analysis has in fact shown that in the repulsive regime the TCS energy eigenvalues did not converge at all when increasing the truncation level.

Fortunately, there exists a way out: since it is expected to find a sensible quantum field theory when the UV cutoff is removed, it should be the case that the *relative energy levels* $\mathcal{E}_\Psi(L) = E_\Psi(L) - E_{vac}(L)$ converge to some limit. This is exactly the behaviour that has been observed. Consequently, in the repulsive regime one can only trust the *relative* scaling functions produced by the TCS method, while in the attractive regime even the *absolute* energy values can be obtained (including the predicted bulk energy constant (1.21), which is completely analytic for $p < 1$ and thus logarithmic corrections are absent as well).

Many numerical results show that the smaller the value of p is the faster the convergence is (with the understanding that in the repulsive regime by convergence of TCS we mean the convergence of the energies relative to the vacuum). On the other hand, even in the attractive regime the convergence is so slow that to get reliable results (which means errors of order $10^{-3} - 10^{-2}$ for the volume l ranging from 0 to somewhere between 5 and 10) requires to work with matrix of dimensions around 4000. This means that the TCS for $c = 1$ theories is far less convergent than the one for minimal models (in the original Lee-Yang example the authors of [15] took a 17 dimensional Hilbert space (!) and arrived to very accurate results).

Chapter 2

LIGHT-CONE LATTICE QFT

In this chapter, the most important tools to deal with Destri-de Vega equation are introduced, with reference to the original papers [4, 6]. Particular attention will be taken to indicate the path that has been done from the light-cone lattice until the definition of a particular system (the 6 vertex model, alias XXZ chain), whose Hilbert space is quite completely known.

2.1 Kinematics on light-cone

It is a usual way to regularize quantum field theories by defining them on a space-like "hamiltonian" lattice (where time is continuous and space discrete) or space and time-like "euclidean" lattice (when both space and time are discrete). In statistical mechanics this is not just a regularization method but can be a right microscopic way to describe physical systems. In two dimensions, the most known approach is to define a rectangular lattice with axis corresponding to space and time directions and associate to each site an interaction depending only on the nearest neighbouring sites. In this case the partition function can be expressed in terms of a transfer matrix.

In what follows, a different approach is adopted: Minkowski and Euclidean space-time can, in fact, be discretized along light-cone directions. Light-cone coordinates are:

$$x_\pm = x \pm t$$

and the choice

$$\mathcal{M} = \{x_\pm = \frac{a}{\sqrt{2}} n_\pm, \quad n_\pm \in \mathbb{Z}\}$$

defines a light-cone lattice of "events" as in figure 2.1 (a) . They are spaced by a in the space and time directions and by $a/\sqrt{2}$ in light-cone directions. At every event $P \in \mathcal{M}$ there is associated a double light-cone (in the past and in the future) and only events within this light-cone can be causally connected (see fig. 2.1 (b)). Then, any rational and not greater than 1 speed is permitted for particles, in an infinite lattice. The shortest displacement of the particle (one lattice spacing) is realized at speed ± 1 and corresponds, from the statistical point of view, to nearest neighbours interactions. Smaller speeds can be obtained with displacements longer than the fundamental plaquette, and correspond to high order neighbours interactions. In quantum field theory, these are nonlocal interactions.

In the following, only the local case (nearest neighbours) is treated. The nearest neighbours of the event P are the four nearest points in the light-cone directions. This implies that particles can have only the speed of light ± 1 and are massless. They are called right-movers (R) and left-movers (L).
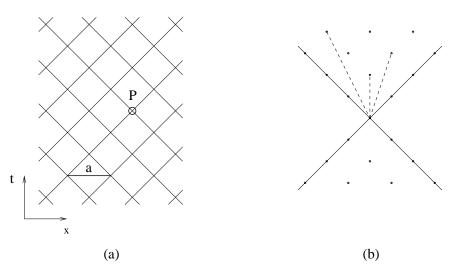
Figure 2.1: (a) light-cone lattice; (b) double light-cone emanating from a point and high-order interactions (dashed)

In this case, it is possible to introduce a useful language for connection with statistical mechanics associating a particle to a link. Consider the two links in the future that come out from a event P. Particles R and L in P, by definition, are respectively associated to the right-oriented link and to the left-oriented link. In this way, the state of a link is defined to be the state of the point where it begins (also the opposite choice, of connecting a link with the site where it ends, can be done; it is simply a matter of convention). For example, if in a point O there is a particle R, one tells that the "right-oriented" link outcoming from it is occupied by R. This correspondence of points and links is possible because only local interactions are assumed, and it is useful because the counting of states is simpler. But the physically correct interpretation is that particles live on events, not on links. Links are the possible world lines for particles.
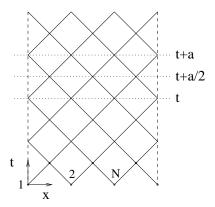
Figure 2.2: Periodicity in space direction; in link language the lines of time must be intended as shifted up by a little bit, as in figure 2.3.

In the following, the lattice is assumed of a finite extent $L = aN$ in space direction (N is the number of sites, counted in the space direction), with periodic boundary conditions, but infinite in time direction, as shown in figure 2.2. In this way a cylinder topology is defined for space time. The Hilbert space of states in an event P is the tensor product

$$\mathcal{H} = \mathcal{H}_L \otimes \mathcal{H}_R$$

of R and L space of states. The fact that particles can be classified in left and right does not

mean, in general, that the two dynamics are independent, as happens for example in conformal field theory. In what follows, exactly the interacting case will be treated.

Call $|\alpha_{Li}, \alpha_{Ri}\rangle$ the generic vector of a basis of $\mathcal{H}_i$ where $i = 1, ..., N$ labels the sites. The notation

$$|\alpha_{2i-1}, \alpha_{2i}\rangle = |\alpha_{Li}, \alpha_{Ri}\rangle$$

is useful and not ambiguous (even number refers to right, odd number refers to left). The total Hilbert space is:

$$\mathcal{H}_N = \bigotimes_{i=1}^{N} \mathcal{H}_i$$

and a basic vector can be represented by

$$|\alpha_1, \alpha_2\rangle \otimes ... \otimes |\alpha_{2N-1}, \alpha_{2N}\rangle = |\alpha_1, \alpha_2, ..., \alpha_{2N}\rangle \in \mathcal{H}_N.$$

Note that in a N sites lattice, due to light-cone, $2N$ labels are required.

If at a given time t there is a line of sites, the particular characteristic of the light-cone is that at time $t + a/2$ there is another line of sites, but not equivalent to the previous one, because it is shifted. Only at $t + a$ there is an equivalent line (see figure 2.2). Then two different evolution operators can be defined, depending on the initial state:

$$U_+ |\alpha_1, \alpha_2, ..., \alpha_{2N}, t\rangle = |\alpha_1', \alpha_2', ..., \alpha_{2N}', t + a/2\rangle$$

$$U_- |\alpha_1', \alpha_2', ..., \alpha_{2N}', t + a/2\rangle = |\alpha_1'', \alpha_2'', ..., \alpha_{2N}'', t + a\rangle$$

(2.1)

where the initial states are chosen as in figure 2.3. Schrödinger form of equations of motion is
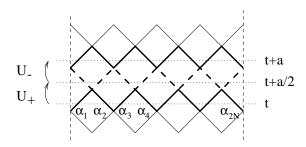
Figure 2.3: Partial evolution operators. The convention used here for the labeling of states will be used also in the following.

used, for a state in Hilbert space.[1] The global time operator can be chosen as

$$U = U_+ U_- \quad \text{or} \quad U' = U_- U_+$$

depending on the initial state. For a consistent quantum theory, both this operators must be unitary. This can be guaranteed if the assumption $U_+^\dagger U_+ = U_-^\dagger U_- = 1$ is made, that is the elementar operators themselves must be unitary.

[1] In Schrodinger form, if $|\alpha\rangle$ is a state vector, its time evolution is given by $|\alpha, t\rangle = U |\alpha, 0\rangle$ where U satisfies motion's equations: $U = Te^{-i \int dt H}$ (Dyson's series)

Another operator plays an important role and is defined as follows (the states are at a certain fixed time):

$$V\,|\alpha_1, \alpha_2, ..., \alpha_{2N}, t\rangle = |\alpha_{2N}, \alpha_1, ..., \alpha_{2N-1}, t\rangle \tag{2.2}$$

it corresponds to an half-space shift in the space direction, with exchange of right and left states(see the figure 2.4). Two applications of V give a shift by an entire lattice spacing, then V^2 is the lattice
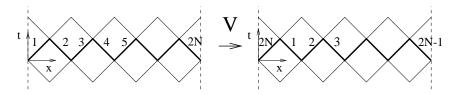
Figure 2.4: Half-shift operator

space evolution operator. It is possible to write an expression for V in terms of the permutation operator:

$$P_{nm}\left(|\alpha_n\rangle \otimes |\alpha_m\rangle\right) = |\alpha_m\rangle \otimes |\alpha_n\rangle\,, \qquad |\alpha_n\rangle \otimes |\alpha_m\rangle \in \mathcal{H}_n \otimes \mathcal{H}_m.$$

that looks like:

$$V = P_{12}P_{23}...P_{2N-1,\,2N} \tag{2.3}$$

The verification is direct:

$$P_{12}P_{23}...P_{2N-1,\,2N}\,|\alpha_1, \alpha_2, ..., \alpha_{2N}\rangle = P_{12}P_{23}...P_{2N-2,\,2N-1}\,|\alpha_1, ..., \alpha_{2N-2}, \alpha_{2N}, \alpha_{2N-1}\rangle =$$

$$= P_{12}P_{23}...P_{2N-3,\,2N-2}\,|\alpha_1, ..., \alpha_{2N}, \alpha_{2N-2}, \alpha_{2N-1}\rangle = ... = |\alpha_{2N}, \alpha_1, ..., \alpha_{2N-1}\rangle\,.$$

Also V is a unitary operator. To show this, one can use the fact that the permutation is self-adjoint. A more complete list of known properties of P is:

$$P = P^{-1} = P^{\dagger}, \qquad P^2 = 1 \tag{2.4}$$

Then, the adjoint of V is:

$$V^{\dagger} = P_{2N-1,2N}...P_{23}P_{12}$$

and $VV^{\dagger} = 1$ simply follows. The operators defined up to now have the following commutation rules:

$$\left[V^2, U_{\pm}\right] = 0; \qquad U_{\pm} = V U_{\mp} V^{\dagger}. \tag{2.5}$$

In figure 2.5, the first case is proved, by showing the equivalence of the two paths $V^2 U_+$ and $U_+ V^2$. "Mutatis mutandis", all the other cases can be simply obtained. Consequently, the two principal evolution operators, V^2 and U, are commuting:

$$\left[V^2, U\right] = \left[U, V^2\right] = 0.$$

As previously shown, they are also unitary. Thanks to all these properties, it is very natural to identify them as the exponential of the hamiltonian operator, and the exponential of the linear momentum:

$$\begin{aligned} U &= e^{-iaH} \\ V^2 &= e^{-iaP}. \end{aligned} \tag{2.6}$$
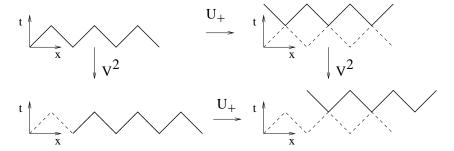
Figure 2.5: Commutation rule: $V^2 U_+ = U_+ V^2$

There are other two important operators, defined as:

$$U_R = U_+ V$$
$$U_L = U_+ V^\dagger \tag{2.7}$$

As clearly shown in figure 2.6 for one of them, they correspond to one step evolution in light-cone directions. They are commuting and give the expressions:
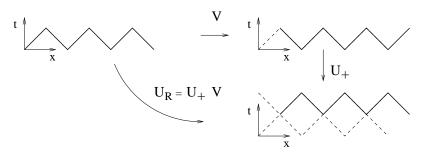
Figure 2.6: Right-oriented shift operator

$$U = U_R U_L \qquad\qquad V^2 = U_R U_L^\dagger$$
$$[U_R, U_L] = 0 \qquad U_R^\dagger U_R = U_L^\dagger U_L = 1$$

then, using also (2.6) yields:

$$U_R = e^{-i\frac{a}{2}(H+P)}, \qquad U_L = e^{-i\frac{a}{2}(H-P)}. \tag{2.8}$$

2.2 Dynamics on light-cone

A dynamics can be defined by giving all the amplitudes of the different processes that can take place. The fundamental assumption is that in every site a whole process can happen, in the sense that if $|\alpha_L, \alpha_R\rangle_{in}$ and $|\beta_L, \beta_R\rangle_{out}$ are the incoming and outgoing states in a certain site, they can be considered asymptotic states and the transition amplitude is an S-matrix element:

$$_{out}\langle \beta_R, \beta_L | \alpha_R, \alpha_L \rangle_{in} = S_{(\alpha_R, \alpha_L)_{in}, (\beta_R, \beta_L)_{out}} \tag{2.9}$$

This, in general, is an $m \to n$ scattering. The system is then defined via its microscopic amplitudes.

From the definition (2.1) of evolution operators, the following expression holds (the "in" state is at time t, the "out" state at $t + a/2$, with reference at the figure 2.3:

$$\langle \alpha_1, \alpha_2, ..., \alpha_{2N}, t | \, U_+ \, | \alpha'_1, \alpha'_2, ..., \alpha'_{2N}, t \rangle =_{in} \langle \alpha_1, \alpha_2, ..., \alpha_{2N} | \, \alpha'_1, \alpha'_2, ..., \alpha'_{2N} \rangle_{out} =$$

$$=_{in} \langle \alpha_1, \alpha_2 \, | \alpha'_1, \alpha'_2 \rangle_{out} \, ..._{in} \langle \alpha_{2N-1}, \alpha_{2N} \, | \alpha'_{2N-1}, \alpha'_{2N} \rangle_{out} = \qquad (2.10)$$

$$= \prod_{i=1,...,N} S^{\dagger}_{(\alpha_{2i-1}, \alpha_{2i})_{in}, (\alpha'_{2i-1}, \alpha'_{2i})_{out}}$$

The operator U_- can be obtained from (2.5). In the last line, the product is on all the sites at a given time.

It is interesting to observe that there is a powerful connection with statistical mechanics, at this point. Assume, for simplicity, that the lattice is euclidean and has a very large (thermodynamics) but finite extension in the "time" direction. In this way there is an initial time (with an initial state $|\alpha\rangle_{in}$) and a final time (with a final state $|\beta\rangle_{out}$). The total transition amplitude is given by the product on all sites of the amplitudes, and the sum on all the internal states (γ', γ''):

$$_{out} \langle \beta | \, \alpha \rangle_{in} = \sum_{int \, states} \prod_{sites} S_{\gamma', \gamma''} \equiv Z$$

The important fact is that if $S_{\gamma', \gamma''}$ is real and positive, it plays the role of a Boltzmann weight for a statistical system whose partition function is given by the previous expression, that was conveniently called Z. It depends only on the external states. The first appearance of this correspondence is in [1].

In both the statistical and the particle interpretation, the integrability (that will be always assumed in what follows) can be obtained by requiring that the scattering amplitude $S_{\gamma, \gamma'}$ or the Boltzmann weight satisfy the Yang-Baxter equation (see [2, 3]). In this case a general $m \rightarrow n$ particles scattering can be factorised in the product of "elementary" $2 \rightarrow 2$ particles scattering. Then at every site there will be associated one of this "elementary" amplitudes:

$$_{out} \langle \beta_L, \beta_R \, | \alpha_R, \alpha_L \rangle_{in} = S^{\beta_R, \beta_L}_{\alpha_R, \alpha_L} \qquad (2.11)$$

and "in" and "out" states are two particle states (as in the previous equation). In statistical language, usually the Boltzmann weight is indicated with R and there is a little change of notation with respect to scattering case:

$$R^{\beta_R, \beta_L}_{\alpha_L, \alpha_R} = S^{\beta_R, \beta_L}_{\alpha_R, \alpha_L} \qquad (2.12)$$

(the lower indices are interchanged). A pictorial interpretation of that is in figure 2.7.
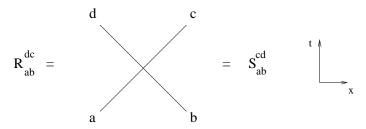

Figure 2.7: Pictorial interpretation of R and S matrix

The Yang-Baxter equation takes the form:

$$S_{12} S_{13} S_{23} = S_{23} S_{13} S_{12} \qquad (2.13)$$

(with the indicated change it holds clearly also for R-matrix).

Apparently, this "phenomenological" approach is quite unusual, because in traditional lattice quantum field theory at every site is associated one interaction potential (ex: $\phi^4(i)$ is the potential on the site i), not a whole scattering process. This can appear as a sort of "macroscopic" approach, not based on fundamental interactions. But the properties of factorisable scattering must be taken into account. Factorization of generic amplitudes in $2 \to 2$ particles amplitudes is a sort of quantum superposition principle and the remarkable fact is that between one scattering and the other, the particles are asymptotic ones, that means that they are free. For example in figure 2.8 (1+1 QFT on the continuum) between the point 1 and the point 2 the motion is free. Every point
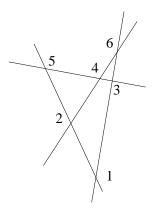
Figure 2.8: Factorizable scattering. Between two interaction points the particles are free.

contain all the interaction. This is what was assumed in the definition of the lattice. Then it is perfectly justified that every site is connected with a whole $2 \to 2$ particles scattering process.[2] The previous equation (2.10) can be written now in a more specific form:

$$\langle \alpha_1, \alpha_2, ..., \alpha_{2N}, t| \, U_+ \left| \alpha_1', \alpha_2', ..., \alpha_{2N}', t \right\rangle = R^{\alpha_1' \alpha_2'}_{\alpha_1 \alpha_2} \, R^{\alpha_3' \alpha_4'}_{\alpha_3 \alpha_4} ... R^{\alpha_{2N-1}' \alpha_{2N}'}_{\alpha_{2N-1} \alpha_{2N}} \tag{2.14}$$

The physical system dynamics is therefore defined by the assignment of an R matrix, and integrability is guaranteed. The consistency on quantum mechanical interpretation is obtained by requiring unitarity, hermitian analyticity and crossing symmetry for the S matrix obtained by (2.12).

It is important to obtain an explicit expression for U_L and U_R :

$$\langle \alpha_1, \alpha_2, ..., \alpha_{2N}, t| \, U_R \left| \alpha_1', \alpha_2', ..., \alpha_{2N}', t \right\rangle = \sum_{\overrightarrow{\gamma}} \langle \overrightarrow{\alpha}, t| \, U_+ \, | \overrightarrow{\gamma} \rangle \langle \overrightarrow{\gamma}| \, V \left| \overrightarrow{\alpha'} t \right\rangle =$$

$$= \sum_{\overrightarrow{\gamma}} R^{\gamma_1 \gamma_2}_{\alpha_1 \alpha_2} \, R^{\gamma_3 \gamma_4}_{\alpha_3 \alpha_4} ... \, \langle \gamma_1, ..., \gamma_{2N} \left| \alpha_{2N}', \alpha_1', ..., \alpha_{2N-1}', t \right\rangle = \tag{2.15}$$

$$= R^{\alpha_{2N}' \alpha_1'}_{\alpha_1 \alpha_2} \, R^{\alpha_2' \alpha_3'}_{\alpha_3 \alpha_4} ... R^{\alpha_{2N-2}' \alpha_{2N-1}'}_{\alpha_{2N-1} \alpha_{2N}}$$

and, in a similar way,

$$\langle \alpha_1, \alpha_2, ..., \alpha_{2N}, t| \, U_L \left| \alpha_1', \alpha_2', ..., \alpha_{2N}', t \right\rangle = R^{\alpha_2' \alpha_3'}_{\alpha_1 \alpha_2} \, R^{\alpha_4' \alpha_5'}_{\alpha_3 \alpha_4} ... R^{\alpha_{2N}' \alpha_1'}_{\alpha_{2N-1} \alpha_{2N}} \tag{2.16}$$

This expression is consistent with the figure 2.6. The important fact is that this operators can be expressed in terms of the transfer matrix of an inhomogeneous lattice model, that will be defined in the next section.

---

[2] In the next paragraphs, it will be explained that, for the particular case of the 6 vertex R matrix, a more traditional lattice QFT approach can be formulated, in terms of a fermionic field.

2.3   Euclidean transfer matrix

Consider a two dimensional euclidean square lattice, with periodic boundary conditions, in both the directions. The links are the physical objects of the system. They can be in different states belonging to the vector spaces $\mathcal{A}$ and $\mathcal{V}$. In principle, this vector states can be different, but in the following they will be identified. At every site can be associated a Boltzmann weight depending on the four links crossing at this site and on a spectral parameter λ (see the figure 2.9). The simplest

(a)   (b)
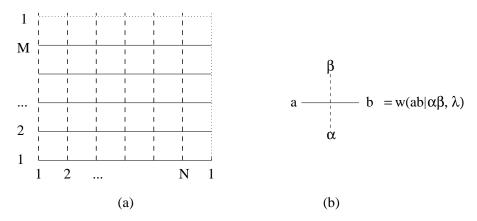
Figure 2.9: (a) periodic (toroidal) square lattice; (b) Boltzmann weight for a site; the labels are: $a, b \in \mathcal{A}, \quad \alpha, \beta \in \mathcal{V}$

case is to take the same Boltzmann weights in all the sites, but more general configurations are possible. In the following an inhomogeneity λ_i will be assumed, where i is the column index (all the sites on a column have the same inhomogeneity), in the sense that the Boltzmann weight in the column i is taken to be:

$$w(ab|\alpha\beta,\ \lambda - \lambda_i).$$

Also for the boundary conditions it is possible to assume more general configurations than the simplest one (i.e. toroidal b.c.). Assume that between the column N and the N+1 (that is 1) there is a nontrivial seam line, in such a way that the Boltzmann weights on the column N (with respect to the normal ones) are given by:

$$w^{(N)}(ab|\alpha\beta,\ \lambda) = e^{i\omega b} w(ab|\alpha\beta,\ \lambda). \tag{2.17}$$

This choice is made because only the link b cross the seam line. This are called *twisted boundary conditions* (obviously the choice $\omega = 0$ reproduces the periodic case).

The partition function for such a model is given by (see the figure 2.9):

$$Z = \sum_{link\ states} \prod_{rows} w(ab|\alpha\beta,\ \lambda - \lambda_1)...w(ab|\alpha\beta,\ \lambda - \lambda_{N-1}) w^{(N)}(ab|\alpha\beta,\ \lambda - \lambda_N) \tag{2.18}$$

(observe the twisted Boltzmann weight in the last column). It is simple to show that it can be expressed, thanks to periodicity, in terms of a row-to-row transfer matrix. To obtain that, it is convenient to define an operator t that acts on both the horizontal and the vertical spaces:

$$\begin{aligned} t(\lambda) : \ & \mathcal{A} \ \to \ \mathcal{A} \\ t_{ab}(\lambda) &= \langle a|\, t(\lambda)\, |b\rangle \end{aligned} \tag{2.19}$$

defines the horizontal action; t_{ab} depends on the horizontal links and acts on the vertical space as:

$$t_{ab}(\lambda):\ \mathcal{V} \to \mathcal{V}$$
$$\langle \alpha | \, t_{ab}(\lambda) \, | \beta \rangle = [t_{ab}(\lambda)]_{\alpha\beta} = w(ab|\alpha\beta,\,\lambda). \qquad (2.20)$$

The twist can be obtained with an appropriate operator that changes the horizontal states by a phase after the seam line:

$$|a_{N+n}\rangle = e^{i\omega A} |a_n\rangle, \qquad |a_i\rangle \in \mathcal{A}_i \qquad (2.21)$$

where ω is a real parameter (twist), A is a self-adjoint operator and n is an horizontal index (in the vertical direction there is no twist). A must be chosen diagonal on the whole horizontal space $\mathcal{A}$, therefore it acts as a phase. Observe that the lattice euclidean structure is a normal periodic one, because the twist acts only on the quantum mechanical structure. For a generic operator B_n acting on the site n the consistency with (2.21) requires that the twist acts as:

$$B_{N+n} = e^{i\omega A} B_n e^{-i\omega A}. \qquad (2.22)$$

This expression can be used for the determination of the t_{ab} operator acting on the last column:

$$_N \langle a | \, t^{(N)}(\lambda) \, | b \rangle_{N+1} =_N \langle a | \, t^{(N)}(\lambda) e^{i\omega A} \, | b \rangle_1 =$$
$$= e^{i\omega b} \,_N \langle a | \, t^{(N)}(\lambda) \, | b \rangle_1 \qquad (2.23)$$

where the "positions" of the states and operators are emphasized; in particular observe that only b crosses the seam line. Using the identification (2.20) the expression (2.17) can be simply obtained.

The row-to-row transfer matrix is an operator $t^{(N)}(\lambda, \{\lambda_i\}, \omega)$ that acts on the vertical space:

$$\mathcal{V}^{(N)} = \bigotimes_{i=1}^{N} \mathcal{V}$$

in the following way:

$$t^{(N)}(\lambda, \{\lambda_i\}, \omega) = \sum_{a_1} T^{(N)}_{a_1 a_1} = \sum_{a_1, \dots a_N} t_{a_1 a_2}(\lambda - \lambda_1) \otimes t_{a_2 a_3}(\lambda - \lambda_2) \otimes \dots \otimes t_{a_N a_1}(\lambda - \lambda_N) e^{i\omega b}$$

$$(2.24)$$

The T_{ab} is called monodromy matrix. The expression for the partition function is:

$$Z = Tr_{V^{(N)}} \left[t^{(N)}(\lambda, \{\lambda_i\}, \omega) \right]^M.$$

Define now a matrix acting on $\mathcal{A} \otimes \mathcal{A}$ given by:

$$R^{\beta b}_{a\alpha}(\lambda) = [t_{ab}(\lambda)]_{\alpha\beta} = w(ab|\alpha\beta,\,\lambda). \qquad (2.25)$$

(observe that in the operator in (2.20) the Latin and Greek index belong to different spaces, while in R matrix they belong to the same space and this differentiation of notation is redundant). An obvious generalization is needed for the last column. This definition (2.25) shows that the R matrix is defined as a Boltzmann weight, as required in the section 2.2. In the following will be explained the importance of (2.25) for the integrability.

It is possible to show, at this point, that the transfer matrix (2.24) can be used to express the operators defined in (2.15, 2.16). Consider the following form for the inhomogeneity:

$$\lambda_i = (-1)^{i+1}\Theta \qquad (2.26)$$

where Θ is a positive real number, and calculate a matrix element of the transfer matrix on vectors of $V^{(2N)}$ (clearly, in this case, the periodicity requires an even number of horizontal sites):

$$\langle \alpha_1, \alpha_2, ..., \alpha_{2N} | \, t^{(2N)}(\Theta, \{\lambda_i\}) \, |\alpha'_1, \alpha'_2, ..., \alpha'_{2N}\rangle =$$

$$= \sum_{a_1...a_{2N}} t_{a_1 a_2}(0)_{\alpha_1 \alpha'_1} \, t_{a_2 a_3}(2\Theta)_{\alpha_2 \alpha'_2} ... t_{a_{2N} a_1}(2\Theta)_{\alpha_{2N} \alpha'_{2N}} =$$

$$= R^{\alpha'_2 \alpha'_3}_{\alpha_1 \alpha_2} \, R^{\alpha'_4 \alpha'_5}_{\alpha_3 \alpha_4} ... R^{\alpha'_{2N} \alpha'_1}_{\alpha_{2N-1} \alpha_{2N}}$$

that is exactly the expression (2.16). In an operatorial form this means that:

$$t^{(2N)}(\Theta, \{\lambda_i\}) = U_L. \tag{2.27}$$

A similar picture holds for the operator U_R, but to take into account this case an assumption on R is necessary. Assume that R matrix is hermitian analytic, that means:

$$R^{ab}_{cd}(\lambda)^* = R^{cd}_{ab}(-\lambda)$$

that in S matrix language is $S^\dagger(s) = S(s^*)$. This is a well known property of an S matrix and, as explained in the section 2.2, the same requirement is necessary for R. Then, as for U_L, the following expression can be obtained:

$$t^{(2N)}(-\Theta, \{\lambda_i\})^\dagger = U_R. \tag{2.28}$$

Here the adjoint conjugation is only on the vertical space.[3] It is given by:

$$\left[t_{ab}(\lambda)^\dagger \right]_{\alpha\beta} = w(ab|\beta\alpha, \, \lambda)^*.$$

Transfer matrix can express the evolution operators.

As introduced in the section 2.2, if the R matrix satisfies the Yang-Baxter equation (2.13), then it is possible to show that the transfer matrix commute with itself at different values of the spectral parameter. In this case the system is integrable. The same conclusion holds also for the inhomogeneous and twisted models. Assume that the R matrix satisfies the Yang-Baxter equation, that in the explicit form is:

$$R^{c_1 c_2}_{a_2 a_1}(\vartheta_1 - \vartheta_2) R^{b_1 c_3}_{a_3 c_1}(\vartheta_1 - \vartheta_3) R^{b_2 b_3}_{c_3 c_2}(\vartheta_2 - \vartheta_3) = R^{c_2 c_3}_{a_3 a_2}(\vartheta_2 - \vartheta_3) R^{c_1 b_3}_{c_3 a_1}(\vartheta_1 - \vartheta_3) R^{b_1 b_2}_{c_2 c_1}(\vartheta_1 - \vartheta_2). \tag{2.29}$$

Using (2.25) it is possible to obtain another form, specific for the t operator:

$$R^{ef}_{ab}(\vartheta - \vartheta') \, [t_{ec}(\vartheta)]_{\alpha\gamma} \, \left[t_{fd}(\vartheta')\right]_{\gamma\beta} = \left[t_{ae}(\vartheta')\right]_{\alpha\gamma} [t_{bf}(\vartheta)]_{\gamma\beta} \, R^{cd}_{ef}(\vartheta - \vartheta') \tag{2.30}$$

For consistency, the R matrix must be of the regular type, that means that at the origin it is the unit operator (or proportional to) on $\mathcal{A} \otimes \mathcal{A}$:

$$R^{\beta b}_{a\alpha}(0) = \delta_{a\beta}\delta_{\alpha b}.$$

This equation fixes a normalization for the R matrix. Then, to fit with the equations (2.27, 2.28) a normalization factor is required. It is fixed by the unitarity requirement. The (2.30) holds also if an identical shift is performed on both the spectral parameters:

$$\vartheta \to \vartheta - \alpha$$

___
[3] The definition of adjoint is $\langle \beta | \, t_{ab} \, |\alpha\rangle^* = \langle \alpha | \, t^\dagger_{ab} \, |\beta\rangle$

(the same for ϑ') because only the difference appears in the R term. This shift is an inhomogeneity for the t operator.

Consider now a group of matrices $g \in \mathcal{G}$ of dimension $\dim \mathcal{A} \times \dim \mathcal{A}$ and determinant one, such that they commute with R:

$$[g \otimes g, R] = 0. \tag{2.31}$$

Then define a transformed ("gauged" or twisted) t operator:

$$t_{(g)ab} = g_{ac} t_{cb}.$$

The twist introduced in (2.23) is the special case of $\mathcal{G} = U(1)^{\dim \mathcal{A}}$. It is simple to verify that also the gauged $t_{(g)}$ satisfies the same (2.30). This is because of the commutation relation (2.31). The group $\mathcal{G}$ is a symmetry group for the Yang-Baxter equation and for the vertex model defined in this way. With some simple algebra, using many times eq. (2.30), it is possible to obtain the form for the monodromy matrix, defined as in (2.24) but with a possibly different gauge g_i in every site of a row (all the column has the same gauge) and clearly an inhomogeneity. If the following synthetic notation is introduced, $G = (g_1, ..., g_N)$, then the final result is:

$$R(\vartheta - \vartheta') \left[T_G^{(N)}(\vartheta) \otimes_{\mathcal{A}} T_G^{(N)}(\vartheta') \right] = \left[T_G^{(N)}(\vartheta') \otimes_{\mathcal{A}} T_G^{(N)}(\vartheta) \right] R(\vartheta - \vartheta').$$

Taking the trace on the horizontal space $\mathcal{A}$ yields:

$$\left[t_G^{(N)}(\vartheta, \{\lambda_i\}), t_G^{(N)}(\vartheta', \{\lambda_i\}) \right] = 0 \tag{2.32}$$

(observe that the gauge must be exactly the same). At the various values of ϑ, $t_G^{(N)}(\vartheta, \{\lambda_i\})$ describes an infinite family of conserved charges. Then the system is integrable. This holds in particular in the inhomogeneous and the twisted cases.

The interesting fact, at this point, is that in some cases the transfer matrix can be exactly diagonalized by Bethe Ansatz methods. This gives an exact expression for eigenstates and eigenvalues of the operator U.

2.4   6 vertex model: main results

The theory developed until now is general and not referred to a specific model. The simplest non trivial case to take into account in the previous framework is the 4×4 R matrix, corresponding to the choice $\mathcal{A} = \mathcal{V}$. As shown in [3], the most general solution is the so called 8 vertex model. This name means that only 8, between the 16 entries of the R matrix, are nonzero. A special case is the 6 vertex model, for which many results have been obtained in the light-cone description: this will be the principal object of this dissertation. The R matrix has the form (lower index are rows and upper index are columns)

$$R(\vartheta, \gamma) = \begin{pmatrix} a & & & \\ & c & b & \\ & b & c & \\ & & & a \end{pmatrix} \tag{2.33}$$

As Boltzmann weights, all this nonvanishing entries must be real and nonnegative. But Yang-Baxter equation is solved for all the values of this variables.[4] As explained in (2.2), the scattering interpretation is possible only assuming the properties indicated in that section.

---

[4] Observe that the upper and lower entries are the same; this is the assumption of parity invariance.

There is a well known mapping between vertex models and spin chains (see [3]), i.e. the transfer matrix is the exponential of the quantum hamiltonian of the chain:

$$t^{(N)} = e^{-H}.$$

In the case of 8 vertex model, the hamiltonian is the XYZ(1/2) chain, while in the special case of 6 vertex, is the XXZ(1/2) chain. In what follows, this identification can be useful to interpret some facts connected with Bethe Ansatz. The XXZ(1/2) chain hamiltonian is given by:

$$H = \sum_{i=1}^{N} \left[\sigma_x^i \sigma_x^{i+1} + \sigma_y^i \sigma_y^{i+1} + (1 - \cos\gamma)\sigma_z^i \sigma_z^{i+1} \right]$$

and γ is the anisotropy. The σ are Pauli matrices. The total z-component of the spin will play an important role in Bethe Ansatz.

This is a statistical approach, but it is possible to give a particle interpretation to the same R matrix (2.33) on the light-cone lattice.

The simplest case of particles obeying Pauli exclusion principle (fermions) and without internal degrees of freedom (color number) is assumed. This means that in an event only one particle of type R and one L at most can take place. In other words, one link has two states: empty or occupied. At every point there are four links, that means 16 possible configurations associated to it. In terms of events, these are the possible configurations that connect a point with the nearest neighbours in the future.

Assume now that only amplitudes that conserves the total number of particles (R+L) are nonvanishing. This reduces to 6 the permitted configurations, as it is shown in the figure 2.10. This is simply the 6 vertex model whose R matrix is written in (2.33). The assumption of

$$\omega_1 \qquad \omega_2 \qquad \omega_3 \qquad \omega_4 \qquad \omega_5 \qquad \omega_6$$
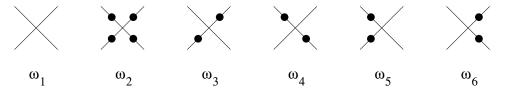
Figure 2.10: 6 permitted amplitudes. Dots are particles.

integrability for this amplitudes gives the general six-vertex model. The requirement of symmetry under parity transformation implies that $\omega_3 = \omega_4$ and $\omega_5 = \omega_6$. The convention adopted in the figure 2.9 and in (2.20, 2.25, 2.33) shows that

$$b = \omega_3 = \omega_4, \quad c = \omega_5 = \omega_6.$$

Now, this R matrix can be written in an operatorial form, by defining a lattice chiral fermion $\psi_{A,n}$, with $A = R, L$, and n labels the sites. The anticommutation rules are the canonical ones:

$$\{\psi_{A,n}, \psi_{B,m}\} = 0, \qquad \left\{\psi_{A,n}, \psi_{B,m}^\dagger\right\} = \delta_{AB}\delta_{nm}. \qquad (2.34)$$

This fermion has some interesting properties, that are exposed in the paper [4], and are sketched in the following list:

1. the R matrix and all the other operators U_{any} can be written in an operatorial form in terms of the fermion;

2. the lattice hamiltonian, in the free case $\omega_1 = \omega_2 = b = 1$, $c = 0$, can be explicitly written; by this, the following dispersion relation can be obtained: $E = \pm k$; this is the dispersion relation for a free massless particle; the unusual fact is that it is monotonous, then there is no doubling of fermions; this is a consequence of the nonlocality of the hamiltonian

3. the lattice hamiltonian admits a continuum limit $N \to \infty$ and $a \to 0$ but with $L = Na$ fixed; the locality is recovered in this limit; the continuum equations of motion are those of the massive Thirring model. The space is compactified on a cylinder.

In the continuum limit, the massive Thirring model emerges as the field theory characterising the scaling behavior of the dynamics on the lattice (remember that L is finite; the scaling behaviour is understood in terms of this L).

2.5   6 vertex model: Bethe Ansatz

The assumptions of unitarity and hermitian analyticity will be taken into account, for the R matrix, and this requires that the variables in (2.33) must have the specific form:

$$a = a(\vartheta, \gamma) = \sinh(i\gamma - \vartheta), \quad b = b(\vartheta, \gamma) = \sinh\vartheta, \quad c = c(\vartheta, \gamma) = i\sin\gamma \qquad (2.35)$$

The transfer matrix defined by this R matrix (2.24, 2.25) can be diagonalized with Bethe Ansatz method. In terms of the spin chain, this means that there are two operators, usually indicated by $B(\vartheta)$ and $C(\vartheta)$, whose expression is known, and there is a "reference state"[5] $|\Omega\rangle$ such that:

$$C(\vartheta) |\Omega\rangle = 0$$

and

$$B(\vartheta_1)...B(\vartheta_M) |\Omega\rangle , \qquad (2.36)$$

for appropriate values of ϑ_j is an eigenstate of the transfer matrix. The "appropriate values" of ϑ_j can be obtained as the solution of a set of M coupled nonlinear equations, that are called Bethe Ansatz equations. In general, because of (2.32), the transfer matrix contains all the conserved charges, in particular the hamiltonian. Then the Bethe Ansatz eigenstates are also eigenstates of the hamiltonian. The Hilbert space of the theory and the action of conserved charges on it are then perfectly know.

All this computations for the 6 vertex model were obtained in [3, 5, 6]; the final results are written here for the eigenvalues of the inhomogeneous and twisted transfer matrix:

$$\tau(\vartheta, \Theta, \omega) = e^{i\omega} \left[a(\vartheta - \Theta) \, a(\vartheta + \Theta) \right]^N \prod_{j=1}^{M} \frac{\sinh \dfrac{\gamma}{\pi} \left[i\dfrac{\pi}{2} + \vartheta_j + \vartheta \right]}{\sinh \dfrac{\gamma}{\pi} \left[i\dfrac{\pi}{2} - \vartheta_j - \vartheta \right]} +$$

$$+ e^{-i\omega} \left[b(\vartheta - \Theta) \, b(\vartheta + \Theta) \right]^N \prod_{j=1}^{M} \frac{\sinh \dfrac{\gamma}{\pi} \left[i\dfrac{3\pi}{2} - \vartheta_j - \vartheta \right]}{\sinh \dfrac{\gamma}{\pi} \left[-i\dfrac{\pi}{2} + \vartheta_j + \vartheta \right]}$$

---

[5] The "reference state" at this point is only a mathematical object. Physically speaking, it corresponds to the ferromagnetic state with all the spins up.

and the values of ϑ_j are defined by the set of coupled nonlinear equations called Bethe Ansatz equations:

$$\left(\frac{\sinh \dfrac{\gamma}{\pi} \left[\vartheta_j + \Theta + \dfrac{i\pi}{2} \right] \sinh \dfrac{\gamma}{\pi} \left[\vartheta_j - \Theta + \dfrac{i\pi}{2} \right]}{\sinh \dfrac{\gamma}{\pi} \left[\vartheta_j + \Theta - \dfrac{i\pi}{2} \right] \sinh \dfrac{\gamma}{\pi} \left[\vartheta_j - \Theta - \dfrac{i\pi}{2} \right]} \right)^N = -e^{2i\omega} \prod_{k=1}^{M} \frac{\sinh \dfrac{\gamma}{\pi} [\vartheta_j - \vartheta_k + i\pi]}{\sinh \dfrac{\gamma}{\pi} [\vartheta_j - \vartheta_k - i\pi]} \qquad (2.37)$$

where $2N$ is the length of the chain and N the number of sites in a row of the light-cone lattice. The ϑ_j are *called Bethe roots*, and in principle, can take any complex value. But there is a periodicity in their imaginary part:

$$\vartheta_j \rightarrow \vartheta_j + \frac{\pi^2}{\gamma} i \qquad (2.38)$$

then only a strip around the real axis must be taken into account for the Bethe roots:

$$\vartheta_j \in \mathbb{R} \times i \left] -\frac{\pi^2}{2\gamma}, \frac{\pi^2}{2\gamma} \right]. \qquad (2.39)$$

Moreover, only the range

$$0 < \gamma < \pi$$

will be examined.

From Bethe Ansatz it is known that the whole spectrum of the theory can be obtained using all the Bethe configurations having $M \leq N$ and $\vartheta_j \neq \vartheta_k$ for every $j \neq k$. In general for a state with M roots the third component of the spin of the chain is

$$S = N - M, \qquad (2.40)$$

because every operator $B(\vartheta_i)$ counts as -1 spin.

This XXZ(1/2) chain has 2 states in every site, then 2^{2N} states. Then the energy spectrum is upper and lower bounded. Changing the sign of the hamiltonian gives another permitted physical system. This means that there are two possible vacua. The first one is the so called ferromagnetic ground state, corresponding to $M = 0$ that is the reference state $|\Omega\rangle$. It has spin $S = N$. The second one is the antiferromagnetic ground state, that can be obtained with $M = N$ and all the roots ϑ_i real. It has spin $S = 0$.

In what follows, only the antiferromagnetic ground state will be considered, because it has one important property: in the thermodynamic limit ($N \rightarrow \infty$) it can be interpreted as a Dirac vacuum (a sea of particles created by B) and the excitations on this vacuum behave as particles.

The energy E and momentum P of a state can be read out by the transfer matrix eigenvalues by use of the equations (2.27, 2.28). The final form is:

$$e^{i\frac{a}{2}(E \pm P)} = e^{\pm i\omega} \prod_{j=1}^{M} \frac{\sinh \dfrac{\gamma}{\pi} \left[i\dfrac{\pi}{2} - \Theta \pm \vartheta_j \right]}{\sinh \dfrac{\gamma}{\pi} \left[i\dfrac{\pi}{2} + \Theta \mp \vartheta_j \right]}. \qquad (2.41)$$

Other integrals of motion can be obtained in a similar way by transfer matrix (see (2.32)). Observe that the second term in the transfer matrix expression vanishes because $b(0) = 0$.

For future analysis, it is more convenient to express the coupling constant γ in terms of a different variable p:

$$p = \frac{\pi}{\gamma} - 1, \qquad 0 < p < \infty.$$

Then all the expressions will be in terms of p.

Chapter 3

A NONLINEAR EQUATION FOR BETHE ANSATZ

In this chapter the fundamental nonlinear integral equation (on the lattice) for the Bethe Ansatz is derived. In literature it is known as Destri-de Vega equation. It was obtained first in [7, 8] and, in the final form, in [9]. On this equation the continuum limit is performed.

3.1 Counting function

It is possible to write the Bethe equations (2.37) in terms of a counting function, that will be called $Z_N(\vartheta)$. To do that, one important preliminar definition is needed:

$$\phi(\vartheta, \nu) = i \log \frac{\sinh \frac{1}{p+1}(i\pi\nu + \vartheta)}{\sinh \frac{1}{p+1}(i\pi\nu - \vartheta)}, \qquad \phi(-\vartheta, \nu) = -\phi(\vartheta, \nu)$$

where the primary interest is in values $\nu = 1/2$, 1 and the oddness on the analyticity strip around the real axis defines a precise logarithmic branch: the so called fundamental branch. In the appendix B the complete structure of the cuts and all the relevant properties of this function are exposed. The counting function[1] can be defined by

$$Z_N(\vartheta) = N[\phi(\vartheta + \Theta, \frac{1}{2}) + \phi(\vartheta - \Theta, \frac{1}{2})] - \sum_{k=1}^{M} \phi(\vartheta - \vartheta_k, 1) + 2\omega \tag{3.1}$$

used to express the logarithm of the Bethe equations, one obtains simply:

$$Z_N(\vartheta_j) = 2\pi I_j, \qquad I_j \in \mathbb{Z} + \frac{1+\delta}{2}, \qquad \delta = (M)_{mod\,2} = (N-S)_{mod\,2} \in \{0,1\}. \tag{3.2}$$

The number I_j plays the role of a quantum number for the Bethe basic vectors (2.36) and it must be chosen depending on the value of δ. Notice that δ and ω play a similar role, because both produce a shift in the quantum numbers I_j (if ω is absorbed in the definition of I_j): in the first case the shift is exactly π, in the second case it is a real (possibly complex) number. This means that the variable δ can be absorbed in ω but the most convenient choice is to use them both.

Observe that Bethe roots can be obtained as zeros of the equation:

$$1 + (-1)^\delta e^{iZ_N(\vartheta_j)} = 0 \tag{3.3}$$

---

[1] The name counting function will became clear in the next paragraphs, where the counting equation will be obtained.

3.2   Classification of Bethe roots

From Bethe Ansatz it is known that a Bethe state (2.36) is uniquely characterized by the set of quantum numbers $\{I_j\}_{j=1,\dots,M}$, $M \leq N$ that appear in (3.2). Notice that $M \leq N$ means $S \geq 0$. The values of ϑ_j to put in (2.36) can be obtained solving Bethe equations. It is also known that only states with

$$\vartheta_j \neq \vartheta_i, \quad \forall\, j \neq i$$

are necessary to form a basis for the space of states. It is a sort of fermionic character for Bethe states [10].

As usual in many cases, Bethe roots can be either real or in complex conjugate pairs (for large N). In the specific case (2.37), there is another possibility, due to periodicity (2.38): if a complex solution has imaginary part $\Im m\,\vartheta = \frac{\pi}{2}(p+1)$ it appears as a single (in (2.37) it produces the left hand side real, then its complex conjugate is not required). It is called *self-conjugate root*. Remember now that the maximal number of real roots ($M = N$) describes the antiferromagnetic ground state. From the point of view of the counting function, a more precise classification of roots is required:

- *real roots*; they are real solutions of (3.2) that appear in the vector (2.36); their number is M_R;

- *holes*; real solutions of (3.2) that do NOT appear in the vector (2.36); their number is N_H;

- *special roots/holes* (special objects); they are real roots or holes where the derivative $Z_N'(\vartheta_j)$ is negative[2] ; their number is N_S; they must be counted both as "normal" and as "special" objects;

- *close pairs*; complex conjugate solutions with imaginary part in the range $0 < |\Im m\,\vartheta| < \pi\min(1,p)$; their number is M_C;

- *wide roots in pairs*; complex conjugate solutions with imaginary part in the range $\pi\min(1,p) < |\Im m\,\vartheta| < \pi\frac{p+1}{2}$;

- *self-conjugate roots* (wide roots appearing as single); $\Im m\,\vartheta = \pi\frac{p+1}{2}$; their number is M_{SC}.

The total number of wide roots appearing in pairs or single is M_W. The following notation will be used (sometimes) for later convenience, to indicate the position of the solutions: h_j for holes, y_j for special objects, c_j for close roots, w_j for wide roots.

Complex roots with imaginary part larger than the self-conjugates are not required because of the periodicity of Bethe equations. This classification is not at all academic; it will play an important role in the physical interpretation of the final equation. A graphical representation of the various types of solutions is given in figure 3.1. An important remark must be made: from the definition itself of Z_N (3.1) it is obvious that only for states without complex roots the fundamental strip for ϕ (see (B.3)), that is the largest strip around the real axis without singularities, is the fundamental strip for Z_N. In all the other cases the analyticity strip for Z_N is narrower, and depends on the imaginary parts of the complex roots.

An important property follows from this classification: the Z_N function is *real analytic* if ω is a real number

$$Z_N\left(\vartheta^*\right) = \left(Z_N(\vartheta)\right)^* \tag{3.4}$$

---

[2] The characteristics of this type of solutions will be completely clarified in the next sections.
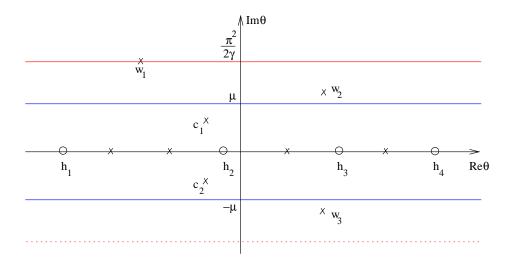
Figure 3.1: The different types of roots and holes and their position in the complex plane. μ denotes $\pi \min\{1, p\}$. The upper line at $\frac{\pi^2}{2\gamma} = \frac{\pi}{2}(p+1)$ is the self-conjugate one.

3.3 Counting equation

It is possible to obtain an equation relating the numbers of all the various types of solutions. The path is simple, and makes use of the asymptotic values obtained in (B.5) to calculate the limits $\vartheta \to \pm\infty$ in Z_N (3.1). Observe that the term $\phi(\vartheta - \vartheta_j, 1)$, in the case of the wide roots, takes contributions from the horizontal strips next to the fundamental, as in figure B.1. This contributions depend from $M_{W\downarrow}$ (number of wide roots below the real axis) and $M_{W\uparrow}$ (number of wide roots over the real axis). The asymptotic limits are then:

$$Z_N(+\infty) = N\pi + \pi\frac{p-1}{p+1}S + 2\pi \operatorname{sign}(p-1) M_{W\downarrow} + 2\omega$$

$$Z_N(-\infty) = -N\pi - \pi\frac{p-1}{p+1}S - 2\pi \operatorname{sign}(p-1) M_{W\uparrow} + 2\omega$$

(3.5)

Observe that the number of self-conjugate roots is: $M_{W\uparrow} - M_{W\downarrow} = M_{SC}$. On the lattice, all the values for N, S are permitted. But in view of the continuum limit, N is expected to be larger than S: $N \gg S$ (also the number of holes and complex roots is expected to be much smaller than N). Then

$$Z_N(+\infty) > Z_N(-\infty).$$

The function is globally increasing (but not necessarily monotonous: in some points it can be a decreasing function). Define now two variables $\zeta_\pm$, choosing $k_\pm$ in such a way that they take value in the indicated interval:

$$\zeta_\pm = \pm Z_N(\pm\infty) + \pi\delta - 2\pi k_\pm, \qquad -\pi < \zeta_\pm \leq \pi$$

Using the previous expressions for Z_N the result is:

$$\zeta_\pm = 2\pi\left(-\frac{S}{p+1} \pm \frac{\omega}{\pi} + \left\lfloor \frac{1}{2} + \frac{S}{p+1} \mp \frac{\omega}{\pi} \right\rfloor\right)$$

where the new symbol $\lfloor x \rfloor$ is the integer part of x, that is the largest integer smaller or equal to x. In this way, the following expression holds:

$$Z_N(+\infty) = 2\pi I_{max} + \pi + \zeta_+$$
$$Z_N(-\infty) = 2\pi I_{min} - \pi - \zeta_- \tag{3.6}$$

where I_{max} is the largest quantum number satisfying $I_{max} < \dfrac{Z_N(+\infty)}{2\pi}$ and I_{min} is the smallest quantum number satisfying $I_{min} > \dfrac{Z_N(-\infty)}{2\pi}$. This very precise definition is required to take into account for the special roots/holes that can appear in the tails (this can happen when $Z_N' < 0$ for very large values of $|\vartheta|$).

The total number of real solutions is the sum of real roots and holes, and in terms of I_{max}, I_{min} it can be written as:

$$M_R + N_H = I_{max} - I_{min} + 1 + 2N_S.$$

Using the equations (2.40, 3.6) and the expression (3.5) the result is:

$$N_H - 2N_S = 2S + M_C + 2\,\theta(p-1)\,M_W +$$

$$- \left\lfloor \frac{1}{2} + \frac{S}{p+1} + \frac{\omega}{\pi} \right\rfloor - \left\lfloor \frac{1}{2} + \frac{S}{p+1} - \frac{\omega}{\pi} \right\rfloor. \tag{3.7}$$

It is the so called *lattice counting equation*. Remember that S is a nonnegative integer. In the case of $\omega = 0$, it turns out that N_H is even (remember that M_C is the number of close roots, and is even).

The most important fact is that in this equation doesn't appear the number of real roots. This fact, together to what will be explained in the next paragraph, allows to consider the real roots as a sea of particles (Dirac vacuum) and all other types of solutions (holes, complex) as excitations on this sea.

3.4   Non linear integral equation (I)

In this section an equation generating Z_N will be obtained. The counting function (3.1) can be written in the following way:

$$Z_N(\vartheta) = N\left[\phi(\vartheta + \Theta, \tfrac{1}{2}) + \phi(\vartheta - \Theta, \tfrac{1}{2}) \right] + \sum_{k=1}^{N_H} \phi(\vartheta - h_k, 1) +$$

$$- \sum_{k=1}^{M_C + M_W} \phi(\vartheta - \xi_k, 1) - \sum_{k=1}^{M_R + N_H} \phi(\vartheta - x_k, 1) \tag{3.8}$$

In this case ξ_k collects close and wide roots, and x_k the real roots and holes. Now, it is convenient to deal with the derivative of this expression:

$$Z_N'(\vartheta) = N\left[\phi'(\vartheta + \Theta, \tfrac{1}{2}) + \phi'(\vartheta - \Theta, \tfrac{1}{2}) \right] + \sum_{k=1}^{N_H} \phi'(\vartheta - h_k, 1) +$$

$$- \sum_{k=1}^{M_C + M_W} \phi'(\vartheta - \xi_k, 1) - \sum_{k=1}^{M_R + N_H} \phi'(\vartheta - x_k, 1) \tag{3.9}$$

Both the previous equations hold for $\vartheta \in \mathbb{C}$. Let $\hat{x}$ be a real solution of the Bethe equation. Assume $Z'_N(\hat{x}) \neq 0$ and define a complex neighbour of $\hat{x}$ by a small $|\nu| \ll 1$: $\mu = \hat{x} + \nu$. Clearly $(-1)^\delta e^{iZ_N(\hat{x})} = -1$. Consider the expression:

$$1 + (-1)^\delta e^{iZ_N(\hat{x}+\nu)} \approx 1 + (-1)^\delta e^{iZ_N(\hat{x})+i\nu Z'_N(\hat{x})} \approx -i\nu Z'_N(\hat{x}) \tag{3.10}$$

then the following identity holds:

$$\frac{1}{\mu - \hat{x}} = \frac{1}{\nu} = \frac{(-1)^\delta e^{iZ_N(\hat{x}+\nu)} i Z'_N(\hat{x}+\nu)}{1 + (-1)^\delta e^{iZ_N(\hat{x}+\nu)}} + ... \tag{3.11}$$

(the dots are regular terms in $\mu - \hat{x}$). From the Cauchy theorem and from (3.11), given an analytic function $f(x)$ on an appropriate strip containing the real axis, yields:

$$f(\hat{x}) = \oint_{\Gamma_{\hat{x}}} \frac{d\mu}{2\pi i} \frac{f(\mu)}{\mu - \hat{x}} = \oint_{\Gamma_{\hat{x}}} \frac{d\mu}{2\pi i} f(\mu) \frac{(-1)^\delta e^{iZ_N(\mu)} i Z'_N(\mu)}{1 + (-1)^\delta e^{iZ_N(\mu)}} \tag{3.12}$$

where $\Gamma_{\hat{x}}$ is a anti-clockwise curve encircling $\hat{x}$ and avoiding other singularities of the denominator, i.e. other Bethe solutions (real or complex). It is always possible to find such a closed curve, because Bethe solutions are finite in number. An equation like (3.12) can be written for all the real roots of (3.2), x_k, $\forall k$. The derivative $\phi'(\vartheta, 1)$ is an analytic function, if poles are avoided, and applying to that the expression (3.12), the last sum in (3.9) becomes:

$$\sum_{k=1}^{M_R+N_H} \phi'(\vartheta - x_k, 1) = \sum_{k=1}^{M_R+N_H} \oint_{\Gamma_{x_k}} \frac{d\mu}{2\pi i} \phi'(\vartheta - \mu, 1) \frac{(-1)^\delta e^{iZ_N(\mu)} i Z'_N(\mu)}{1 + (-1)^\delta e^{iZ_N(\mu)}} =$$
$$= \oint_{\Gamma} \frac{d\mu}{2\pi i} \phi'(\vartheta - \mu, 1) \frac{(-1)^\delta e^{iZ_N(\mu)} i Z'_N(\mu)}{1 + (-1)^\delta e^{iZ_N(\mu)}} \tag{3.13}$$

The sum on the contours was modified to a unique curve Γ encircling all the real solutions x_k, and avoiding the complex Bethe solutions (this is possible because they are finite in number), as in the figure 3.2.
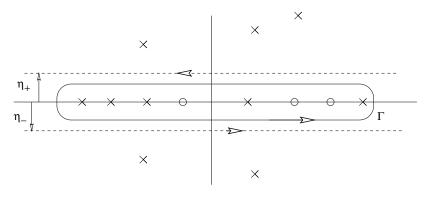

Figure 3.2: Contours for the integration. The crosses are roots while the circles are holes.

Clearly the Γ curve must be contained in the strip

$$0 < \eta_+, \eta_- < \min\{\pi, \pi p, |\Im m\, c_k| \,\forall\, k\}$$

Without loss of generality, assume that $\eta_+ = \eta_- = \eta$, and deform Γ to the contour of the strip characterized by η. The regions at $\pm\infty$ do no contribute because of the vanishing of ϕ', then the integral can be performed only on the lines $\mu = x \pm i\eta$, where x is real[3]:

$$
\oint_\Gamma \frac{d\mu}{2\pi i} \phi'(\vartheta - \mu, 1) \frac{(-1)^\delta e^{iZ_N(\mu)} i Z'_N(\mu)}{1 + (-1)^\delta e^{iZ_N(\mu)}} =
$$

$$
= \int \frac{dx}{2\pi i} \phi'(\vartheta - x + i\eta, 1) \frac{(-1)^\delta e^{iZ_N(x-i\eta)} i Z'_N(x - i\eta)}{1 + (-1)^\delta e^{iZ_N(x-i\eta)}} + \tag{3.14}
$$

$$
- \int \frac{dx}{2\pi i} \phi'(\vartheta - x - i\eta, 1) \frac{(-1)^\delta e^{iZ_N(x+i\eta)} i Z'_N(x + i\eta)}{1 + (-1)^\delta e^{iZ_N(x+i\eta)}}
$$

The first term at the right can be written as:

$$
\frac{(-1)^\delta e^{iZ_N(x-i\eta)} i Z'_N(x - i\eta)}{1 + (-1)^\delta e^{iZ_N(x-i\eta)}} =
$$
$$
\frac{-(-1)^\delta e^{-iZ_N(x-i\eta)} i Z'_N(x - i\eta)}{1 + (-1)^\delta e^{-iZ_N(x-i\eta)}} + i Z'_N(x - i\eta) \tag{3.15}
$$

Putting this in (3.15) the integral contribution from $Z'_N(x - i\eta)$ is independent from η because no singularities are crossed if $\eta \to 0$ and at the infinity the integrand is zero. The following convenient redefinition can be introduced (see (B.4)):

$$
K(x) \equiv \frac{\phi'(x, 1)}{2\pi} = \frac{1}{\pi(p + 1)} \frac{\sin \dfrac{2\pi}{p + 1}}{\cosh \dfrac{2\vartheta}{p + 1} - \cos \dfrac{2\pi}{p + 1}} \tag{3.16}
$$

In general, for every complex value of ϑ:

$$
\int dx \left[\delta(x) Z'_N(\vartheta - x) + K(\vartheta - x) Z'_N(x) \right] = N \left[\phi'\left(\vartheta + \Theta, \frac{1}{2}\right) + \phi'\left(\vartheta - \Theta, \frac{1}{2}\right) \right] +
$$
$$
+ \sum_{k=1}^{N_H} \phi'(\vartheta - h_k, 1) - \sum_{k=1}^{M_C + M_W} \phi'(\vartheta - \xi_k, 1) +
$$
$$
- \int \frac{dx}{2\pi i} \phi'(\vartheta - x + i\eta, 1) \frac{-(-1)^\delta e^{-iZ_N(x-i\eta)} i Z'_N(x - i\eta)}{1 + (-1)^\delta e^{-iZ_N(x-i\eta)}} + \tag{3.17}
$$
$$
+ \int \frac{dx}{2\pi i} \phi'(\vartheta - x - i\eta, 1) \frac{(-1)^\delta e^{iZ_N(x+i\eta)} i Z'_N(x + i\eta)}{1 + (-1)^\delta e^{iZ_N(x+i\eta)}}
$$

The second term on the left takes the form

$$
\int dx\, K(\vartheta - x, 1)\, Z'_N(x) = \int dx\, K(x, 1)\, Z'_N(\vartheta - x);
$$

that can be obtained by shifting the integration line: $x \to x + \Im m\, \vartheta$. But if poles are crossed (this can happen if the imaginary part is sufficiently large), their contribution must appear in the right hand side of the equation.

---

[3] $\int = \int_{-\infty}^{+\infty}$ In all the cases where the limits of integration are not explicitly specified, the integral is taken on the whole real axis.

Using Fourier transformations, the convolution in the left hand side of (3.17) can be simply handled. Observe first that the Fourier transform of $[\delta(\vartheta - x) + K(\vartheta - x)]$ is simply $1 + \tilde{K}$. In the appendix B the form of $\tilde{K}$ is given (as $\tilde{\phi}'$ in (B.6)). It is obvious that $1 + \tilde{K}$ is nonvanishing, so it can be reversed. Call $\tilde{\Delta}$ the inverse:

$$\tilde{\Delta}(k) \equiv \frac{1}{1 + \tilde{K}(k)}.$$

The inverse Fourier transform of $\tilde{\Delta}$, indicated as $\Delta(x)$, is a distribution, because $\tilde{\Delta}(k) \to 1$ for $k \to \pm\infty$. The following obvious equation holds:

$$\int dx \, \Delta(x) \, (\delta(\theta - x) + K(\vartheta - x)) = \delta(\theta)$$

and this allows to invert the convolution in (3.17). Calling globally $\mathcal{F}(\vartheta)$ the right hand side of (3.17) the inversion is:

$$Z'_N(\vartheta) = \int dx \, \Delta(\vartheta - x) \, \mathcal{F}(x). \tag{3.18}$$

The various terms in $\mathcal{F}$ give different contributions, that shall be computed in the following.

For the two terms $\phi'(\vartheta \pm \Theta, \frac{1}{2})$ the convolution can be completely performed using (A.3):

$$\int dx \, \Delta(\vartheta - x) \, \phi'(x \pm \Theta, \frac{1}{2}) = \frac{1}{\cosh(\vartheta \pm \Theta)}. \tag{3.19}$$

The effect of the inversion on $\phi'(\vartheta, 1)$ gives an important object, that will be called G :

$$\int dx \, \Delta(\vartheta - x) \frac{\phi'(x, 1)}{2\pi} = \int dx \, \Delta(\vartheta - x) \, K(x) \equiv G(\vartheta) \tag{3.20}$$

Using Fourier transforms (see A.3) for Δ and ϕ' (B.6) the following expression can be obtained:

$$
\begin{aligned}
G(\theta) &= \frac{1}{p+1} \int \frac{dk}{2\pi} e^{ik\theta} \frac{1}{p+1} \tilde{K}(k) \frac{1}{1 + \tilde{K}(k)} = \\
&= \frac{1}{2\pi} \int dk \, e^{ik\theta} \frac{\sinh \frac{\pi(p-1)k}{2}}{2 \sinh \frac{\pi p k}{2} \cosh \frac{\pi k}{2}}.
\end{aligned}
\tag{3.21}
$$

The expression (B.6) used in the previous computation for the Fourier transform of ϕ' holds only for θ in the fundamental strip (B.3), i.e. for real solutions or close pairs, as in section 3.2. This means that contributions to Z'_N coming from wide roots require a different approach (see later). Instead the terms containing holes and close roots are completely arranged in this way.

The Fourier transform of (3.21) is obviously

$$\tilde{G}(k) = \frac{\tilde{K}(k)}{1 + \tilde{K}(k)}.$$

This is an even function, real on the real axis (*real analyticity*), positive if $p > 1$ and negative in the opposite case. The same properties, clearly, hold for $G(\theta)$. The function $\tilde{G}$ vanishes exponentially for large values of $|k|$:

$$\tilde{G} \sim e^{-\frac{\pi \, \min(1,p)}{p+1} |k|}.$$

(consequently also the function $G(\theta)$ has a similar asymptotic behaviour). Because of this, the Fourier transform in (3.21) at the points

$$|\Im m\,\theta| = \pm\pi\,\min(1,p)$$

has a singularity. As before, this points correspond exactly to the limit between close roots and wide roots. This confirms exactly that wide roots require a different analysis. Call *source* the contribution to (3.18) by one wide root put in w:

$$source = \int dx\,\Delta(x)\,\phi'(\vartheta - x - w, 1) =$$

$$= \frac{1}{p+1}\int dx\int \frac{dk}{2\pi}e^{ikx}\frac{1}{p+1}\tilde{\Delta}(k)\,\phi'(\vartheta - x - w, 1).$$

Using the known expression (B.4) for ϕ' the computation can be performed into a closed form. The integral in x must be performed first. It is a Fourier transform, but because of the w contribution, it is different from the Fourier transform of ϕ' calculated in (B.6), that holds for ϑ near the real axis. This is because $\Im m\,w$ is larger than the position of the first singularity of ϕ', and the poles to take into account in the two cases are different. The result can be written in the following form:

$$source = 2\pi G_{II}(\vartheta - w) \tag{3.22}$$

where the function G_{II} is defined by (for $|\Im m\theta| > \pi\min(1,p)$):

$$2\pi G_{II}(\theta) = \begin{cases} \dfrac{i}{p}\left[\coth\dfrac{\theta}{p}\,\text{sign}\Im m(\theta) + \coth\dfrac{(i\pi - \theta\,\text{sign}\Im m(\theta))}{p}\right] & \text{if } p > 1 \\[4ex] \text{sign}\Im m(\theta)\,i\left[\dfrac{1}{\sinh\theta} + \dfrac{1}{\sinh(\theta - i\pi p\,\text{sign}\Im m(\theta))}\right] & \text{if } p < 1 \end{cases} \tag{3.23}$$

A quite singular property, pointed out in [8], is that this function can be interpreted as the so called *second determination* of the previous function G. The general definition of the second determination is:

$$f_{II}(\theta) = \begin{cases} f(\theta) + f(\theta - i\pi\,\text{sign}\Im m(\theta)) & \text{if } p > 1 \\[2ex] f(\theta) - f(\theta - i\pi p\,\text{sign}\Im m(\theta)) & \text{if } p < 1 \end{cases} \quad \text{for } |\Im m\theta| > \pi\min(1,p) \tag{3.24}$$

Applied to (3.21), it yields exactly (3.22).

Taking into account (3.19, 3.20, 3.22) in (3.18), the equation (3.17) takes the form of an integro-differential equation for Z'_N:

$$Z'_N(\vartheta) = N\left[\frac{1}{\cosh(\vartheta + \Theta)} + \frac{1}{\cosh(\vartheta - \Theta)}\right] + \sum_{k=1}^{N_H} 2\pi G(\vartheta - h_k) +$$

$$- \sum_{k=1}^{M_C} 2\pi G(\vartheta - c_k) - \sum_{k=1}^{M_W} 2\pi G_{II}(\vartheta - w_k) +$$

$$+ \frac{1}{i}\int dx\,G(\vartheta - x - i\eta)\frac{(-1)^\delta e^{iZ_N(x+i\eta)}iZ'_N(x+i\eta)}{1 + (-1)^\delta e^{iZ_N(x+i\eta)}} +$$

$$- \frac{1}{i}\int dx\,G(\vartheta - x + i\eta)\frac{-(-1)^\delta e^{-iZ_N(x-i\eta)}iZ'_N(x-i\eta)}{1 + (-1)^\delta e^{-iZ_N(x-i\eta)}} \tag{3.25}$$

This equation holds for both the cases of ω real or complex. The most common case is $\omega \in \mathbb{R}$. This allows to write the last two lines in a more compact form, valid only if ϑ is on the real axis. The real analyticity of Z_N and of G is used:

$$2\Im m \int dx G(\vartheta - x - i\eta) \frac{(-1)^\delta e^{iZ_N(x+i\eta)} i Z'_N(x+i\eta)}{1 + (-1)^\delta e^{iZ_N(x+i\eta)}} \qquad \text{if } \vartheta \in \mathbb{R}.$$

Observe that the second factor in the integral terms seems to be the derivative of $\log\left[1 + (-1)^\delta e^{\pm iZ_N(x\pm i\eta)}\right]$, but this substitution requires some care, because of the polydromy of the logarithmic function. Call, for the sake of simplicity, the argument of the log:

$$f(x) = 1 + (-1)^\delta e^{iZ_N(x+i\eta)} \tag{3.26}$$

and use the fundamental branch as in the appendix B. If $f(x)$ cross the cut of the log on the negative real axis, the function $\log_{FD} f(x)$ has a jump by $\pm 2\pi i$. The exact real point $y_\uparrow$ where this happens (suppose for simplicity only one such point; the extension is trivial) is given (see the figure 3.3)by the condition $f(y_\uparrow) \in \,]-\infty, 0[$, that is:

(a)   (b)
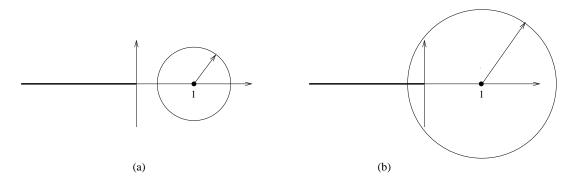
Figure 3.3: Plane of the log. The circles have radius $\left|e^{iZ_N(x+i\eta)}\right|$. In (a) it is < 1, in (b) it is > 1.

$$1 + (-1)^\delta e^{i\,\Re e\,Z_N(y_\uparrow + i\eta)} = 0 \qquad \text{and} \qquad \Im m Z_N(y_\uparrow + i\eta) < 0. \tag{3.27}$$

Only the expression

$$\log_{FD} f(x) - 2\pi i \theta(x - y_\uparrow)\epsilon$$

gives rise to a continuous function. $\epsilon = \pm 1$ is a sign that is positive if the cross is in the clockwise direction (from below to up) as in figure 3.4 and negative in the opposite case. An important observation can be made by the following Taylor expansion:

$$\Re e\, Z_N(y_\uparrow + i\eta) = Z_N(y_\uparrow) - \frac{\eta^2}{2} Z''_N(y_\uparrow) + \dots \tag{3.28}$$

$$\Im m\, Z_N(y_\uparrow + i\eta) = \eta \left(Z'_N(y_\uparrow) - \frac{\eta^2}{6} Z'''_N(y_\uparrow) + \dots \right). \tag{3.29}$$

It is clear that if and only if $\eta \to 0$ the condition (3.27) becomes the definition of a special solution, i.e. $y_\uparrow$ is a special object only in the limit of η going to zero because in this case the second terms in (3.28, 3.29) are negligible. Then the condition (3.27) becomes $Z'_N(y_\uparrow) < 0$ and

$Z_N = 2\pi I$. The sign must be chosen positive: $\epsilon = 1$.[4] For the general case $\eta \neq 0$, $y_\uparrow$ is a special object y shifted by a little bit.

A completely analogous analysis can be performed for the lower integral, obtaining a $y_\downarrow$. From (3.28), because of the real analyticity of Z_N, the following equation holds: $y_\uparrow = y_\downarrow \equiv \hat{y}$. The result is:

$$\frac{(-1)^\delta e^{\pm i Z_N(x \pm i\eta)}(\pm i) Z_N'(x \pm i\eta)}{1 + (-1)^\delta e^{\pm i Z_N(x \pm i\eta)}} = \frac{d}{dx} \log_{FD} \left(1 + (-1)^\delta e^{\pm i Z_N(x \pm i\eta)} \right) \mp 2\pi i \delta(x - \hat{y}). \quad (3.30)$$

Using this expression in (3.25), a new source term appears every times there is a such point $\hat{y}$:

$$Z_N'(\vartheta) = N \left[\frac{1}{\cosh(\vartheta + \Theta)} + \frac{1}{\cosh(\vartheta - \Theta)} \right] + \sum_{k=1}^{N_H} 2\pi G(\vartheta - h_k) +$$

$$- \sum_{k=1}^{M_C} 2\pi G(\vartheta - c_k) - \sum_{k=1}^{M_W} 2\pi G_{II}(\vartheta - w_k) - 2\pi \sum_{k=1}^{N_S} \left(G(\vartheta - \hat{y}_k + i\eta) + G(\vartheta - \hat{y}_k - i\eta) \right)$$

$$+ \frac{1}{i} \int dx \, G(\vartheta - x - i\eta) \frac{d}{dx} \log_{FD} \left[1 + (-1)^\delta e^{i Z_N(x + i\eta)} \right] +$$

$$- \frac{1}{i} \int dx \, G(\vartheta - x + i\eta) \frac{d}{dx} \log_{FD} \left[1 + (-1)^\delta e^{-i Z_N(x - i\eta)} \right]. \quad (3.31)$$

The sum on $\hat{y}_k$ has been indicated as sum on the specials, even if they are not exactly in the position of specials, because in the usual computations made on the NLIE η takes a small value. The condition to be used for the correct position is (3.27). In the following, we omit the label
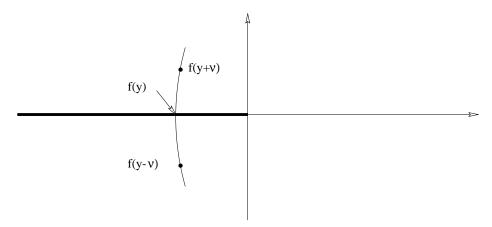
Figure 3.4: Jump in the log: $\log f(\hat{y} + \nu) - \log f(\hat{y} - \nu) = 2\pi i$

FD, intending always the log in the fundamental branch. It is very important to note that special objects are not completely independent degrees of freedom, unlike the holes and complex solutions, that are fixed "a priori". Special objects appear when the derivative of Z_N on a root or on a hole becomes negative. A special object then apparently appears two times in (3.31), both as a real root/hole and as a special root/hole.

3.5   Non linear integral equation (II)

From a Bethe Ansatz point of view, only the function Z_N (and not the derivative) has a physical meaning, because it is required to obtain the position of various types of solution, given the

---
[4] In what follows, always this case will be assumed.

quantum numbers (3.2). To obtain Z_N, an integration in ϑ must be performed in (3.31). All the source terms must be integrated. For the case of holes, specials and closes this is given by the function:

$$\chi(\theta) = \int_0^\theta dx\, 2\pi G(x) \tag{3.32}$$

It is and odd and real analytic function. It asymptotic value is known by direct integration:

$$\chi_\infty = \chi(+\infty) = \frac{\pi}{2}\frac{p-1}{p} \tag{3.33}$$

Because G has always the same sign for every x, the $\chi(\theta)$ is a monotonous function.

The integration of the source for wide roots is simply the integral of (3.23). But this integration produces logarithms, then there is a problem of definition of the appropriate branch. The Z_N function is continuous in the analyticity strip, then the most correct choice for the wide sources satisfies this continuity. The forms that are proposed in the following do so (they have no jumps) for θ with imaginary part $\pi\max(1,p) > |\Im m\theta| > \pi\min(1,p)$ (the log is in the fundamental determination):

$$\chi_{II}(\theta) = \begin{cases} i\,\mathrm{sign}(\Im m\theta)\left(\log\sinh\left(\dfrac{\theta}{p}\right) - \log\sinh\left(\dfrac{\theta - i\pi\,\mathrm{sign}\Im m\theta}{p}\right)\right) & \text{if } p > 1 \\[2em] i\,\mathrm{sign}(\Im m\theta)\left(\log\left(-\tanh\dfrac{\theta}{2}\right) + \log\left(\tanh\dfrac{\theta - i\pi p\,\mathrm{sign}\Im m\theta}{2}\right)\right) & \text{if } p < 1 \end{cases} \tag{3.34}$$

The notation χ_{II} is used to indicate the integral of the G_{II}. As in the previous case of G, this is the same as taking the second determination of χ in (3.32). The two forms corresponding to the opposite signs of the variable are related by the oddity:

$$\chi_{II}(-\theta) = \chi_{II}(\theta) \qquad \text{if } |\Im m\theta| > \pi\min(1,p).$$

This function can be continued to smallest values of the imaginary part, but obviously it has a line of discontinuity. The asymptotic limits are (now ϑ is real):

$$\lim_{\vartheta\to\pm\infty}\chi_{II}(\vartheta - w) = \begin{cases} \pm(2\chi_\infty - \pi) & \text{if } p > 1 \\[1em] \pm\pi & \text{if } p < 1 \end{cases} \tag{3.35}$$

The final form obtained in this way is the so called *fundamental non linear integral equation,* also known as *Destri-de Vega equation* (see [8]) for the counting function:

$$Z_N(\vartheta) = 2N\arctan\frac{\sinh\vartheta}{\cosh\Theta} + g(\vartheta|\vartheta_j) +$$

$$+ \int \frac{dx}{i}G(\vartheta - x - i\eta)\log\left(1 + (-1)^\delta e^{iZ_N(x+i\eta)}\right) + \tag{3.36}$$

$$- \int \frac{dx}{i}G(\vartheta - x + i\eta)\log\left(1 + (-1)^\delta e^{-iZ_N(x-i\eta)}\right) + \alpha$$

where

$$g(\vartheta|\vartheta_k) = \sum_{k=1}^{N_H} \chi(\vartheta - h_k) - \sum_{k=1}^{N_S} \left(\chi(\vartheta - \hat{y}_k + i\eta) + \chi(\vartheta - \hat{y}_k - i\eta) \right) +$$

$$- \sum_{k=1}^{M_C} \chi(\vartheta - c_k) - \sum_{k=1}^{M_W} \chi_{II}(\vartheta - w_k)$$

(3.37)

Both the previous equations hold for ϑ in the fundamental strip. Out of that, the analytic continuation of Z_N is required, because the first singularity of G is crossed. To obtain an equation expressing the analytic continuation of Z_N beyond this singularity, the second determination of the various terms appearing in the right hand side of (3.36) must be taken, as defined in (3.24). Notice that it is not the second determination of Z_N but its analytic continuation:

$$\text{for } |\Im m\, \vartheta| > \min(1,\, p): \qquad Z_N(\vartheta) = 2N \left[\arctan \frac{\sinh \vartheta}{\cosh \Theta} \right]_{II} +$$

$$+ g(\vartheta|\vartheta_k)_{II} + \int \frac{dx}{i} G(\vartheta - x - i\eta)_{II} \log \left(1 + (-1)^\delta e^{iZ_N(x+i\eta)} \right) +$$

(3.38)

$$- \int \frac{dx}{i} G(\vartheta - x + i\eta)_{II} \log \left(1 + (-1)^\delta e^{-iZ_N(x-i\eta)} \right) + \alpha_{II}$$

This explicit form of the analytic continuation requires to compute $g(\vartheta|\vartheta_k)_{II}$. Remembering (3.37), it is clear that for holes, specials and close roots the second determination of $\chi(\vartheta - \vartheta_j)$ (see (3.34)) appears. For the wide roots the second determination of $\chi_{II}(\vartheta - w_j)$ appears. It must be determined considering that

$$\chi_W(\vartheta, w_j) \equiv \chi_{II}(\vartheta - w_j)$$

is a function of ϑ:

$$\chi_{II}(\vartheta - w_j)_{II} \equiv (\chi_W(\vartheta, w_j))_{II}.$$

(3.39)

The explicit forms are not given there but they can be simply computed from the definition of second determination.

The integral of the convolution term is possible because G vanishes exponentially at infinity. α is the integration constant and must be determined.

There is a useful way to write the log term in (3.36), valid for real x and if $\eta \to 0$:

$$\mathcal{Q}_N(x) \equiv \lim_{\eta \to 0} 2\Im m \, \log \left(1 + (-1)^\delta e^{iZ_N(x+i\eta)} \right) =$$

$$= \lim_{\eta \to 0} \frac{1}{i} \log \frac{1 + (-1)^\delta e^{iZ_N(x+i\eta)}}{1 + (-1)^\delta e^{-iZ_N(x-i\eta)}} = (Z_N(x) + \pi\delta) \mod 2\pi$$

(3.40)

The expression $(A) \mod 2\pi$ means exactly $-\pi < A \leq \pi$. The second line in (3.40) holds only if $Z_N'(x) > 0$, because the branch cut of the log is not crossed and $|\Im m \log f(x)| < \pi$ (the notation (3.26) is used). In the opposite case the branch cut is crossed and the previous expression can take values larger than π: $|\Im m \log f(x)| < 2\pi$. In the limit case $Z_N'(x) = 0$ (for example this happens when $x \to \infty$) the values permitted are $-\pi \leq \Im m \log f(x) \leq \pi$.

At this point it is possible to explicitly calculate, from (3.36), the limit $Z_N(+\infty)$, using (3.36, 3.7, 3.33, 3.35). The limit gives:

$$Z_N(+\infty) = N\pi + \chi_\infty \left(N_H - 2N_S - M_C - 2\theta(p-1)M_W \right) +$$

$$+\pi \operatorname{sign}(p-1)\, M_W + \int dx\, G(x)\, \mathcal{Q}_N(+\infty) + \alpha. \tag{3.41}$$

The limit $\mathcal{Q}_N(+\infty)$ can be calculated by using in (3.40) the limit of Z_N (3.5). By a comparison of the (3.41) with the asymptotic values of Z_N calculated in (3.5) the value of α can be obtained:

$$\alpha = \omega \frac{p+1}{p} + \chi_\infty \left(\left\lfloor \frac{1}{2} + \frac{S}{p+1} + \frac{\omega}{\pi} \right\rfloor - \left\lfloor \frac{1}{2} + \frac{S}{p+1} - \frac{\omega}{\pi} \right\rfloor \right) \tag{3.42}$$

In this expression the following term has been omitted: $-\pi \operatorname{sign}(p-1)\, M_{SC}$. It is a multiple of π and can be taken into account simply changing the value of δ from 0 to 1 (or viceversa) if M_{SC} is odd, and shifting of an integer quantity the quantum numbers

$$\delta = (M + M_{SC})_{mod\,2} = (N - S + M_{SC})_{mod\,2} \in \{0,1\}. \tag{3.43}$$

This sort of manipulation on the quantum numbers has been explained at the end of the section 3.1.

Observe that the result is exactly $\alpha = 0$ if there is no twist. There is another important observation. In (2.37) the twist term ω is invariant for the shift

$$\omega \to \omega + \pi.$$

The same sort of invariance is required in α for the NLIE (which is equivalent to Bethe equations). It is simple to verify that the expression for α (3.42) displays the following symmetry

$$\alpha \to \alpha + 2\pi \quad \text{when} \quad \omega \to \omega + \pi.$$

Note that shifting α by 2π is an invariance of the NLIE (3.36), if an appropriate redefinition of the Bethe quantum numbers is made: $I_j \to I_j + 1$. This shift does not affects physical quantities, that depend only on the variables ϑ_j.

With the given value of the integration constant the equation (3.36) is complete. The quantization condition (3.2) can now be written as:

$$Z_N(\vartheta_j) = 2\pi I_j, \qquad I_j \in \mathbb{Z} + \frac{1+\delta}{2} \tag{3.44}$$

for the various solutions. For the wide roots remember the previous warning about the analytic continuation of the Z_N function.

The previous equation is completely equivalent to Bethe equations. No new physics has been introduced, until this point. Simply an equation that generates the counting function Z_N has been obtained (the NLIE).

3.6   Energy and momentum

The expression (2.41) can be written using the function ϕ as:

$$E = \frac{1}{a} \sum_{j=1}^{M} \left(\phi(\Theta - \vartheta_j, 1/2) + \phi(\Theta + \vartheta_j, 1/2) - 2\pi \right)$$

$$\tag{3.45}$$

$$P = \frac{1}{a} \sum_{j=1}^{M} \left(\phi(\Theta - \vartheta_j, 1/2) - \phi(\Theta + \vartheta_j, 1/2) \right) + 2\omega$$

The choice of the logarithmic branch in the energy ensures that the contribution of each real root is negative definite. This is consistent with the known ground state structure (as in section 2.5), that is given by the maximal number of real roots. It will be clear that excitations give only positive contributions.

It is possible to relate the previous expressions to the counting function. To do that, consider first the following quantity:

$$W(\theta) = \sum_{j=1}^{M} \phi'(\theta - \vartheta_j, 1/2) \qquad \theta \in \mathbb{R}. \tag{3.46}$$

It can be integrated to obtain the pieces appearing in (3.45). Clearly the following expressions hold:

$$\sum_{j=1}^{M} \phi(\Theta - \vartheta_j, 1/2) = \int_{asymp}^{\Theta} dx\, W(x)$$

$$\sum_{j=1}^{M} \phi(\Theta + \vartheta_j, 1/2) = -\sum_{j=1}^{M} \phi(-\Theta - \vartheta_j, 1/2) = -\int_{asymp}^{-\Theta} dx\, W(x). \tag{3.47}$$

The integration requires to fix a constant. This can be simply done by computing for $\Theta \to +\infty$ the left hand side in (3.47) and imposing the equality with the primitive of W at the same limit. This has been indicated by the symbol

$$\int_{asymp}^{\pm\Theta}$$

The function W admits an expression in terms of the counting function. The sum over roots in (3.46) can be expressed as in (3.8) and using the same notations:

$$W(\theta) = \sum_{j=1}^{M_R+N_H} \phi'(\theta - x_j, 1/2) - \sum_{j=1}^{N_H} \phi'(\theta - h_j, 1/2) + \sum_{j=1}^{M_C+M_W} \phi'(\theta - \xi_j, 1/2).$$

Using now the same trick used for Z'_N, as in (3.13, 3.14, 3.15), and the expression (3.30) generating the "special" contribution, the following expression yields:

$$W(\vartheta) = \int \frac{dx}{2\pi i} \phi'(\vartheta - x + i\eta, 1/2) \frac{d}{dx} \log_{FD}\left[1 + (-1)^\delta e^{-iZ_N(x-i\eta)}\right] +$$
$$-\int \frac{dx}{2\pi i} \phi'(\vartheta - x - i\eta, 1/2) \frac{d}{dx} \log_{FD}\left[1 + (-1)^\delta e^{iZ_N(x+i\eta)}\right] +$$
$$-\sum_{k=1}^{N_H} \phi'(\vartheta - h_k, 1/2) + \sum_{k=1}^{M_C} \phi'(\vartheta - c_k, 1/2) + \sum_{k=1}^{M_W} \phi'(\vartheta - w_k, 1/2) +$$
$$+\sum_{k=1}^{N_S} \left(\phi'(\vartheta - \hat{y}_k + i\eta, 1/2) + \phi'(\vartheta - \hat{y}_k - i\eta, 1/2)\right) + \int \frac{dx}{2\pi} \phi'(\vartheta - x, 1/2)\, Z'_N(x). \tag{3.48}$$

Now the equation (3.31) can be put in the last integral in the previous expression. The terms "similar" can be collected (i.e. holes with holes, close roots with close roots, and so on) to obtain

the following form:

$$
W(\vartheta) = -\sum_{k=1}^{N_H} \left[\phi'(\vartheta - h_k, 1/2) - \int dx\, \phi'(\vartheta - x, 1/2)\, G(x - h_k) \right] +
$$
$$
+ \sum_{k=1}^{M_C} \left[\phi'(\vartheta - c_k, 1/2) - \int dx\, \phi'(\vartheta - x, 1/2)\, G(x - c_k) \right] +
$$
$$
+ \sum_{k=1}^{M_W} \left[\phi'(\vartheta - w_k, 1/2) - \int dx\, \phi'(\vartheta - x, 1/2)\, G_{II}(x - w_k) \right] +
$$
$$
+ \sum_{k=1}^{N_S} \left[\phi'(\vartheta - \hat{y}_k + i\eta, 1/2) + \phi'(\vartheta - \hat{y}_k - i\eta, 1/2) + \right.
$$
$$
\left. - \int dx\, \phi'(\vartheta - x, 1/2)\, (G(x - \hat{y}_k + i\eta) + G(x - \hat{y}_k - i\eta)) \right] +
$$
$$
+ \int \frac{dx}{2}\phi'(\vartheta - x, 1/2) N \left[\frac{1}{\cosh(\vartheta + \Theta)} + \frac{1}{\cosh(\vartheta - \Theta)} \right] +
$$
$$
-2\Im m \int \frac{dx}{2\pi}\phi'(\vartheta - x - i\eta, 1/2) \int dy\, [\delta(x - y) - G(x - y)] \frac{d}{dy} \log_{FD} \left[1 + (-1)^\delta e^{iZ_N(y + i\eta)} \right] =
$$
$$
= W_H + W_C + W_W + W_S + W_{bulk} + W_I
$$

where the notation introduced on the last line is obvious (the meaning of bulk will be clear in the following; label I is for interaction term or, that is the same, for integral).

As in section 3.4, there are different terms to analyze.

First, rearranging a little bit the terms and introducing a delta-function, it is possible to see that in the case of holes, closes, specials and in the integral term there is a contribution by:

$$
\delta(x - y) - G(x - y) = \Delta(x - y)
$$

(this equality is a simple consequence of the definition of Δ). The corresponding terms contain the integral:

$$
\int dx\, \phi'(x - \vartheta_j, 1/2)\, \Delta(\vartheta - x) = \frac{1}{\cosh(\vartheta - \vartheta_j)}
$$

that is well known because it has been used in (3.19). This holds in the case of holes and closes and ϑ_j is the corresponding rapidity. For the integral term and the specials the contribution is exactly:

$$
\frac{1}{\cosh(\vartheta - y - i\eta)}.
$$

where y is the integration variable or the special rapidity.

The wide computation is more involved. The expression to be computed is

$$
W_W(\vartheta) = \sum_{k=1}^{M_W} \left[\phi'(\vartheta - w_k, 1/2) - \int dx\, \phi'(\vartheta - x, 1/2)\, G_{II}(x - w_k) \right]
$$

and the most convenient way to do that is to use the Fourier transformation of all the terms. For $\phi'(\vartheta - w_k, 1/2)$ and G_{II} it has been used in the computation for (3.23). For ϕ' on the real axis it is in (B.6). The result is

$$
W_W(\vartheta) = \begin{cases} 0 & \text{for } p > 1 \\ \left[\dfrac{1}{\cosh(\vartheta)} \right]_{II} + O(\vartheta) & \text{for } p < 1 \end{cases}
$$

In the case of $p > 1$ it simply cancels out. In the other case, there is no such cancellation, for generic wide positions. The explicit form of the contribution $O(\vartheta)$ is quite long and shall not be written out at this point. The important fact is that it is a fast vanishing contribution for large ϑ. Observe that the second determination (3.24) of a whatever trigonometric hyperbolic function, for $p > 1$, is exactly zero, then the notation $[1/\cosh(\vartheta)]_{II}$ will be used also in this case.

The final form is:

$$
W(\vartheta) = -\sum_{k=1}^{N_H} \frac{1}{\cosh(\vartheta - h_k)} + \sum_{k=1}^{N_S} \left(\frac{1}{\cosh(\vartheta - \hat{y}_k - i\eta)} + \frac{1}{\cosh(\vartheta - \hat{y}_k + i\eta)} \right) +
$$
$$
+ \sum_{k=1}^{M_C} \frac{1}{\cosh(\vartheta - c_k)} + \sum_{k=1}^{M_W} \left[\frac{1}{\cosh(\vartheta - w_k)} \right]_{II} + O(\vartheta) +
$$
$$
+ \int \frac{dx}{2\pi} \phi'(\vartheta - x, 1/2) N \left[\frac{1}{\cosh(x + \Theta)} + \frac{1}{\cosh(x - \Theta)} \right] +
$$
$$
-2\Im m \int \frac{dx}{2\pi} \frac{1}{\cosh(\vartheta - x - i\eta)} \frac{d}{dx} \log_{FD} \left[1 + (-1)^\delta e^{iZ_N(x+i\eta)} \right]
$$

Integrating this function, as in (3.47), the energy and momentum of this lattice system can be obtained. In all the terms appears $1/\cosh x$; its primitive is

$$
\int \frac{dx}{\cosh x} = \arctan \sinh x = 2 \arctan \tanh(x/2). \tag{3.49}
$$

The last form is the most convenient, to calculate the continuum limit. Then:

$$
a\frac{E \pm P}{2} = -\sum_{k=1}^{N_H} 2 \arctan \tanh((\Theta \mp h_k)/2) + \sum_{k=1}^{M_C} 2 \arctan \tanh((\Theta \mp c_k)/2) +
$$
$$
+ \sum_{k=1}^{N_S} 2 \left(\arctan \tanh((\Theta \mp \hat{y}_k - i\eta)/2) + \arctan \tanh((\Theta \mp \hat{y}_k + i\eta)/2) \right) +
$$
$$
+ \sum_{k=1}^{M_W} 2 \arctan \tanh((\Theta \mp w_k)/2)_{II} + O(\Theta) \mp \int \frac{dx}{2\pi} \frac{1}{\cosh(\pm\Theta - x)} Q_N(x) + S\pi +
$$
$$
+ \int \frac{dx}{2\pi} \phi(\Theta \mp x, 1/2) N \left[\frac{1}{\cosh(x + \Theta)} + \frac{1}{\cosh(x - \Theta)} \right] \pm \omega - N\pi
\tag{3.50}
$$

The term $O(\Theta)$ vanishes for large Θ.

The function (3.40) has been used, by putting $\eta \to 0$, and observing that x is real.

3.7   Continuum limit

At the conclusion of the previous long computations there is an important observation: in the final expressions for energy and momentum there is no explicit contribution from the real roots. This also happens in the NLIE (3.36). On the lattice it is not a relevant observation, but in this section it shall be shown that it can justify a continuum limit procedure, $N \to \infty$ and $a \to 0$, and a particle interpretation. In the lattice energy expression there is a bulk term (see later) i.e. a term increasing with N and completely independent from the solutions ϑ_j of Bethe equations. This bulk term can be subtracted and the remaining terms (due only to holes and complex roots) can be chosen in such a way that they describe particle excitations.

To do that, in the limit procedure, they must be chosen in finite number (order $O(1)$) and also its "rapidity" ϑ_j must be finite. From (3.2) this means that only real roots can appear in the

asymptotic tails of Z_N. All the other lattice states must be discarded (as usual, lattice theory contains more states than the continuum theory).

A state where holes and complex roots are not considered, is the hamiltonian vacuum. If they are considered, they give positive contribution to the energy, behaving as particle excitations on a vacuum state. Real roots are completely disappeared, in this limit. They can be interpreted (in the limit procedure) as a sort of Dirac sea that is the hamiltonian vacuum on with holes and complex roots built particle excitations.

This is the structure required to have a consistent quantum field theory.

All this interpretation is possible only because of the antiferromagnetic vacuum choice, made in section (2.5).

What will be proved now is that there is a consistent way to do continuum limit in the NLIE and in the expression of the energy.

In [11] it was shown that the correct way to do the continuum limit for this model on the light-cone is to send $N, \Theta \to \infty$ connected in the following way:

$$\Theta \approx \log \frac{4N}{\mathcal{M}L}. \tag{3.51}$$

$L = N\,a$ is the spatial dimension of the lattice (as in section 2.1) and stay fixed in the limit. $\mathcal{M}$ is the renormalized physical mass. As in section 2.5, the light-cone lattice is periodic in space direction. Then its continuum limit yields a compactified space of length L (space-time is a cylinder of circumference L). The lattice 6 vertex model becomes a field theory defined on this cylinder. The interpretation of what field theory is defined by this continuum limit, at the various values of the twist, is the job of the next chapter.

To do the limit, consider first the counting equation. It takes the following form, on the continuum

$$N_H - 2N_S = 2S + M_C + 2\,\theta(p-1)\,M_W \tag{3.52}$$

because the structures in the tails are extremely simplified. The other terms appearing in the lattice counting equation (3.7) in fact came from the configurations where in the tails there are special root/holes or self-conjugate of the so called first class (see the original paper [8]). Such configurations completely disappear in the continuum limit.

The principal interest is to obtain the limit of the energy and momentum eigenvalues (3.50). Clearly, to fix the positions of the roots ϑ_j the limit of (3.44) is required. This can be made using a *continuum counting function* that is defined by:

$$Z(\vartheta) = \lim_{N \to \infty} Z_N(\vartheta). \tag{3.53}$$

This limit computation is made on the sequence of counting functions that are implicitly defined in (3.36) at the various values of N; the (3.51) must be also taken onto account. The interesting fact is that this limit can be done explicitly in all the terms appearing in (3.36), i.e. a *continuum NLIE* can be obtained. To show that, the various terms are analyzed.

The first term and the integral in (3.36) are trivial matter to compute. The source terms for holes, complex solutions and specials don't have any explicit dependence from N. Only the positions that appear in this terms must be determined, obviously, by the continuum NLIE. Then the term $g(\vartheta|\vartheta_j)$ is unchanged. The result is:

$$\begin{aligned}
Z(\vartheta) = \mathcal{M}L \sinh\vartheta + g(\vartheta|\vartheta_j) + \\
+ \int \frac{dx}{i} G(\vartheta - x - i\eta) \log\left(1 + (-1)^\delta e^{iZ(x+i\eta)}\right) + \\
- \int \frac{dx}{i} G(\vartheta - x + i\eta) \log\left(1 + (-1)^\delta e^{-iZ(x-i\eta)}\right) + \alpha
\end{aligned} \tag{3.54}$$

The quantization conditions (3.2, 3.44) can now be written as:

$$Z(\vartheta_j) = 2\pi I_j \,, \qquad I_j \in \mathbb{Z} + \frac{1+\delta}{2} \tag{3.55}$$

for the various solutions. This terminates the limit procedure on NLIE. Observe that on the continuum only the implicit "definition" of Z by (3.54) is available, instead of and explicit expressions as in the case (3.1).

Consider now in the energy expression (3.50) the terms with the form $2/a \arctan \tanh((\Theta - \theta)/2)$. Using the following hyperbolic trigonometric identity

$$\arctan \tanh(x) = \frac{\pi}{4} - \arctan e^{-x}$$

the following asymptotic behaviour can be obtained:

$$\frac{N}{L} 2 \arctan \tanh(\Theta - \theta) \approx \frac{N\pi}{L2} - \frac{1}{2}\mathcal{M} e^{\theta}.$$

Then, collecting in the expression for $(E \pm P)/2$ the contribution of this type, yields (remember that there is a $S\pi$ in (3.50)):

$$\frac{\pi}{2}(2S - N_H + 2N_S + M_C + 2\theta(p-1)M_W) = 0 \tag{3.56}$$

(the (3.52) has been used).

One of the two integral contributions is

$$\lim_{N \to \infty} \mp \frac{N}{L} \int \frac{dx}{2\pi} \frac{1}{\cosh(\pm\Theta - x)} \mathcal{Q}_N(x) =$$
$$= \mp \frac{\mathcal{M}}{2} \int \frac{dx}{2\pi} e^{\pm x} \mathcal{Q}(x).$$

The final result has been obtained by exchanging the limit and the integral.

The other one is the last line in (3.50). It can be handled by shifting the integration variable and observing that one term in the square brackets is odd and gives a vanishing integral:

$$E_{N, bulk}^{\pm} = \frac{N^2}{L} \left[\int \frac{dx}{2\pi} \phi(\Theta \mp x, 1/2) \left[\frac{1}{\cosh(x+\Theta)} + \frac{1}{\cosh(x-\Theta)} \right] - \pi \right] \pm \omega =$$
$$= \frac{N^2}{L} \left[\int \frac{dx}{2\pi} \left[\frac{\phi(x, 1/2)}{\cosh(2\Theta - x)} \right] - \pi \right] \pm \omega \,.$$

This energy contribution is "source independent". It has been labeled by "bulk" because it will be shown that it diverges as N. It is interesting to compute the contribution to E and P, instead of the diverging contribution to $(E \pm P)/2$:

$$E_{N\,bulk} = E_{N, bulk}^{+} + E_{N, bulk}^{-} = \frac{N^2}{L} \left[\int \frac{dx}{\pi} \left[\frac{\phi(x, 1/2)}{\cosh(2\Theta - x)} \right] - 2\pi \right] = -\frac{N^2}{L}(\pi + \gamma)$$

$$P_{N\,bulk} = E_{N\,bulk}^{+} - E_{N\,bulk}^{-} = 2\omega$$

The first integral can be computed observing that ϕ is a constant for very large values of x, and can be put out of the integral sign. The second one contains the difference of two equal contributions and only ω is not deleted.

Collecting all the terms follows:

$$
\begin{aligned}
\frac{E \pm P}{2} = \frac{\mathcal{M}}{2} \Bigg(&\sum_{k=1}^{N_H} e^{\pm h_k} - \sum_{k=1}^{N_S} \left(e^{\pm \hat{y}_k + i\eta} + e^{\pm \hat{y}_k - i\eta} \right) + \\
&- \sum_{k=1}^{M_C} e^{\pm c_k} - \sum_{k=1}^{M_W} e_{II}^{\pm w_k} \mp \int \frac{dx}{2\pi} e^x \mathcal{Q}_N(x) \Bigg) + E_{N\,bulk}^{\pm}
\end{aligned}
\tag{3.57}
$$

or, subtracting all the diverging contributions,

$$
\begin{aligned}
E = \mathcal{M} \Bigg(&\sum_{k=1}^{N_H} \cosh h_k - \sum_{k=1}^{N_S} \left(\cosh(\hat{y}_k + i\eta) + \cosh(\hat{y}_k - i\eta) \right) + \\
&- \sum_{k=1}^{M_C} \cosh c_k - \sum_{k=1}^{M_W} \cosh_{II} w_k - \int \frac{dx}{2\pi} \sinh x \mathcal{Q}(x) \Bigg)
\end{aligned}
\tag{3.58}
$$

and

$$
\begin{aligned}
P = \mathcal{M} \Bigg(&\sum_{k=1}^{N_H} \sinh h_k - \sum_{k=1}^{N_S} \left(\sinh(\hat{y}_k + i\eta) + \sinh(\hat{y}_k - i\eta) \right) + \\
&- \sum_{k=1}^{M_C} \sinh c_k - \sum_{k=1}^{M_W} \sinh_{II} w_k + \int \frac{dx}{2\pi} \cosh x \mathcal{Q}(x) \Bigg)
\end{aligned}
\tag{3.59}
$$

Observe that for $p > 1$ the second determination of hyperbolic functions vanishes. This means that wide roots contribute to the energy only in an implicit way, because they contribute to the position of other objects, by (3.54).

3.8 Physical interpretation

The limit procedure described in the previous section is mathematically consistent, but the question is if from the physical point of view it describes a consistent quantum theory and allows for a meaningful physical interpretation.

Before to propose it, an important remark must be made about the allowed values for S. It is clear from (2.40) that on the lattice only integer and nonnegative values can be taken into account for S. But on the continuum the definition of S is no more related to the Bethe state (that is undefined), instead it is given implicitly by (3.52). Then, *"a priori"*, there are no arguments that fixes its values to be integers. As our group showed in [28], the half-integer choice for S is necessary (and gives completely consistent results) to describe odd numbers of particles.

At this point the following physical interpretation can be proposed. It will be refined to describe the correspondence with particles. Also it will be supported by many arguments that will be clarified in the next chapters.

Physical interpretation:

- the physical vacuum (hamiltonian ground state) corresponds to absence of sources (i.e. holes, complex); all the sources are excitations on this vacuum

- for $\omega = 0$ and at the various values of S this theory describes the sine-Gordon/massive Thirring model on a finite space of size L; $2S$ is the topological charge and can take non-negative integer values.

- for the values

$$\omega = \frac{k\pi}{s}, \qquad k = 1, ..., q' - 1 \tag{3.60}$$

it describes the quantum reduction of sine-Gordon model, i.e. the massive integrable theory obtained perturbing the minimal model $Vir(r, s)$ with the operator $\Phi_{(1,3)}$.

Observe that it has been assumed that only nonnegative values of S are required to describe the whole Hilbert space of the theory. Indeed the theory is assumed charge-conjugation invariant then negative topological charge states have the same energy and momentum as their charge conjugate states. The assumption that all the states can be described by the NLIE is absolutely not trivial, or better still until this moment it is not available a general proof of this fact, but only a number of specific cases supports this conjecture.

All this things are the argument of the next chapters.

Chapter 4

ANALYSIS OF THE CONTINUUM THEORY

4.1 Principal questions

In the next sections, a carefull analysis of the vacuum and of some excited states from NLIE will be performed at the various scales (various L), to completely understand the physical interpretation suggested at the end of the section 3.7. The principal question is what theory is described by equations (3.54, 3.58, 3.59).

As scale parameter, as appears in (3.54), can be chosen equivalently the size L or the *adimensional size* $l = \mathcal{M}L$, where $\mathcal{M}$ plays the role of a mass scale. The limit of very large l can be interpreted both as large size (that reproduces infinite Minkowski space-time) or large mass scale, that is an *infrared point* in a renormalization flow (IR). Finite size effects do not appear, in that limit.

At the opposite limit of small l, important finite size effects are expected; a small value of l can be obtained with a small mass $\mathcal{M}$, then this case is an *ultraviolet point* in a renormalization flow (UV). The complete control on the scaling functions can be obtained analyzing the whole range of values $l > 0$.

4.2 Connection with sine-Gordon/massive Thirring

The section 3.7 ends with a conjecture about the physical meaning of the model described by the continuum NLIE and the corresponding energy and momentum expressions. There are many arguments to support this interpretation. Some of them came from the well known properties of the 6-vertex Bethe Ansatz, other from the analysis of the NLIE itself.

Consider the R matrix in (2.33, 2.35). It has the same entries as the R_{sG} matrix that appears by putting sine-Gordon on a lattice, and obtaining the corresponding Bethe Ansatz equations (lattice Thirring B.A. gives exactly the same). The equality of R matrix and of Bethe Ansatz equations means that there is a common integrable structure in the two systems.

Moreover, the lattice sine-Gordon B.A. can be obtained as the continuum limit $N \to \infty$ (and with $\Theta = \log \dfrac{4N}{\mathcal{M}L}$) of the inhomogeneous 6-vertex Bethe equations (2.37). The Bethe Ansatz techniques, then, strongly suggest the previous interpretation.

The 6-vertex model in its thermodynamics limit is critical, as shown in [3], then there is a conformal field theory describing this critical point. From the eigenvalues of the transfer matrix (obtained by B.A.) it is possible to extract the conformal properties, as shown in [24]. As shown

in [23], for 6-vertex model they reproduce exactly the equation (1.4) for $\omega = 0$ (that is the UV structure of sine-Gordon and massive Thirring) and the minimal models conformal weights for ω chosen as in (3.60).

It has been shown, in [4], that a fermion satisfying massive Thirring equations of motion can be constructed, as described in section (2.4). It describes the scaling behaviour of the inhomogeneous 6-vertex light-cone lattice dynamics. A similar argument can be made on the XXZ chain quantum hamiltonian, whose exponential is the transfer matrix of 6-vertex model. In [10] a (classical) field satisfying sine-Gordon equations is built from this XXZ chain.

There is one more suggestion, that comes from the NLIE itself: the χ function obtained in the derivation of the NLIE (3.32) is well known in literature, because it is exactly the logarithm of the soliton-soliton sine-Gordon S matrix:

$$\chi(\vartheta) = -i \log S_{++}^{++}(\vartheta) \tag{4.1}$$

as in [2].

This arguments are the starting points for the analysis of NLIE itself that will be performed in the next sections. They completely confirm the physical interpretation given in section 3.7.

4.3   Some general facts about the IR limit

This IR analysis is important, because it can connect NLIE with the (minkowskian) scattering theory. The limit $L \to \infty$ is not at all a thermodynamic limit, because the size of the system is scaled, but the number of particles is fixed. Then, the interaction among the physical particles is expected to cease affecting the energy and momentum, because their density is vanishing. Hence, E and P should approach finite limits equal to a free massive spectrum. In fact, for large l, the dominant term in (3.54) is the $l \sinh \vartheta$. Using it as first iteration in the convolution terms of (3.54, 3.58, 3.59), they become small (of order $O\left(e^{-l}\right)$) and can be dropped. The surviving part in NLIE can be seen as a dressed Bethe Ansatz giving constraints on the asymptotic states:

$$Z(\vartheta) = l \sinh \vartheta + g(\vartheta|\vartheta_k) + \alpha \qquad \text{for} \quad l \to \infty. \tag{4.2}$$

Out of the fundamental strip where this equation holds, a similar expression can be written, using the second determination. Assume for the moment $\alpha = 0$. Taking the exponential of the previous equation and imposing the quantization condition yields:

$$e^{il \sinh \vartheta_j} e^{ig(\vartheta_j|\vartheta_k)} = \pm 1$$

that has a structure similar to the usual quantization condition of particles in a box:

$$e^{iLP(\lambda_j)} \prod_{k \neq j} S(\lambda_j - \lambda_k) = \pm 1 \tag{4.3}$$

($+$ is referred to periodic and $-$ to antiperiodic boundary conditions). The equation (4.3) is not a Bethe Ansatz equation[1] , in general, because the λ_k that appear in it are real rapidities of particles, instead of the rapidities of the pseudoparticles (ϑ_j) required to built Bethe states. But in (4.2) can appear complex "rapidities". The correct correspondence between the box quantization (4.3) and the infrared NLIE (4.2) will be carefully analyzed later. The important fact, for the moment, is that the comparison between this two equations allows to read out scattering data from NLIE and this can be compared with the known S-matrix of the models to which the NLIE is referred.

---

[1] It is called Dressed Bethe Ansatz because it contains real particles instead of pseudoparticles appearing in usual B.A.

Another important IR observation is that the derivative of the counting function is a very large positive number and no one special root/hole can takes place

$$Z'(\vartheta) = l \cosh \vartheta + g'(\vartheta|\vartheta_k) \qquad \text{for} \quad l \to \infty.$$

This suggest that special roots/holes are not physical particles. Instead, as it is clearly shown in section 3.4, they are a mathematical artifact of the logarithmic contribution that appears in the convolution term.

The final important observation in IR analysis comes from quantization conditions (3.44)

$$2\pi I_j = l \sinh \vartheta_j + g(\vartheta_j|\vartheta_k) + \alpha$$

The number I_j is real. Distinguishing the real and imaginary part of this equation gives:

$$2\pi I_j = l \sinh \Re e\, \vartheta_j \, \cos \Im m\, \vartheta_j + \Re e\, (g(\vartheta_j|\vartheta_k) + \alpha)$$
$$0 = l \cosh \Re e\, \vartheta_j \, \sin \Im m\, \vartheta_j + \Im m\, (g(\vartheta_j|\vartheta_k) + \alpha)$$

To deal with the first equation, the real part of the ϑ_j for increasing values of the large scale l moves toward the origin as

$$\Re e\, \vartheta_j \propto \frac{1}{l \cos \Im m\, \vartheta_j}.$$

From the second equation, the imaginary part must develops a singularity from $\Im m\, (g(\vartheta_j|\vartheta_k))$ to annihilate the rapidly diverging term $l \sin \Im m\, \vartheta_j$. Because the positions of singularities are known, this simple argument can be used to fix (at the IR) the imaginary part of the sources. Being the real part zero, the source position at IR is completely fixed.

4.4 The intermediate regions

The NLIE (3.54) contains a source term $g(\vartheta|\vartheta_j)$ which is specified by giving the root/hole structure of the given state and depends on the positions of the holes, special roots/holes and complex roots. These positions in turn are fixed by the Bethe quantization conditions (3.55). The NLIE supplemented by the quantization conditions gives a set of coupled nonlinear equations in the function $Z(\vartheta)$ and the variables ϑ_j that can be solved numerically by an iterative procedure. First one chooses a starting position for the sources ϑ_j. Then one iterates the integral equation (using fast Fourier transform to evaluate the convolution) to update the counting function Z. Using this new Z, an improved determination of position of the ϑ_j can be obtained, and is fed back into the integral equation for a new iteration cycle. The process is repeated until the solution is found to a prescribed precision (usually 10^{-6}). As explained in section 4.3, for large l the source term dominates, while the correction coming from the integral term is exponentially small. Therefore it is reasonable to expect that the further one goes to the IR regime the faster the iteration converges which is in fact what happens in the computations. Hence it is preferable to start iterating at the largest desired value of l and decrease the volume gradually, always taking as a starting point at the next value of the volume the solution found at the previous value.

As a preliminar analysis, the general behaviour of the $Z(x)$ function is that of $\sinh x$ for large l. Decreasing the scale, the tangent in the central portion of $Z(x)$ for $x \in \mathbb{R}$ becomes more and more horizontal; instead for large $|x|$ the leading term is always the hyperbolic sine. This central position broadens to a single or double plateau system that extends to all $|x|$'s smaller than $\log(2/l)$, and rapidly disappears for greater values, in favor of the dominant exponential growth.

It can happens, when decreasing l, that special holes appear. But there is the so called *number of effective holes*, that is given by

$$N_{H,eff} = N_H - 2N_S \tag{4.4}$$

that is a constant independent of l. This is a consequence of one simple fact: when a globally increasing function (as Z is) makes a small oscillation as in figure 4.1 there are an odd number of points that intersect the horizontal line corresponding to a certain quantum number. Then to
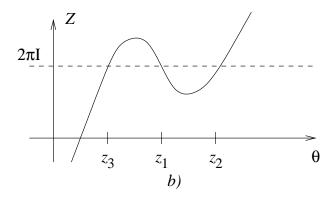
Figure 4.1: The typical behaviour of the Z function when z_1 is a special root/hole

every real solution (when Z is increasing) correspond three (of five or seven or ...) real solutions in the case of specials. Of this odd number of solutions, only one is a real root (no Bethe roots can have the same quantum numbers). All the other must be holes (specials or normal). Then (as in figure 4.1)

1 root for large $l = 1$ root $+ 2$ holes $- 2 \times 1$ special r. or h. for small l.

The general case is (4.4). The physical meaning of the holes, then, must be related to the effective number $N_{H,eff}$, not to N_H.various

For the finite values of the scale, it is interesting to made the comparison of the numerical data from the NLIE predictions with those obtained with the Truncated Conformal Space Approach (TCSA, see section (1.4)) at several values of the parameter p. For illustration, some interesting cases will be presented. For the various values of the coupling constant, our group obtained a spectacular agreement between the results obtained by the two methods, up to deviations of order $10^{-4} - 10^{-3}$(see [9, 27, 28]). The deviation grows with the volume L, exactly as expected for truncation errors. As also told in (1.4), in the attractive regime ($p < 1$) the TCSA convergence is fast. The opposite happens for the NLIE, i.e. it converges faster in the repulsive regime ($p > 1$) and for large volume L, but in general it is possible to have precisions of order 10^{-7} (and higher) in both the regimes.

By studying other parameters such as the mass gap, the breather-soliton mass ratios and the rate of convergence of the energy levels with increasing the value of E_{cut}, the small differences between the two methods can be clearly attributed to the inaccuracy in the TCS data.

4.5   The UV limit computation

The ultraviolet limit of the states described by the NLIE will be examined, in order to compare it with the known facts about the UV limit of sG/mTh theory and conformal minimal models, outlined in sections (1.2, 1.3).

More explicitly, it is known, from conformal perturbation theory, that the behaviour of energy and momentum for very small L are given by:

$$E(L) = -\frac{\pi \tilde{c}(l)}{6L} = -\frac{\pi}{6L} \left(c - 12(\Delta + \bar{\Delta}) \right) + \dots$$
$$P(L) = \frac{2\pi}{L}(\Delta - \bar{\Delta}) + \dots \tag{4.5}$$

where the ellipsis are most regular terms in the space size L. Therefore, to determine the UV behaviour, in E and P only terms containing $\frac{1}{L}$ must be retained. Consider, e.g., the hole contribution to the energy: $\mathcal{M} \cosh h$. In order to have this hole, this term must behaves as $1/L$, that is possible only if

$$h = \text{finite} \pm \log \frac{2}{l}. \tag{4.6}$$

This means that only holes with this rapidity can contribute to UV. The same argument applies to specials and complex solutions.

The behaviour of the sources for $l \to 0$ can be classified by three possibilities: they can remain finite (they are called *central*), or they can move towards the two infinities as $\pm \log \frac{2}{l}$ (*right/left-movers*). The finite parts of their positions can be obtained by extracting the divergent part:

$$\{\vartheta_j(l)\} = \left\{ \vartheta_j^{\pm} \pm \log \frac{2}{l}, \vartheta^0 \right\}. \tag{4.7}$$

(the l dependence of the roots has been made manifest). The number of right/left moving resp. central holes is indicated by $N_H^{\pm,0}$ and similarly the numbers $N_S^{\pm,0}$, $M_C^{\pm,0}$ and $M_W^{\pm,0}$ are introduced. The finite parts in (4.7) satisfy a modified version of the NLIE, known as *kink equation*. To obtain that, observe that Z has an implicit dependence from l that can be made manifest writing $Z(\lambda, l)$. Define the *kink functions* with the following expression:

$$Z_{\pm}(\vartheta) = \lim_{l \to 0} Z \left(\vartheta \pm \log \frac{2}{l}, l \right) \tag{4.8}$$

The term "kink" has its origin in the fact that the asymptotic form of the function $Z(\vartheta)$ has two plateaus stretching between the central region and the regions of the left/right movers. The functions $Z_{\pm}(\vartheta)$ describe the interpolation between the plateaus and the asymptotic behaviour of $Z(\vartheta)$ at the corresponding infinity. Note that if there are no central objects then the two plateaus merge into a single one stretching from the left movers' region to the right movers' one. Using (4.7, 4.8) in the NLIE (3.54), the source terms may behave in different ways. Consider e.g. one hole $h(l)$ of the type h^+. Its source term for the kink "+" is:

$$\lim_{l \to 0} \chi \left(\vartheta + \log \frac{2}{l} - h(l) \right) = \chi(\vartheta - h^+).$$

There are N_H^+ terms of this of type. For a h^- hole the source contribution to the same "+" kink is

$$\lim_{l \to 0} \chi \left(\vartheta + \log \frac{2}{l} - h(l) \right) = \lim_{l \to 0} \chi \left(\lambda - h^- + 2 \log \frac{2}{l} \right) = \chi_{\infty}$$

(χ_∞ is defined in (3.33)). One h^0 hole behaves in the same way. Then there are $N_H - N_H^+ = N_H^- + N_H^0$ such terms. Analogous arguments apply to "–" kink and to the other roots. For wide roots the limits of second determination are given in (3.35).

The following definitions are introduced, according to (3.52):

$$S^{\pm,0} = \frac{1}{2}[N_H^{\pm,0} - 2N_S^{\pm,0} - M_C^{\pm,0} - 2M_W^{\pm,0}\theta(p-1)]$$

Observe that S is always integer, whereas $S^{\pm,0}$ can be half integer; moreover, in some cases, S^0 can be negative. All this numbers are interpreted as the spin of the right, left movers and fixed solutions. Clearly

$$S = S^+ + S^- + S^0.$$

Using all this computations in the definition (4.8), the NLIE for the "+" and "–" kinks reads:

$$Z_\pm(\vartheta) = \pm e^{\pm\vartheta} + \alpha + g_\pm(\vartheta) + \int dx G(\vartheta - x)\mathcal{Q}_\pm(x) \tag{4.9}$$

where the following definitions are used:

$$g_\pm(\vartheta) = \lim_{l\to 0} g\left(\vartheta \pm \log\frac{2}{l}\bigg|\vartheta_k\right) = \pm 2\chi_\infty(S - S^\pm) + 2\pi l_W^\pm + \sum_{k=1}^{N_H^\pm}\chi(\vartheta - h_k^\pm) +$$

$$-\sum_{k=1}^{N_S^\pm}\left(\chi(\vartheta - \hat{y}_k^\pm + i\eta) + \chi(\vartheta - \hat{y}_k^\pm - i\eta)\right) - \sum_{k=1}^{M_C^\pm}\chi(\vartheta - c_k^\pm) - \sum_{k=1}^{M_W^\pm}\chi_{II}(\vartheta - w_k^\pm)\,; \tag{4.10}$$

$$l_W^\pm = \pm\text{sign}(p-1)\frac{1}{2}\left(M_W - M_W^\pm\right)$$

and the function $\mathcal{Q}_\pm(x)$ is related to $Z_\pm$ as Z to $\mathcal{Q}$ in (3.40).

This equations allow to write the quantization conditions as:

$$Z_\pm\left(\vartheta_j^\pm\right) = 2\pi I_j^\pm. \tag{4.11}$$

It is a matter of convenience to put the apex $\pm$ on the quantum numbers. Indeed, they do not change in the limit procedure: they are exactly the same as for finite l.

By simply taking the limit $l \to 0$ in NLIE reads an equation for the fixed objects ϑ^0:

$$Z_0(\vartheta) = \lim_{l\to 0} Z(\vartheta, l) = \alpha + g_0(\vartheta) + \int dx G(\vartheta - x)\mathcal{Q}_0(x) \tag{4.12}$$

where

$$g_0(\vartheta) = \lim_{l\to 0} g\left(\vartheta|\vartheta_k\right) = 2\chi_\infty(S^- - S^+) + 2\pi l_W^0 + \sum_{k=1}^{N_H^0}\chi(\vartheta - h_k^0) +$$

$$-\sum_{k=1}^{N_S^0}\left(\chi(\vartheta - \hat{y}_k^0 + i\eta) + \chi(\vartheta - \hat{y}_k^0 - i\eta)\right) - \sum_{k=1}^{M_C^0}\chi(\vartheta - c_k^0) - \sum_{k=1}^{M_W^0}\chi_{II}(\vartheta - w_k^0)\,;$$

$$l_W^0 = \text{sign}(p-1)\frac{1}{2}\left(M_W^- - M_W^+\right).$$

As in the previous case the function $\mathcal{Q}_0(x)$ is related to the corresponding $Z_0(x)$ by the usual expression (3.40).

In the following the asymptotic values of $Z_{\pm,0}$ and the corresponding values for $\mathcal{Q}$ will play an important role. Equations (4.9) simply gives

$$Z_+(+\infty) = +\infty = -Z_-(-\infty), \tag{4.13}$$

consequently the value for $\mathcal{Q}(x)$ can be obtained using (3.40):

$$\mathcal{Q}_\pm(\pm\infty) = 0 \tag{4.14}$$

(to compute it, before do the limit in x and later the limit in η, because the NLIE holds with a finite η). Moreover it can be shown that

$$g_+(-\infty) = g_0(+\infty) = 2\chi_\infty(S - 2S^+) + 2\pi k_W^+$$
$$g_-(+\infty) = g_0(-\infty) = -2\chi_\infty(S - 2S^-) + 2\pi k_W^-$$

and

$$k_W^\pm = \pm\frac{1}{2} \operatorname{sign}(p-1)(M_W - 2M_W^\pm) = \frac{M_{SC}}{2} + \text{integer}.$$

A direct consequence of this is that

$$Z_+(-\infty) = Z_0(+\infty) \qquad \text{and} \qquad Z_-(+\infty) = Z_0(-\infty) \tag{4.15}$$

because they satisfy the same equation. Remember that for small l the counting function gives, in the central region, one or two plateaus that stretch to the infinities. Then the previous equations simply mean that $Z_0(+\infty)$ is the right plateau height and and $Z_0(-\infty)$ the left plateau height. If there are no central objects, they take the same value, yielding so a one plateau system.

The explicit values can be computed, using the kink equations. The integral can be handled because the $\mathcal{Q}$ in the asymptotic limit takes a constant value and the kernel G rapidly converges to zero:

$$\begin{aligned} Z_+(-\infty) &= \alpha + g_+(-\infty) + \frac{\chi_\infty}{\pi}\mathcal{Q}_+(-\infty) \\ Z_-(+\infty) &= \alpha + g_-(+\infty) + \frac{\chi_\infty}{\pi}\mathcal{Q}_-(+\infty). \end{aligned} \tag{4.16}$$

They are called *plateau equations*. From the definition of $\mathcal{Q}$ in (3.40), and making attention to the warning concerning the range of values allowed for it, it follows that

$$Z_\pm(\mp\infty) = \mathcal{Q}_\pm(\mp\infty) + \pi\delta + 2\pi k_\pm$$

with an appropriate choice of the integers $k_\pm$ such that the condition $-\pi \le \mathcal{Q}_+(-\infty) \le \pi$ holds (remember that $k_W^\pm$ can be half-integer).The solution of the plateau equation is then

$$\omega_\pm \equiv \mathcal{Q}_\pm(\mp\infty) = \pm 2\pi\frac{p-1}{p+1}(S - 2S^\pm) + 2\pi\frac{p}{p+1}\left(\frac{\alpha}{\pi} - \delta + 2k_W^\pm - 2k_\pm\right). \tag{4.17}$$

Notice that for $p > 1$ there can be cases without solution. If instead it is there, there is no ambiguity in the choice of $k_\pm$, because its contribution is a multiple of $4\pi\dfrac{p}{p+1} > 2\pi$, that is larger than the range of values allowed for $\mathcal{Q}_\pm$. Instead, for $p < 1$ the solution always exists, but it can happens that two or more choices of $k_\pm$ satisfy the condition on the range of $\mathcal{Q}_\pm$. It

will be clear later, that this phenomenon is related to the fact that wide roots become excitations independent of the other one's, which is manifestly evident from the fact that they no longer contribute to the spin of the state S and that the asymptotic value of their source contribution χ_{II} in the attractive regime is simply a π (see 3.35).

Before to continue the general computation, the kink equations for the wide roots will be explicitly written. They can be obtained by using the same procedure used for (4.9), applied to the correct expression for $Z(\vartheta)$ given in (3.38):

$$
Z_{\pm}(\vartheta) = \pm e_{II}^{\vartheta} + \sum_{k=1}^{N_H^{\pm}} \chi_{II}(\vartheta - h_k^{\pm}) - \sum_{k=1}^{N_S^{\pm}} \left(\chi_{II}(\vartheta - \hat{y}_k^{\pm} + i\eta) + \chi_{II}(\vartheta - \hat{y}_k^{\pm} - i\eta) \right)
$$

$$
- \sum_{k=1}^{M_C^{\pm}} \chi_{II}(\vartheta - c_k^{\pm}) - \sum_{k=1}^{M_W^{\pm}} \chi_{II}(\vartheta - w_k^{\pm})_{II} \pm \theta(p-1)4\chi_{\infty}(S - S^{\pm}) + 2\pi L_W^{\pm}(\text{sign}\Im m\vartheta) + \tag{4.18}
$$

$$
+ \int dx \, G_{II}(\vartheta - x)\mathcal{Q}(x) + \alpha_{II} \qquad \text{for } |\Im m \, \vartheta| > \min(1, \, p)
$$

where the notation introduced for L_W is so complicated because it depends on the sign of the imaginary part of ϑ:

$$
L_W^{\pm}(\text{sign}\Im m\vartheta) = - \sum_{k=1}^{M_W - M_W^{\pm}} \lim_{x \to \pm\infty} \left[\chi_{II}(\vartheta - w_k + x)_{II} \mp 4(\chi_{\infty} - \pi)\theta(p-1) \right] = \pi \, \cdot \text{integer}
$$

$$
\tag{4.19}
$$

The explicit form is quite complicated. Then this contribution must be computed case by case. Observe that the term e_{II}^{ϑ} vanishes for $p > 1$ and α_{II} vanishes for $p < 1$.

Now, the ultraviolet limit on the energy and momentum expressions will be done. To this end, substitute in the energy and momentum expressions (3.58, 3.59) the ultraviolet behaviour of the roots (4.7) and retain only terms in $\dfrac{1}{L}$. The kinetic terms give contributions as

$$
\mathcal{M} \cosh \vartheta_k \sim \frac{1}{L} e^{\pm\vartheta_k^{\pm}}. \tag{4.20}
$$

The integral terms must be calculated separately. Their form in the energy and momentum expressions is, respectively:

$$
-\mathcal{M} \int \frac{dx}{2\pi} \sinh x \, \mathcal{Q}(x) = -\mathcal{M} \int \frac{dx}{2\pi} \frac{1}{2} [e^x \, \mathcal{Q}(x) - e^{-x} \, \mathcal{Q}(x)],
$$
$$
-\mathcal{M} \int \frac{dx}{2\pi} \cosh x \, \mathcal{Q}(x) = -\mathcal{M} \int \frac{dx}{2\pi} \frac{1}{2} [e^x \, \mathcal{Q}(x) + e^{-x} \, \mathcal{Q}(x)],
$$

where the contribution depending on e^x is called "+" kink contribution, and the other term is the "−" kink contribution. From the definition itself of $\mathcal{Q}_{\pm}$ observe that, in the limit of very small l, it is possible to write for $\mathcal{Q}$:

$$
\mathcal{Q}\left(x \pm \log \frac{2}{l}, l \right) \sim \mathcal{Q}_{\pm}(x) + q_{\pm}(x, l), \tag{4.21}
$$

where the two functions $q_{\pm}(x, l)$ vanishes in the $l \to 0$ limit. The expression (4.21) can be substituted in the integral form for the two kinks. The integration variable can be shifted by

$x \rightarrow x + \log(2/l)$ then

$$\mathcal{M} \int \frac{dx}{2\pi} \frac{1}{2} e^{x} \, \mathcal{Q}(x) \doteq \frac{1}{L} \int \frac{dx}{2\pi} e^{x} \, \mathcal{Q}_{+}(x) \,, \tag{4.22}$$

where the symbol $\doteq$ means that only the terms of order $1/L$ are retained. Similarly for the "–" kink term

$$\mathcal{M} \int \frac{dx}{2\pi} \frac{1}{2} e^{-x} \, \mathcal{Q}(x) \doteq \frac{1}{L} \int \frac{dx}{2\pi} e^{-x} \, \mathcal{Q}_{-}(x) \,. \tag{4.23}$$

At this point, it is possible to express energy and momentum in a way dependent only on quantities which are finite in the UV limit. Using then (4.20, 4.22, 4.23) in (4.5), and rearranging the expression in terms of Δ, $\bar{\Delta}$ (i.e. restoring the light-cone coordinates) follows:

$$\Delta^{\pm} = \frac{c}{24} + \frac{1}{2\pi} \left(\sum_{j=1}^{N_{H}^{\pm}} e^{\pm h_{j}^{\pm}} - \sum_{j=1}^{N_{S}^{\pm}} \left(e^{\pm \hat{y}_{j}^{\pm} + i\eta} + e^{\pm \hat{y}_{j}^{\pm} - i\eta} \right) + \right.$$

$$\left. - \sum_{j=1}^{M_{C}^{\pm}} e^{\pm c_{j}^{\pm}} - \sum_{j=1}^{M_{W}^{\pm}} e_{II}^{\pm w_{j}^{\pm}} \mp \int \frac{dx}{2\pi} e^{\pm x} \, \mathcal{Q}_{\pm}(x) \right) \,.$$

As a notation, $\Delta = \Delta^{+}$ and $\bar{\Delta} = \Delta^{-}$. The NLIE can be used now to express the various terms appearing in the sums and the integrals. Consider, for example, the quantization condition (4.11) for the holes $h_{j}^{\pm}$. Using the oddity of the $\chi(x)$ function, it can be arranged in a more convenient way:

$$\pm \sum_{j=1}^{N_{H}^{\pm}} e^{\pm h_{j}^{\pm}} = 2\pi \sum_{j=1}^{N_{H}^{\pm}} I_{h_{j}}^{\pm} + \sum_{j=1}^{N_{H}^{\pm}} \left(\sum_{k=1}^{N_{S}^{\pm}} \left(\chi(h_{j}^{\pm} - \hat{y}_{k}^{\pm} + i\eta) + \chi(h_{j}^{\pm} - \hat{y}_{k}^{\pm} - i\eta) \right) + \right.$$

$$\left. + \sum_{k=1}^{M_{C}^{\pm}} \chi(h_{j}^{\pm} - c_{k}^{\pm}) + \sum_{k=1}^{M_{W}^{\pm}} \chi_{II}(h_{j}^{\pm} - w_{k}^{\pm}) \right) - N_{H}^{\pm} \left(\alpha \pm 2\chi_{\infty}(S - S^{\pm}) + 2\pi l_{W}^{\pm} \right) +$$

$$- \sum_{j=1}^{N_{H}^{\pm}} 2 \Im m \int \frac{dx}{i} G(h_{j}^{\pm} - x - i\eta) \log \left(1 + (-)^{\delta} e^{iZ_{\pm}(x+i\eta)} \right)$$

(the nonzero η has been restored for later convenience). For the other objects, similar forms hold (remember that the $\hat{y}_{k}$ are defined by (3.27)). All the equations so obtained must be substituted in the expression for $\Delta^{\pm}$. Now, observe that all the sums of $\chi(\vartheta)$, $\chi_{II}(\vartheta)$ and $\chi_{II}(\vartheta)_{II}$ cancel completely for the oddity of the functions. Moreover in the integral term the following substitution (for all the type of sources) can be made

$$2\pi G(h_{j}^{\pm} - x) = \chi'(x - h_{j}^{\pm}). \tag{4.24}$$

The result is:

$$\Delta^{\pm} = \frac{c}{24} \pm \left(I_{H}^{\pm} - 2I_{S}^{\pm} - I_{C}^{\pm} - I_{W}^{\pm} \right) - \frac{2\chi_{\infty}}{\pi} \left(S - S^{\pm} \right) S^{\pm} \mp S^{\pm} \left(\frac{\alpha}{\pi} + l_{W}^{\pm} \right) +$$

$$\pm \mathcal{L}_{W}^{\pm} \mp 2 \Im m \int \frac{dx}{(2\pi)^{2} i} \varphi_{\pm}'(x + i\eta) \log \left(1 + (-)^{\delta} e^{iZ_{\pm}(x+i\eta)} \right) \,.$$

The following notation has been introduced:

$$I_H^\pm = \sum_{j=1}^{N_H^\pm} I_{h_j}^\pm \, , \; I_C^\pm = \sum_{j=1}^{M_C^\pm} I_{c_j}^\pm \, , \; I_W^\pm = \sum_{j=1}^{M_W^\pm} I_{w_j}^\pm \text{ and } I_S^\pm = \sum_{j=1}^{N_S^\pm} I_{y_j}^\pm \, .$$

The new constant appearing in that equation takes into account for wide roots, and is given by (see also (4.18)):

$$\mathcal{L}_W^\pm = \sum_{j=1}^{M_W^\pm} L_W^\pm (\text{sign} \Im m \, w_j^\pm) = -\pi \text{sign}(p-1) M_W^\pm 2(S-S^\pm) +$$

$$-\sum_{j=1}^{M_W^\pm} \sum_{k=1}^{M_W - M_W^\pm} \lim_{x \to \pm\infty} \left[\chi_{II}(w_j^\pm - w_k + x)_{II} \mp 4(\chi_\infty - \pi)\theta(p-1) \right] = \pi \; \cdot \text{integer}$$

It must be computed case by case.

The following function has been introduced:

$$\varphi_\pm(\vartheta) = \pm e^{\pm\vartheta} + \sum_{k=1}^{N_H^\pm} \chi(\vartheta - h_k^\pm) - \sum_{k=1}^{N_S^\pm} \left(\chi(\vartheta - y_k^\pm + i\eta) + \chi(\vartheta - y_k^\pm - i\eta) \right) -$$

$$\text{(4.25)}$$

$$-\sum_{k=1}^{M_C^\pm} \chi(\vartheta - c_k^\pm) - \sum_{k=1}^{M_W^\pm} \chi_{II}(\vartheta - w_k^\pm) = Z_\pm(\vartheta) - \int dx G(\vartheta - x)\mathcal{Q}_\pm(x) - \alpha$$

Now, with the help of the computations shown in appendix C the integral becomes:

$$2 \Im m \int \frac{dx}{(2\pi)^2 i} \varphi_\pm'(x + i\eta) \log \left(1 + (-)^\delta e^{iZ_\pm(x+i\eta)} \right) = \pm \left(\frac{1}{24} - \frac{\mathcal{Q}_\pm^2(\mp\infty)}{16\pi^2} \frac{p+1}{p} \right)$$

and the UV limit computation ends with a close form for the conformal dimensions:

$$\Delta^\pm = \frac{c-1}{24} \mp \frac{\alpha}{\pi} S^\pm \pm \left(I_H^\pm - 2I_S^\pm - I_C^\pm - I_W^\pm \right) \mp S^\pm 2 l_W^\pm +$$

$$\pm \mathcal{L}_W^\pm - \frac{2\chi_\infty}{\pi} \left(S - S^\pm \right) S^\pm + \frac{\mathcal{Q}_\pm^2(\mp\infty)}{16\pi^2} \frac{p+1}{p}$$

$$\text{(4.26)}$$

This means that the UV limit admits an exact computation of the spectrum. The identification of the UV states is one of the fundamental steps to understand the physical interpretation of the continuum model so far defined.

An interesting phenomenon is that the conformal weights obtained depend only on very generic features of the source configuration such as the asymptotics of the left and right moving sources, the total spin and the number of self-conjugate roots. This means that if a certain source configuration is given, one can add new sources separately to the right and the left moving part in such a way that they are separately neutral (i.e. do not change S^+ and S^-, the total spin and the number of self-conjugate roots). In this way the primary weights do not change, but generally the term $I_H^\pm - 2I_S^\pm - I_C^\pm - I_W^\pm$ is increased and so descendents of the initial state are created. An example: states which have $S = 0 = M_{SC}$ and $S^\pm = 0$ are all descendents of the vacuum, however complicated their actual source configurations are.

It is important also to drive attention to the well known fact (see the section 3.8) that (at the moment) there is no proof that the scaling functions obtained by the method of NLIE span

the complete space of states. This is an extremely difficult problem due to the following two circumstances: (1) the dependence of the UV conformal weights from the parameters of the source configuration is rather complicated and (2) to obtain the allowed values of the complex roots one has to carefully examine the IR limit as suggested in section 4.3. It will be also clear that the same state can be realized by different root configurations depending on the regime (e.g. the $(s\bar{s})_\pm$ states: scattering of soliton and antisoliton in even and odd wave functions; see later).

4.6 Sine-Gordon and massive Thirring

As suggested in section (3.7), the choice $\omega = \alpha = 0$ is supposed to describe the sine-Gordon and massive Thirring models on a cylinder. In this section the corresponding NLIE will be analyzed, starting with the vacuum state. Obviously, the coupling p is expected to be the same that appears in the s-G and mTh lagrangians via the equation (1.12).

Starting from a lattice with $2N$ sites one finds that the antiferromagnetic ground state which has spin $S = 0$, when written in terms of Bethe vectors depends on $M = N$ roots of the Bethe equations, all of which are real, as indicated in (2.5). This ground state is expected to correspond to the vacuum of the field theory. However, there are two possibilities: one for N even and the other for N odd, corresponding in the continuum to the choices $\delta = 0$ or $\delta = 1$. As it will be shown in the sequel, only one of these states can be identified with the vacuum for a local field theory having a $c = 1$ UV limiting CFT. The UV dimensions of the vacuum are $\Delta^\pm = 0$ (because the theory is assumed unitary). Choosing $\delta = 0$, the expression (4.26) gives a value consistent with the interpretation proposed, i.e.

$$c = 1,$$

as obtained in the paper [7]. At the IR, because no holes neither complex roots are considered, the energy and momentum (3.58, 3.59) vanishes, that is what is expected for the vacuum. The numerical iteration of the NLIE gives the scaling energy shown in figure 4.2. In that figure, the value of the predicted bulk energy (1.21) has been subtracted from TCSA data in order to normalize them at the same way as the NLIE data are. The agreement of the two data is to order $10^{-4} - 10^{-3}$.

As a consequence of this vacuum analysis, the equations for the asymptotic behaviour (4.17) and for the conformal dimensions (4.26) take a simpler form ($\alpha = 0$ and $c = 1$). If the physical interpretation is consistent, the expected conformal dimensions must have the form (1.4), that is a sum of powers of $R^2 = \frac{p+1}{2p}$ (as is (1.12)). Then it is convenient to express $\Delta^\pm$ in powers of $\frac{p+1}{p}$, using also the expression (4.17) for $\mathcal{Q}_\pm^2(\mp\infty)$. The final form is

$$\Delta^\pm = \frac{p}{p+1}n_\pm^2 + \frac{m^2}{16}\frac{p+1}{p} \pm \frac{n_\pm m}{2} + N_\pm =$$
$$= \frac{1}{2}\left(\frac{n_\pm}{R} \pm \frac{1}{2}mR^2\right)^2 + N_\pm \tag{4.27}$$

where the following identifications have been made:

$$m = 2S$$
$$n_\pm = \left(\frac{\delta}{2} - k_W^\pm + k_\pm\right) \mp (S - 2S^\pm) \tag{4.28}$$

and

$$N_\pm = \pm\left(I_H^\pm - 2I_S^\pm - I_C^\pm - I_W^\pm\right) \mp S^\pm 2l_W^\pm \pm \mathcal{L}_W^\pm - 2\left(S^\pm\right)^2 \mp 2S^\pm\left(\frac{\delta}{2} - k_W^\pm + k_\pm\right). \tag{4.29}$$
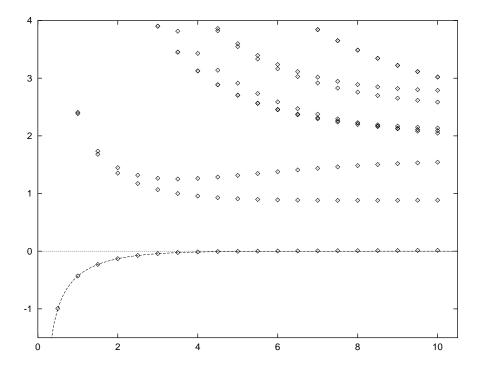
Figure 4.2: The first few energy levels (TCSA) in the vacuum ($m = 0$) sector at $p = \frac{2}{7}$ (plotted with diamonds) for $E_{cut} = 17.0$ (the dimension of the space is 4141) and the NLIE prediction for the vacuum scaling function (shown with a dotted line).

The similarity with (1.4) is manifest. To match an exact correspondence two conditions are required. The first one requires that

$$|n_+| = |n_-|. \tag{4.30}$$

The second condition is that one must be able to chose the sign of n in such a way that the left and right descendent numbers are integer. Consider the case where $n_+ = n_-$: then (using (4.27)) follows that both $N_\pm$ must be integers. Instead, in the case $n_+ = -n_-$ a combination of $N_\pm$ and $\pm\dfrac{n_\pm m}{2}$ must be integer.

Since the R^{-2} contribution comes exclusively from the last term in (4.26), the one-plateau systems (i.e. when $\mathcal{Q}_+(-\infty) = \mathcal{Q}_-(+\infty)$) satisfy trivially the condition (4.30), but even in that case it is not clear whether the descendent numbers are integers. At the time of this writing the analysis of our group cannot exclude the possibility that there exist some states for which the conformal weights cannot be interpreted within the framework of $c = 1$ CFT. However, in the numerous explicit examples we have calculated so far we have not found any configuration of sources which lead to such behaviour. If it happens for some configuration of the sources then the corresponding scaling function must be excluded from the spectrum.

From the second line of (4.28) one obtains a useful relation ($m = 2S \in \mathbb{Z}$)

$$n_\pm = \frac{m + \delta + M_{SC}}{2} + \text{integers}.$$

Using now the classification of UV conformal operators for s-G and mTh in the two algebras $\mathcal{A}_b$

and $\mathcal{A}_f$ given in section 1.3, one can obtain the following rule:

$$
\begin{aligned}
\frac{m + \delta + M_{SC}}{2} \in \mathbb{Z} &\qquad \text{for} \qquad \text{sine Gordon} \\
\frac{\delta + M_{SC}}{2} \in \mathbb{Z} &\qquad \text{for} \qquad \text{massive Thirring.}
\end{aligned}
\tag{4.31}
$$

With reference to figure 1.2, from this rule follows that all the four sectors can be accessed by NLIE, because the sectors **I** and **II** describe sine-Gordon, **I** and **III** describe massive Thirring and the sector **IV** can be obtained by m even and $\dfrac{\delta + M_{SC}}{2}$ half-integer. If there are no self-conjugate roots, the rule simplifies: $\delta = 0$ for mTh (**I** and **III**) and $\delta = 1$ for the sectors **II** and **IV**. The sector **IV**, that also is accessible by NLIE, contains non local states. Then NLIE describes also this non local sector.

4.6.1 "–" vacuum

Consider the case of $g(\vartheta|\vartheta_j) = 0$ (i.e. no sources). There are two possibilities $\delta = 0, 1$. One is the vacuum, considered previously, the other is $\delta = 1$. The (4.17) yields

$$
\mathcal{Q}_{\pm}(\mp\infty) = -2\pi\frac{p}{p+1}(1 + 2k_{\pm})\,,
\tag{4.32}
$$

which admits solution only in the attractive regime when

$$
|\mathcal{Q}_+(-\infty)| = |\mathcal{Q}_-(+\infty)| = 2\pi\frac{p}{p+1}\,.
\tag{4.33}
$$

The value is not determined uniquely due to the contribution of wide roots, but it can be fixed using information from the repulsive regime.

In that case, by performing the usual iteration procedure described in section 4.4, one finds that only for $l > l_0$ the iteration converges. For smaller values of l there is no convergence. The "breakdown" volume l_0 depends by p: for $p = 1.5$ it is $l_0 = 0.3$ (no breakdown in attractive regime). What happens is that the real root at the origin is a special one with $Z'(0) < 0$. By (3.52), because $S = 0$, also two holes must appear. All of which sources have Bethe quantum number zero. One of the holes moves to the left and the other one to the right and so $S^{\pm} = \dfrac{1}{2}$, while the special root is central (the configuration is completely symmetric, then $Z(-x) = -Z(x)$). This allows for a unique solution of the plateau equations:

$$
\mathcal{Q}_+(-\infty) = \pm\frac{2\pi}{p+1}\,, \qquad Z_+(-\infty) = -Z_-(+\infty) = \pi\frac{1-p}{p+1} < 0\,.
$$

Observe that $Z_-(+\infty) > Z_+(-\infty)$. This compared with (4.15) means that there are two plateaus and the left is higher than the right, i.e. $Z'(0) < 0$. The picture is completely consistent. This phenomenon can be thought of as the splitting of the root at the origin into a special root and two holes and is one of the general mechanisms in which the special sources are generated (see figure 4.3). Another mechanism will be explored when the UV limit of the soliton-antisoliton states will be examined.Let us suppose that the counting function Z is analytic as a function of p which is plausible because all terms in the NLIE for this state are analytic in the coupling. This determines which branch to choose for the plateau values in the attractive regime. One obtains the final result (for both the attractive and the repulsive regime)

$$
\Delta^{\pm} = \frac{1}{4}\frac{p}{p+1} = \frac{1}{8R^2} = \Delta^{\pm}_{\pm 1/2, 0}\,,
$$

which are the conformal weights of the vertex operators $V_{(\pm 1/2, 0)}$. The actual UV limit can be a linear combination of these operators; in any case, it is not contained in the UV spectrum of the sG/mTh theory, but is a state in the nonlocal sector (sector **IV** in figure 1.2).
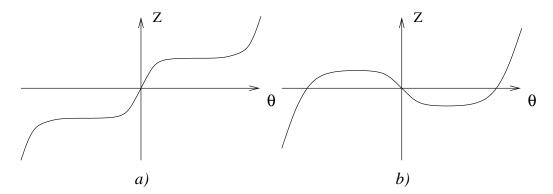
Figure 4.3: The UV behaviour of Z(two plateaus system) for (a) $p < 1$ and (b) $p > 1$. In (b) the root at the origin turned into a special one and two normal holes appeared at the points where Z crosses the horizontal axis with a positive derivative.

4.6.2   Pure hole states

The analysis of pure holes states is the simplest one. In the IR limit one such state gives (using (4.2):

$$Z(\vartheta) = l \sinh \vartheta + \sum_{j=1}^{N_H} \chi(\vartheta - h_j) \quad , \quad Z(h_j) = 2\pi I_j. \tag{4.34}$$

The holes "rapidities" are real. Using the observation (4.1) the equations (4.34) show the same structure of the box quantization equations for physical particles (4.3). Then the holes can be interpreted as particles with rapidity h_j, i.e. they are the solitons of sine-Gordon. Pure holes states are states with only solitons.

The IR limit puts no restriction on the quantum numbers I_k of the holes; instead the rapidities converge to zero. This seems to be a very general feature that remains true even when complex roots are allowed.

The UV calculations, for **one hole**, give for $\delta = 1$ (the hole can be put fixed in the origin):

$$S = \frac{1}{2}; \quad S^\pm = 0.$$

Solving the equation for $\mathcal{Q}_\pm(\mp\infty)$ gives:

$$m = 1$$
$$n_+ = n_- = 0$$

that correspond to the operators $V_{0,\pm 1}$. They create the sine-Gordon soliton (see also [20]). For one hole with $\delta = 0$, using

$$S^+ = \frac{1}{2}; \quad S^- = S = 0,$$

the UV computation gives the dimensions of $V_{1/2,\,1}$ or $V_{-1/2,\,-1}$ that describe the Thirring fermion. The UV picture is consistent with the IR. The behaviour at intermediate values of l is shown in figure 4.4where it appears that the interpretation of the hole with the soliton in consistent. This is the simplest case where the NLIE was used, in [28], for an odd number of particles. Table 4.1 gives
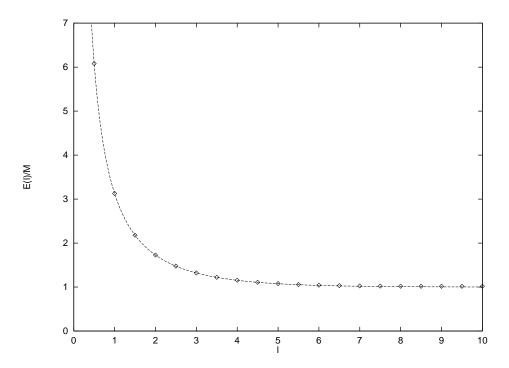
Figure 4.4: Comparison of the results for the one-soliton state coming NLIE and TCSA at $p = \frac{2}{7}$. Continuous line is the NLIE result, while the diamonds represent the TCSA data.

l	NLIE	TCS	Relative deviation
.5	6.080571	6.08062	0.000008
1	3.126706	3.12685	0.00005
1.5	2.177411	2.17791	0.0002
2	1.727224	1.72776	0.0003
2.5	1.475004	1.47593	0.0006
3	1.320353	1.32168	0.001
4	1.153188	1.15548	0.002
5	1.075376	1.07908	0.003

Table 4.1: Numerical comparison of the energy levels predicted by the NLIE to the TCS data for the case depicted in figure 4.4. The NLIE data are exact to the precision shown.

an idea about the numerical magnitude of the difference. Note that the deviations are extremely small for small values of l and they grow with the volume, exactly as expected for truncation errors.

For **two solitons** case the two possibilities, corresponding to $\delta = 0, 1$ must be checked. The simplest cases are:

1. Two holes quantised with $I_{1,2} = \pm\frac{1}{2}$, $\delta = 0$. It yields:

$$\Delta^{\pm} = \frac{p+1}{4p} = \frac{R^2}{2} = \Delta^{\pm}_{0,2}\,,$$

   corresponding to the operator $V_{(0,2)}$, which is the UV limit of the lowest-lying two-soliton state. as it can also be seen from the TCS data. If instead of the minimal choice $I_{1,2}$ we take a nonminimal one $I_+ = 3/2, 5/2, ...$, $I_- = -3/2, -5/2, ...$, we obtain

$$\Delta^{\pm} = \Delta^{\pm}_{0,2} \pm I_{\pm} - \frac{1}{2}\,,$$

   which corresponds to descendents of $V_{(0,2)}$. This is a general phenomenon: the "minimal" choice of quantum numbers yields the primary state, while the nonminimal choices give rise to descendents.

2. Two holes quantized with $I_{1,2} = \pm 1$, $\delta = 1$, as proposed in [8]. In the repulsive regime a special root is required, as in the case of the $\delta = 1$ vacuum state. The result (in both regimes) is:

$$\Delta^{\pm} = 1 + \frac{1}{4}\frac{1}{p(p+1)} = \Delta^{+}_{1/2,2} = \Delta^{-}_{1/2,2} + 1\,.$$

   This state is a linear combination of $\bar{a}_{-1}V_{(1/2,2)}$ and $a_{-1}V_{(-1/2,2)}$ which means that it is *not* contained in the local operator algebras of sG/mTh theories.

3. Two holes quantized with $I_1 = 0$, $I_2 = \pm 1$, $\delta = 1$. Consider in detail the case of $I_2 = +1$ since the other one is similar. Suppose that the hole with $I_1 = 0$ is a left mover and the other one is a right mover (the other possibilities lead to a contradiction). We find a solution to the plateau equation only in the attractive regime:

$$\mathcal{Q}_+(-\infty) = \pm 2\pi\frac{p}{p+1}, \quad \mathcal{Q}_-(+\infty) = \pm 2\pi\frac{p}{p+1}\,.$$

   In the repulsive regime the hole with quantum number 0 becomes a special hole y and emits other two ordinary holes each quantised with zero. We obtain for the plateau values

$$\mathcal{Q}_+(-\infty) = \mathcal{Q}_-(+\infty) = 2\pi\frac{1}{p+1}\,.$$

   The conformal weights turn out to be:

$$\begin{aligned}
\Delta^+ &= 1 + \frac{1}{4}\frac{1}{p(p+1)} = \Delta^+_{1/2,2}\,, \\
\Delta^- &= \frac{1}{4}\frac{1}{p(p+1)} = \Delta^+_{1/2,2}\,.
\end{aligned}$$

   These are the conformal weights of the vertex operator $V_{(1/2,2)}$. Performing a similar calculation for $I_2 = -1$ we obtain the weights of $V_{(-1/2,2)}$.

The calculation for a **generic number of holes** proceeds in complete analogy with the cases treated until now, we only give a summary of the results. The conformal families which we obtain depend on how many holes move to the left and to the right. The primaries are obtained for the minimal choice of the hole quantum numbers; increasing the quantum numbers we obtain secondary states, as it was pointed out in the case with two holes. The states we obtain are in the conformal family of a vertex operator $V_{n,m}$ with

$$m = N_{H,eff} \, , \; n \in \mathbb{Z} + \frac{\delta}{2} \, .$$

As a consequence, all states with $\delta = 0$ are contained in the UV spectrum of the sG/mTh theory while the ones with $\delta = 1$ are not, in agreement with the relation (4.31). The complete expression for n is somewhat complicated, but we give it in the case of symmetric $(N_H^+ = N_H^- = N_{H,eff}/2)$ configurations:

$$n = 0 \, , \quad \delta = 0 \, ,$$
$$n = \pm\frac{1}{2} \, , \quad \delta = 1 \, .$$

The comparison with TCSA completely confirms the analysis made until now. The example of four solitons states in repulsive regime is in figure 4.5.As usual in TCSA, one can see that
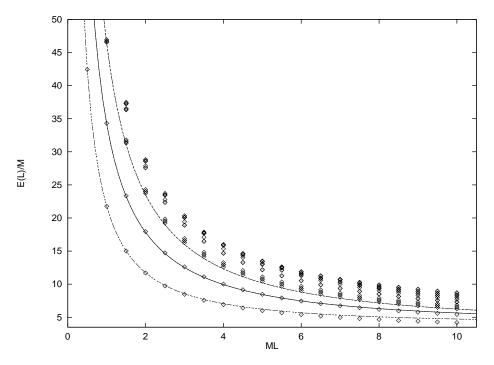
Figure 4.5: The first few energy levels (TCSA) for $m = 4$ solitons at $p = 1.5$ (plotted with diamonds) for $E_{cut} = 22.5$ (the dimension of the space is 4149) and the NLIE prediction for the four holes scaling functions with quantum numbers $(-\frac{3}{2}, -\frac{1}{2}, \frac{1}{2}, \frac{3}{2})$, $(-\frac{5}{2}, -\frac{1}{2}, \frac{1}{2}, \frac{5}{2})$ and $(-\frac{5}{2}, -\frac{3}{2}, \frac{3}{2}, \frac{5}{2})$ (shown wit continuous lines).

the truncation errors become larger; at values of the volume l close to 10 the deviation can be observed even from the figures. For $l < 5$ the agreement is still within an error of order 10^{-3}. More comments and examples can be found in [27, 28].

4.6.3   Holes and close roots

Let us now extend our investigation to situations with complex roots and consider the two particle states in more detail. Forgetting for the moment the breathers, we have to consider the two-soliton states. The soliton-antisoliton come in doublets so there are four different polarizations for two particle states of which the ss and $\bar{s}\bar{s}$ have topological charge $Q = \pm 2$ instead $s\bar{s}$ and $\bar{s}s$ have zero topological charge. The first two states are expected to have exactly the same scaling function for energy and momentum because the sG/mTh theory is charge conjugation invariant. Instead there are two different situations for the neutral $s\bar{s}$ state, which have spatially symmetric and antisymmetric wavefunctions (denoted by $(s\bar{s})_+$ and $(s\bar{s})_-$, respectively). To separate the symmetric and antisymmetric part one simply has to diagonalize the 4×4 SG two particle S-matrix and see that it has 2 coinciding eigenvalues (equal to $e^{i\chi(\vartheta)}$, corresponding to ss and $\bar{s}\bar{s}$), and two different eigenvalues in the $Q = 0$ channel.

Now we proceed to demonstrate that the IR limit restricts the possible quantum numbers of the complex roots. To simplify matters we consider only the repulsive regime $p > 1$.

In the repulsive regime $p > 1$, the scaling function $(s\bar{s})_-$ is realized as the solution to the NLIE with two holes (at positions $h_{1,2}$) and a complex pair at the position $\rho \pm i\sigma$. In the IR limit we have

$$
\begin{aligned}
Z(\vartheta) &= l\sinh\vartheta + \chi(\vartheta - h_1) + \chi(\vartheta - h_2) - \chi(\vartheta - \rho - i\sigma) - \chi(\vartheta - \rho + i\sigma),
\end{aligned}
$$

$$
Z(h_{1,2}) = 2\pi I_{1,2}\,,
$$
$$
Z(\rho \pm i\sigma) = 2\pi I_C^\pm\,.
$$

(4.35)

The quantization condition for the complex roots explicitly reads (we write down the equation only for the upper member of the complex pair, since the other one is similar)

$$
l\sinh(\rho + i\sigma) + \chi(\rho + i\sigma - h_1) + \chi(\rho + i\sigma - h_2) - \chi(2i\sigma) = 2\pi I_C^+.
$$

(4.36)

Now observe that as $l \to \infty$, the first term on the left hand side acquires a large imaginary part, but the right hand side is strictly real. The imaginary contribution should be cancelled by some other term. The function χ is bounded everywhere except for isolated logarithmic singularities on the imaginary axis. For the cancellation of the imaginary part the argument $2i\sigma$ of the last term on the left hand side should approach one of these singularities (similarly to the analysis in TBA [18]).

In the repulsive regime, taking into account that for a close pair $\sigma < \pi$, the only possible choice for σ is to approach $\dfrac{\pi}{2}$ as $l \to \infty$. The soliton-soliton scattering amplitude has a simple zero at $\vartheta = i\pi$ with a derivative which we denote by C (the exact value does not matter). To leading order in l, the cancellation of the imaginary part reads

$$
l\cosh\rho + \Re\log C\left(\sigma - \frac{\pi}{2}\right) = 0\,,
$$

(4.37)

from which we deduce

$$
\left|\sigma - \frac{\pi}{2}\right| \sim \exp\left(-l\cosh\left(\rho\right)\right)\,,
$$

(4.38)

so the imaginary part of the complex pair approaches its infrared limit exponentially fast. This approach is modified by taking into account the finite imaginary contributions coming from the source terms of the holes and from the convolution term. These contributions lead to corrections of the order e^{-l} and so they modify only the value of the constant C.

The behaviour of the real part near the singularity is:

$$\Re e\,\chi(z - i\pi) \to 0 \qquad \text{if} \qquad \Re e\,z < 0.$$

Assume, for the moment, that σ moves toward $\frac{\pi}{2}$ from below (i.e. $\sigma - \frac{\pi}{2} < 0$).

For the real part we get, again to the leading order

$$\Re e\chi\left(\rho + i\frac{\pi}{2} - h_1\right) + \Re e\chi\left(\rho + i\frac{\pi}{2} - h_2\right) = 2\pi I_C^+. \tag{4.39}$$

It can be shown that (in the repulsive regime $p > 1$)

$$\xi\left(\vartheta\right) \equiv \Re e\chi\left(\vartheta + i\frac{\pi}{2}\right) = -\frac{i}{2}\log\frac{\sinh\dfrac{1}{p}\left(i\dfrac{\pi}{2} - \vartheta\right)}{\sinh\dfrac{1}{p}\left(i\dfrac{\pi}{2} + \vartheta\right)}\,, \tag{4.40}$$

where the the fundamental branch of the logarithm is taken into account. ξ is an odd monotonous function bounded by

$$|\xi(\vartheta)| \leq |\xi(\infty)| = \frac{\pi(p-1)}{2p} \tag{4.41}$$

from below and above. This means that for any allowed value of $I_C^{\pm}$ the real position of the complex pair is determined uniquely and that

$$\left|I_C^{\pm}\right| < \left|\frac{p-1}{2p}\right|\,, \tag{4.42}$$

and since in the repulsive regime $p > 1$, the only possible choice is $I_C^{\pm} = 0$. Then the solution for ρ is

$$\rho = \frac{h_1 + h_2}{2}\,, \tag{4.43}$$

so it approaches the central position between the two holes (the corrections to this asymptotic are also exponentially small for large l). In fact, for the symmetric hole configuration $I_1 = -I_2$ we expect $h_1 = -h_2$ and $\rho = 0$ to be valid even for finite values l.

However, the above derivation is valid only if $\sigma < \dfrac{\pi}{2}$ and so we do not cross the boundary of the analyticity strip of the $\chi(\vartheta)$ function which is at $\Im m\,\vartheta = \pi$. If $\sigma > \dfrac{\pi}{2}$, we must use a consider that:

$$\Re e\,\chi(z - i\pi) \to \pi \qquad \text{if} \qquad \Re e\,z > 0.$$

The conclusion that σ approaches $\frac{\pi}{2}$ exponentially fast as $l \to \infty$ is unaffected by this change, but now the real part of $\chi(2i\sigma)$ is not zero but instead $\pm\pi$ (modulo 2π). We choose the branches of the logarithm in such a way that $\Re e\,\chi(\pm 2i\sigma) = \mp\pi$ (the structure of the cuts is displayed in figure 4.6). In this way we obtain that

$$I_C^{\pm} = \mp\frac{1}{2}\,,$$

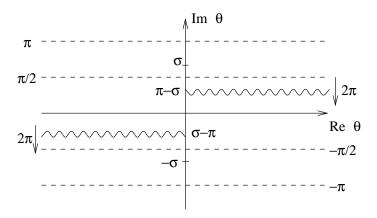and the asymptotic value of ρ is just as before.

Figure 4.6: The analytic structure of the counting function if $\sigma > \frac{\pi}{2}$. The logarithmic cuts are indicated with the wiggly lines. The one lying in the upper half plane originates from the root in the lower half plane and vice versa. We also indicated the value of the discontinuity across the cuts.

The S-matrix of the $(s\bar{s})_-$ configuration can be obtained by substituting the asymptotic values

$$\rho = \frac{h_1 + h_2}{2} \; , \; \sigma = i\frac{\pi}{2} \tag{4.44}$$

into the expression for $Z(\vartheta)$ and considering now the quantization rules of the holes. We obtain

$$Z(h_1) = l\sinh(h_1) - i\log S_-(h_1 - h_2) = 2\pi I_1 \; , \tag{4.45}$$

and a similar equation for the second hole, with

$$S_-(\vartheta) = -\frac{\sinh\left(\dfrac{\vartheta + i\pi}{2p}\right)}{\sinh\left(\dfrac{\vartheta - i\pi}{2p}\right)} S_{++}^{++}(\vartheta) \; , \tag{4.46}$$

which is the correct scattering amplitude for the antisymmetric configuration of the soliton-antisoliton system. The amplitude has poles at $\vartheta = i\pi(1 - 2kp)$, $k = 1, 2, \ldots$, corresponding to breathers with mass

$$m_{2k} = 2\mathcal{M}\sin kp\pi \; .$$

The equation (4.45) describes an approximation to the full NLIE valid for large l which is called the dressed or asymptotic Bethe Ansatz. There are three levels of approximations to the scaling functions: the full NLIE (which is in fact exact), the higher level Bethe Ansatz (HLBA) obtained from the NLIE by dropping the convolution term and the asymptotic BA. The difference between the BA and the HLBA is that while the former keeps the complex pair in its asymptotic position, the latter takes into account the corrections coming from the fact that σ changes with l (to first order as given in (4.38)). However, since the convolution term is of the same order in l as the dependence of σ derived from the HLBA, the HLBA is not a self-consistent approximation scheme. Therefore we are left with the exact NLIE, which is valid for all scales and with the BA as its IR asymptotic form.

The above conclusions about the $(s\bar{s})_-$ state an be extended into the attractive regime as long as $p > \frac{1}{2}$. At the point $p = \frac{1}{2}$, however, the pair situated at the asymptotic position $\pm i\frac{\pi}{2}$ hits the boundary of the fundamental analyticity strip situated at $i\pi p$. This phenomenon has a

physical origin: this point is the threshold for the second breather bound state which is the first pole entering the physical strip in the $(s\bar{s})_-$ channel. To continue our state further, it requires to go to configurations having an array of complex roots of the first type (see [8]). Without going into further details, let us mention only that any such array contains a close pair plus some wide pairs depending on the value of p.

The symmetric state $(s\bar{s})_+$ can be obtained from a configuration with two holes and one selfconjugate wide root. Considerations similar to the above lead to the scattering amplitude

$$S_+(\vartheta) = \frac{\cosh\left(\dfrac{\vartheta + i\pi}{2p}\right)}{\cosh\left(\dfrac{\vartheta - i\pi}{2p}\right)} S_{++}^{++}(\theta)\,, \tag{4.47}$$

which agrees with the prediction from the exact S-matrix. The poles are now at $\vartheta = i\pi(1 - (2k + 1)p)$, $k = 0, 1, \ldots$ and correspond to breathers with mass

$$m_{2k+1} = 2\mathcal{M}\sin\frac{(2k+1)p\pi}{2}\,.$$

This configuration extends down to $p = 1$, where the selfconjugate root collides with the boundary of the fundamental analyticity strip at $i\pi$. This is exactly the threshold for the first breather which is the lowest bound state in the $(s\bar{s})_+$ channel. For $p < 1$ the $(s\bar{s})_+$ state contains a degenerate array of the first kind (see [8]), which consists of a close pair, a selfconjugate root and some wide pairs, again depending on the value of p.

We remark that it is easy to extend the above considerations to a state with four holes and a complex pair. In this case the only essential modification to the above conclusions is that the limit for the complex pair quantum number becomes

$$\left|I_c^\pm\right| < \left|\frac{p-1}{p}\right| \tag{4.48}$$

when $\sigma < \dfrac{\pi}{2}$, and

$$\left|I_c^\pm \pm \frac{1}{2}\right| < \left|\frac{p-1}{p}\right|\,, \tag{4.49}$$

when $\sigma > \dfrac{\pi}{2}$, since now there are four χ sources coming from the holes. In the range $1 < p < 2$ this gives the same constraints

$$I_c^\pm = \begin{cases} 0\,, & \sigma < \dfrac{\pi}{2}\,, \\ \mp\dfrac{1}{2}\,, & \sigma > \dfrac{\pi}{2} \end{cases}\,,$$

as for the $(s\bar{s})_-$ state (for $p > 2$ it allows for more solutions, which however we will not need in the sequel).

From the UV point of view, the results shown in this paragraph about the quantum numbers of the close roots are quite interesting. Consider the conformal dimensions (4.26) or the specific form (4.27). There is no proof that the terms $N_\pm$ give always the correct descendent numbers. In particular there is no proof that the sum of quantum numbers $\left(I_H^\pm - 2I_S^\pm - I_C^\pm - I_W^\pm\right)$ is bounded from below (and nonnegative). Then we don't know if the so called "vacuum" is really the hamiltonian ground state. The IR analysis done until now shows exactly that states with only holes and with holes and close roots have the correct hamiltonian behaviour.

We now turn ourselves to the UV limits of the previous states. In particular we consider the state of two holes and a close pair (in the repulsive regime), which describes the antisymmetric soliton-antisoliton two-particle state. According to the results from the IR asymptotic, the quantum numbers of the complex roots can be 0 or $\pm\frac{1}{2}$. Therefore, we are left two possibilities: either the holes are quantised with integers or with half-integers.

Let us start with the half-integer choice $\delta = 0$ and suppose that one of the holes is right moving (which is the case if its quantum number $I_1 = I_+$ is positive) and the other one is left moving (i.e. $I_2 = I_- < 0$). Using the general formula (4.17) and $S^\pm = \frac{1}{2}$, $S = 0$, by a simple calculation we obtain

$$\mathcal{Q}_+(-\infty) = Z_+(-\infty) = -2\pi\frac{p-1}{p+1}\,,$$

which is valid for $1 < p < 4$ (the complex pair remains central). The other plateau values follow by oddity of the function Z. For the other half of the repulsive regime we have to include two new normal holes, one moving to the left and the other to the right, and two special holes that remain central (a justification for this will be given shortly) so that $S^\pm = 1$. We then find

$$\mathcal{Q}_+(-\infty) = 4\pi\frac{1}{p+1}\,, \ Z_+(-\infty) = -2\pi\frac{p-1}{p+1}\,,$$

which is valid for $p \geq 4$. In both cases the result for the UV weights turns out to be

$$\Delta^\pm = \frac{p}{p+1} \pm I_\pm - \frac{1}{2} = \frac{1}{2R^2} \pm I_\pm - \frac{1}{2} = \Delta_{(\pm1,0)} \pm I_\pm - \frac{1}{2}\,.$$

The primary state is obtained for the minimal choice $I_+ = -I_- = \frac{1}{2}$ and coincides with a linear combination of the vertex operators $V_{(\pm1,0)}$ which is correct for the state to be included in the spectrum of the sG/mTh theory and agrees with the behaviour of the $(s\bar{s})_-$ state observed from TCS. If both of the holes move to the right or to the left, we obtain descendents of the identity operator, i.e. states in the vacuum module of the UV CFT.

Figure 4.7 shows how the special holes are generated in this case. Starting from $p < 4$ and increasing the value of p the UV asymptotic form of the counting function varies analytically. Since the real roots/holes are quantised by half-integers, they are at positions where the function Z crosses a value of an odd multiple of π. As the plots demonstrate, the behaviour of Z is in fact continuous at the boundary $p = 4$: it is our interpretation in terms of the sources that changes, exactly because we try to keep the logarithm in the integral term of the NLIE in its fundamental branch. The price we pay is that we have to introduce two new normal holes (one moves left and the other one moves right) and two special holes which are central.Let us comment on the extension to the attractive regime. The complex root configuration changes only by the possible presence of wide pairs, which however have no effect on the plateau values (4.17) as their contribution can be absorbed in redefinition of the values $k_\pm$. The other effect the wide roots have is to shift the terms $\Sigma_\pm$ by multiples of 2π, but this affects only the integers $N_\pm$ in (4.29). Therefore we again obtain states which are descendents of $V_{(\pm1,0)}$.

For the state with integer quantization of the holes, we only give the result. If one of the holes is moving left and the other one to the right, we obtain

$$\Delta^\pm = \frac{1}{4}\left(\frac{p}{p+1}\right) \pm I_\pm = \frac{1}{8R^2} \pm I_\pm = \Delta_{(\pm1/2,0)} \pm I_\pm,$$

i.e. some linear combinations of descendents of the vertex operators $V_{(\pm1/2,0)}$. If both of the holes move to the left or to the right, we obtain other descendents of the same primary states. Again, this excludes the integer quantised states from the spectrum of sG/mTh theory.
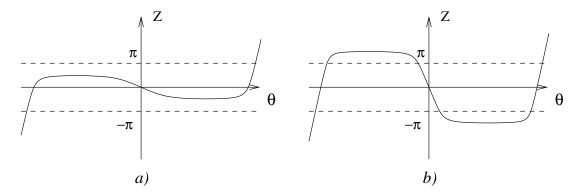
Figure 4.7: The UV behaviour of Z for a) $p < 4$ and b) $p > 4$.

4.6.3.1   Two holes and a selfconjugate complex root

Taking the integer quantised state, the plateau values are given by the same formulas as for the case with the close pair above, since the plateau equation is identical. The only difference is that the numbers $l_W^{\pm}$ (4.10) take a nonzero value

$$l_W^{\pm} = -S^{\pm}.$$

If the one of the holes is a right mover, while the other one is a left mover, the conformal weights turn out to be

$$\Delta^{\pm} = \frac{p}{p+1} \pm I_{\pm} - 1 = \Delta_{(\pm 1, 0)} \pm I_{\pm} - 1.$$

If the two holes move in the same direction, we again obtain secondaries of the vacuum state.

Concerning the extension to the attractive regime, one can again check that the plateau solution remains unchanged for the root configuration of two holes and two close roots, therefore the conformal family to which the state belongs remains the same, similarly to the case of the $(s\bar{s})_{-}$ state.

One can ask what happens if we quantize with half-integers. The result is, similarly to the case with the complex pair, that we obtain descendants of the operators $V_{(\pm 1/2, 0)}$. Therefore we conclude that in this case the integer quantised configuration must be accepted, while the half-integer one is ruled out, in full accordance with the rule (4.31).

4.6.4   Breather S-matrices and IR limit

In the infrared limit $l \to \infty$ the term $l \sinh(\vartheta)$ develops a large imaginary part in the first determination away from the real axis, forcing the close complex roots to fall into special configurations called *arrays* (we use the terminology of [8]). An array is a set of complex roots in which the roots are placed at specific intervals in the imaginary direction and have the same real part. In the attractive regime $l \sinh(\vartheta)_{II}$ is nonzero and so this is true for nonselfconjugate wide pairs as well (in the repulsive case wide roots do not have such driving force), while self-conjugate roots have a fixed imaginary part anyway. The deviation of the complex roots from their positions in the array decays exponentially with l (section 4.6.3).

For the rest of this subsection, whenever it is not explicitly stated, we restrict ourselves to the attractive regime $p < 1$. The possible arrays fall into two classes:

1. *Arrays of the first kind* are the ones containing close roots, which describe the polarization states of solitons.

There are two degenerate cases: *odd degenerate* arrays, which have a self-conjugate root at

$$\vartheta_0 = \vartheta + i\frac{\pi(p+1)}{2}$$

and accompanying complex pairs at

$$\vartheta_k = \vartheta \pm i\frac{\pi(1 - (2k+1)p)}{2} \ , \ \ k = 0, \dots, \left[\frac{1}{2p}\right]$$

and *even degenerate* ones, which only contain complex pairs, at the positions

$$\vartheta_k = \vartheta \pm i\frac{\pi(1 - 2kp)}{2} \ , \ \ k = 0, \dots, \left[\frac{1}{2p}\right]$$

These arrays always contain exactly one close pair. The odd degenerate arrays in the repulsive regime reduce to single self-conjugate roots and the even degenerate ones to a single close complex pair.

2. *Arrays of the second kind* describe breather degrees of freedom. The odd ones contain a self-conjugate root

$$\vartheta_0 = \vartheta + i\pi(p+1)/2$$

and wide pairs as follows:

$$\Im m\vartheta_k = \vartheta \pm i\frac{\pi(1 - (2k+1)p)}{2} \ , \ \ k = 0, \dots, s \ ,$$

where

$$0 \leq s \leq \left[\frac{1}{2p}\right] - 1 \ ,$$

while the even ones only contain wide pairs

$$\Im m\vartheta_k = \vartheta \pm i\frac{\pi(1 - 2kp)}{2} \ , \ \ k = 0, \dots, s \ ,$$

and s runs in the same range. They correspond to the $(2s+1)$-th breather B_{2s+1} and the $(2s+2)$-th breather B_{2s+2}, respectively.

As one can see, arrays of the second kind become degenerate ones of the first kind, if we analytically continue increasing p. The reason is that breathers are of course soliton-antisoliton bound states, while degenerate arrays of the first kind describe scattering states of a soliton and antisoliton, as we will see shortly.

One can compute the energy and momentum contribution of a array of the second kind corresponding to the breather B_s. The energy-momentum contribution turns out to be

$$2\mathcal{M}\sin\frac{\pi sp}{2}\,(\cosh\vartheta, \sinh\vartheta) \ , \tag{4.50}$$

where ϑ is the common real part of the roots composing the array. This is just the contribution of a breather B_s moving with rapidity ϑ. Arrays of the first kind do not contribute to the energy-momentum in the infrared limit, which lends support to their interpretation as polarization states of solitons.

Now we proceed to show that with the above interpretation the NLIE correctly reproduces the two-body scattering matrices of sine-Gordon theory including breathers.

Let us start with breather-soliton matrices. The Bethe quantization conditions for a state containing a soliton (i.e. a hole) with rapidity ϑ_1 and a breather B_s with rapidity ϑ_2 take the following form in the infrared limit. For the hole we get

$$Z(\vartheta_1) = \mathcal{M} \sinh \vartheta_1 - \sum_{k=0}^{s} \chi_{II}(\vartheta_1 - \vartheta_2 - i\rho_k) = 2\pi I_1,$$

where we denoted the prescribed imaginary parts of the roots in the array B_s by ρ_k. Here we used $\chi(0) = 0$ to eliminate the source term for the hole. Now we can compute the second determination of χ as in (3.34). Now it is a matter of elementary algebra to arrive at

$$Z(\vartheta_1) = \mathcal{M} \sinh \vartheta_1 - i \log S_{SB_s}(\vartheta_1 - \vartheta_2) = 2\pi I_1 \ ,$$

where $S_{SB_s}(\vartheta_1 - \vartheta_2)$ is the soliton-breather S-matrix conjectured in [2].

One can start with the breather quantization conditions, too. Writing

$$Z(\vartheta_2 + i\rho_k) = \mathcal{M} \sinh(\vartheta_2 + i\rho_k)_{II} + \chi_{II}(\vartheta_2 - \vartheta_1 + i\rho_k) + \ldots = 2\pi I_2^{(k)} \ , k = 0, \ldots, s \quad (4.51)$$

(the dots are terms due to wide root sources themselves, which cancel out up to multiples of 2π in the next step). Summing up these equations one arrives at

$$2\mathcal{M} \sin \frac{sp\pi}{2} \sinh(\vartheta_2) - i \log S_{SB_s}(\vartheta_2 - \vartheta_1) = 2\pi I_2 \ ,$$

where I_2 is essentially minus the sum of the quantum numbers of the wide roots composing the array (shifted by some integer coming from summing up the terms omitted in equation (4.51)).

Using a similar line of argument we also reproduced the breather-breather S-matrices by writing down the Bethe quantization conditions for a state with two degenerate strings B_s and B_r of the second kind. One has to be careful that when $Z(\vartheta)$ contains wide root sources which are expressed in terms of $\chi_{II}(\vartheta)$, the second determinations of these terms will appear in $Z(\vartheta)$ for large $\Im m \, \vartheta$, i.e. terms that can be written roughly like $(\chi_{II}(\vartheta))_{II}$, as in (3.39).

Scattering state of a soliton and an antisoliton can be described by taking two holes and a degenerate array of the first kind. There are two possibilities now, corresponding to scattering in the parity-odd and parity-even channels. Following the procedure outlined in section 4.6.3, we were once again able to reproduce the corresponding scattering amplitudes. The results presented here together with those of section 4.6.3 exhaust all two-particle scattering amplitudes of sine-Gordon theory, both in the repulsive and attractive regime.

4.6.5 Some examples of breather states

So we proceed to take a look at the simplest neutral excited state, which is the one containing a first breather B_1 at rest. The source term to be written into the NLIE turns out to be

$$g(\vartheta - w_R) = -\chi_{II}(\vartheta - w) = -i \log \frac{\cos \dfrac{\pi p}{2} - i \sinh(\vartheta - w_R)}{\cos \dfrac{\pi p}{2} + i \sinh(\vartheta - w_R)} \ , \qquad (4.52)$$

where w_R is the real part of the position of the self-conjugate root (the imaginary part is $w_I = \pi(p+1)/2$. In this case $w_R = 0$ since the breather has zero momentum. There is no need to look at the Bethe quantization condition as the root does not move due to the left-right symmetry

l	TCS	NLIE	TCS	NLIE
1.0	2.38459	n/a	1.84996	n/a
1.5	1.68168	n/a	1.30438	n/a
2.0	1.35391	n/a	1.05038	n/a
2.5	1.17420	n/a	0.91152	n/a
3.0	1.06692	1.0655810539	0.82903	0.8285879853
3.5	0.99985	0.9980153379	0.77773	0.7771857432
4.0	0.95664	0.9542867454	0.74499	0.7443106400
4.5	0.92845	0.9254766107	0.72381	0.7229895177
5.0	0.91000	0.9063029141	0.71006	0.7090838262

Table 4.2: The first breather state at $p = \dfrac{2}{7}$ and $p = \dfrac{2}{9}$. Energies and distances are measured in units of the soliton mass $\mathcal{M}$, and we have subtracted the predicted bulk energy term from the TCS data.

of the problem. This state is quantized with integer Bethe quantum numbers, i.e. $\delta = 1$, as in (4.31).

Table 4.2 presents the energy values obtained by iterating the NLIE in comparison to results coming from TCS, at the values $p = 2/7$ and $p = 2/9$.

The table shows that iteration of the NLIE fails for values of l less than 3 (the actual limiting value is around 2.5). What is the reason?

We plot the counting function Z on the real line for $l = 3$ and $l = 2$ in figure 4.8. In a first approximation we can safely neglect the integral term for these values of the volume to see the qualitative features that we are interested in. What we see is that the behaviour of the function
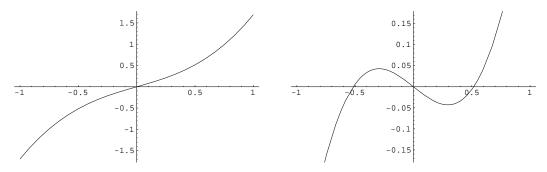
Figure 4.8:   The behavior of the function $Z(\vartheta)$ at $l = 3$ and $l = 2$, respectively.

changes: its derivative changes sign at the origin. As a result, two new holes appear where the new real zeros of the function are. But the topological charge remains zero, due to the fact that now we have a special root at the origin and so $N_S = 1$ and $N_H = 2$. The two new holes do not give us any new dynamical degrees of freedom: their quantum numbers are fixed to be 0 and so their positions are uniquely determined.

Of course when we calculated the UV dimension, the appearance of the new sources had to be taken into account. It turns out that for $\dfrac{1}{3} < p < 1$ the two holes are left/right movers, while for $p < \dfrac{1}{3}$ they remain central. Calculating the UV conformal dimensions we obtain

$$\Delta^{\pm} = \frac{p}{p+1} \, , \tag{4.53}$$

so the ultraviolet limit of this state is a linear combination of the vertex operators $V_{\pm 1,0}$ of the

$c = 1$ UV CFT. This is in perfect agreement with the TCS calculations performed by us as in table 4.2.

How does this change of sign in the derivative of Z affect the iteration scheme for the NLIE (see section 4.4)? The two new zeros of $Z(\vartheta)$, which is a complex analytic function apart from logarithmic branch cuts, actually correspond to singularities of the logarithmic term in the NLIE (3.54). They come along the imaginary axis in the ϑ plane as we decrease l, and at a certain point they cross our integration contour which runs parallel to the real axis at distance η. As they make the logarithmic term in our NLIE (3.54) singular, they blow up our iteration scheme. After reaching the origin of the ϑ plane (at exactly the radius where the derivative of Z becomes 0), they continue to move along the real axis, which corresponds to crossing a square root branch cut.

This problem of numerically solve NLIE appears in all the cases where special roots/holes are taken into account (e.g. the "-" vacuum, the two holes-close quantized with "-" and so on).

We do not go into details here as this problem is currently under investigation[2]. We just remark that these issues prove to be highly nontrivial and for the time being, unfortunately, they prevent us from having a reliable numeric scheme for the NLIE below the critical volume.

One can estimate the volume where the slope of the counting function changes sign by neglecting the integral of the logarithmic term. The result is

$$l_{critical} = \frac{2}{\cos \dfrac{p\pi}{2}} \tag{4.54}$$

which gives a value of around 2.22 for $p = 2/7$ and 2.13 for $p = 2/9$. The actual limiting value is a bit higher, partly due to the finite value of η used in the iteration program and partly because the iteration already destabilizes when the singularities come close enough to the contours. It must also be noted that the integral term cannot eventually be neglected when the singularities are close to the contour, which is an additional reason why (4.54) is just a crude estimate.

We make a short digression to examine the UV limit of the second breather B_2. The second breather at rest is described by a wide pair at positions

$$\vartheta = \pm i \frac{\pi}{2} \ .$$

Calculating the UV conformal dimension we get

$$\Delta^+ = \Delta^- = \frac{p}{p+1} \ ,$$

which turns out to be the same as that of the first one (4.53), i.e. this state must originate from the other linearly independent combination of the vertex operators $V_{\pm 1,0}$ in the ultraviolet. This is again in perfect agreement with TCS and confirms a result by Pallua and Prester [29] who used XXZ chain in transverse magnetic field to regularize sine-Gordon theory. They calculated scaling functions numerically on a finite lattice for several concrete values of p, and arrived at this conclusion by looking at the numerical data. However, our method to compute UV dimensions gives us an *exact analytic formula* and therefore much stronger evidence. This result is interesting because it invalidates a conjecture made previously by Klassen and Melzer [20] who identified the second breather as a linear combination of $V_{\pm 2,0}$.

To close this section, we present the lowest lying example of a two-breather state, containing two B_1 particles with zero total momentum. It turns out that this is a state for which the numerical iteration of the NLIE is not plagued with the problem found above for the first breather. Locality

---

[2] Work in progress in collaboration with P. E. Dorey and C. Dunning, Durham.

constrains the state to be quantized with half-integers and for lowest energy the quantum numbers of the self-conjugate roots must take the values

$$I_1 = \frac{1}{2} \ , \ I_2 = -\frac{1}{2}$$

We remark that in contrast to the case of holes, the self-conjugate root with $I > 0$ moves to the left, while the one with $I < 0$ moves to the right. This is due to the fact that the second determination of Z is in general a monotonically decreasing function on the self-conjugate line. In order to determine the position of the two self-conjugate roots we need the second determination of Z. The second determination of the self-conjugate root source turns out to be

$$(\chi_{II}(\vartheta))_{II} = i \log \frac{i \sin \pi p - \sinh \vartheta}{i \sin \pi p + \sinh \vartheta} \ .$$

Up to some signs, this is just the phase shift which arises when two breathers scatter on each other, which is exactly why the IR analysis gives the correct scattering amplitude. Using this formula, we obtained the numerical data presented in table 4.3. The UV limit for this state can

l	TCS	NLIE
1.0	12.1601	12.159257
1.5	8.20139	8.2006130
2.0	6.24771	6.2465898
2.5	5.09489	5.0937037
3.0	4.34132	4.3397021
3.5	3.81513	3.8129798
4.0	3.43020	3.4275967
4.5	3.13912	3.1357441
5.0	2.91308	2.9089439

Table 4.3:   The two-breather state at $p = \frac{2}{7}$.

be calculated from NLIE to be a symmetric first level descendent of the vacuum with weights

$$\Delta^+ = \Delta^- = 1 \ ,$$

which agrees with TCS. (Note that this descendent exists due to the fact that there is a $\hat{U}(1)_L \times \hat{U}(1)_R$ Kac-Moody symmetry at $c = 1$: this state exactly corresponds to the combination of the left and right moving currents $J\bar{J}$.)

4.7 α twist and minimal models (the ground state)

It is known from [23] that by twisting the Bethe Ansatz Equations of the six vertex model as indicated in section 2.5, the twisted model shows the critical behaviour of conformal minimal models (the untwisted critical behaviour corresponds to $c = 1$). Moreover, in recent papers, Al. Zamolodchikov has put forward the idea of modifying sine-Gordon theory by a twist α [30] to deal with conformal minimal models. As a consequence of this two ideas, the Bethe equations used to obtain NLIE contained the twist (2.37) ω. In the NLIE, as shown in section 3.5, the twist is parametrized by α (3.42).

Looking at the ground state, that in analogy with sine-Gordon is expected to be a sea of real roots, the source in NLIE is put to zero $g(\vartheta) = 0$ (3.37).

In analogy with the sine-Gordon ground state, we can choose half-integer quantization rule with $\delta = 0$. The expression for conformal dimensions (4.26) gives:

$$\Delta^{\pm} = \frac{c-1}{24} + \frac{1}{4}\frac{p}{p+1}\left(\frac{\alpha}{\pi}\right)^2$$

corresponding to an effective central charge

$$\tilde{c} = 1 - \frac{6p}{p+1}\left(\frac{\alpha}{\pi}\right)^2 \tag{4.55}$$

(the effective central charge is defined in (4.5)). Only in the unitary models the $\tilde{c}$ is the Virasoro central charge. Furthermore, it is well-known that the perturbation of the Virasoro minimal model $Vir(r,s)$ by its relevant primary operator $\Phi_{(1,3)}$ is integrable and is described by an RSOS restriction of sine-Gordon theory [31] with

$$p = \frac{r}{s-r} \ . \tag{4.56}$$

We will use for this model the shorthand notation $Vir(r,s) + \Phi_{(1,3)}$. Using the rule suggested in (3.60) for ω and the expression (3.42) for α gives: $\alpha = \pi/r$ (the additional integer terms are excluded, for the moment). Then

$$\tilde{c} = 1 - \frac{6}{rs} \ ,$$

which is exactly the *effective central charge* of the minimal model $Vir(r,s)$. Therefore one can expect that the twisted equation describes the ground state of the model $Vir(r,s) + \Phi_{(1,3)}$. In fact, Fioravanti et al. [32] calculated these scaling functions for the unitary case $s = r+1$ and showed that they match perfectly with the TBA predictions already available. Moreover, choosing the following values for the twist

$$\alpha = \pm\frac{k\pi}{r} \ , \ k = 1\dots r-1 \tag{4.57}$$

they obtained the conformal weights of the operators $\Phi_{(k,k)}$, $k = 1\dots r-1$ in the UV limit (the sign choice is just a matter of convention). In our notation, $\Phi_{(q,q')}$ denotes the primary field with conformal weights

$$h^+ = h^- = \frac{(qs - q'r)^2 - (s-r)^2}{4sr} \ . \tag{4.58}$$

The models $Vir(r,s) + \Phi_{(1,3)}$ have exactly $r-1$ ground states. In fact, one can see from the fusion rules that the matrix of the operator $\Phi_{(1,3)}$ is block diagonal with exactly $r-1$ blocks in the Hilbert space made up of states with the same left and right primary weights. In each of these blocks, there is exactly one ground state and for the unitary series $s = r+1$, it was conjectured in [33] that their UV limits are the states corresponding to $\Phi_{(k,k)}$. One can check that in the general nonunitary case the twists (4.57) correspond in the UV limit to the lowest dimension operators among each of the $r-1$ different blocks of primaries (see explicit examples later).

These ground states are degenerate in infinite volume, but for finite l they split; their gaps decay exponentially as $l \to \infty$. In the unitary case, they were first analyzed in the context of the NLIE in [32] where it was shown that the NLIE predictions perfectly match with the TBA results already available for the unitary series.

However, ground states for nonunitary models have not been treated so far and therefore now we proceed to give examples of that. The models we select are the ones that will be used for

comparison in the case of excited states as well. The first is for the scaling Lee-Yang model $Vir(2,5) + \Phi_{(1,3)}$, for which we have also given data from TCS [15] and TBA [16] for comparison (table 4.4).

$$M_B = 2\mathcal{M} \sin \frac{\pi p}{2} = \sqrt{3}\mathcal{M}$$

is the mass of the fundamental particle of the Lee-Yang model (this is more natural here than using the mass $\mathcal{M}$ of the soliton of the unrestricted sine-Gordon model as a scale, since the soliton disappears entirely from the spectrum after RSOS restriction) and call

$$l_B = M_B L = \sqrt{3}l$$

where l is the variable appearing in NLIE. There is only one independent value of the twist, which we choose to be

$$\alpha = \frac{\pi}{2} \ .$$

Here and in all other subsequent calculations the TCS data were normalized using the analogue of the coupling-mass gap relation (1.18) from [25]. There is only one ground state in this model,

l_B	TCS	NLIE	TBA
0.1	-2.0835015786	-2.0835015787	-2.0835015786
0.5	-0.3803475256	-0.3803475281	-0.3803475281
1.0	-0.1532068463	-0.1532068801	-0.1532068801
1.5	-0.0763483319	-0.0763484842	-0.0763484842
2.0	-0.0406269362	-0.0406273676	-0.0406273676
2.5	-0.0222292932	-0.0222302407	-0.0222302407
3.0	-0.0123492438	-0.0123510173	-0.0123510173
3.5	-0.0069309029	-0.0069338817	-0.0069338817
4.0	-0.0039198117	-0.0039244430	-0.0039244430
5.0	-0.0012721417	-0.0012816882	-0.0012816882

Table 4.4: The vacuum of the Virasoro minimal model $Vir(2,5)$ perturbed by $\Phi_{(1,3)}$. The energy and the volume are normalized to the mass of the lowest excitation M_B, which is the first breather of the unrestricted sine-Gordon model. The TCS data shown have the predicted bulk energy term subtracted.

which corresponds to the primary field with conformal weights

$$\Delta^+ = \Delta^- = -\frac{1}{5} \ ,$$

which is in agreement with TBA and TCS predictions. We have also found a perfect agreement for the models $Vir(2,7) + \Phi_{(1,3)}$ and $Vir(2,9) + \Phi_{(1,3)}$, but we do not present those data here. We remark that the TCS for the minimal models converges much better than the one for $c = 1$ theories: all TCS data in table 4.4 and subsequent ones were produced by taking a few hundred states and in some fortunate cases (e.g. the ground state of the scaling Lee-Yang model for small values of l) we were able to produce data with up to $9 - 10$ digits of accuracy! The better convergence meant that all the computation could be done with the computer algebra program *Mathematica*, greatly simplifying the programming work.

All the models of the class $Vir(2, 2n+1) + \Phi_{(1,3)}$ have only one ground state. For models with two ground states, we can take a look at $Vir(3,5)$ ($Vir(3,7)$ was taken into account in [34]). For

$Vir(3,5)$ the ultraviolet spectrum is defined by the following Kac table, where the weight (4.58) of the field $\Phi_{(k,l)}$ is found in the k-th row and l-th column.

0	$-\frac{1}{20}$	$\frac{1}{5}$	$\frac{3}{4}$
$\frac{3}{4}$	$\frac{1}{5}$	$-\frac{1}{20}$	0

The two blocks of the perturbing operator $\Phi_{(1,3)}$ are defined by the fields $\{\Phi_{(1,2)}, \Phi_{(1,4)}\}$ and $\{\Phi_{(1,1)}, \Phi_{(1,3)}\}$, respectively. The ground states correspond in the UV to the operators $\Phi_{(1,2)}$ and $\Phi_{(1,1)}$, as can be checked directly using formulae (4.55), (4.56) and (4.57).

We also have TBA data to compare with, using the TBA equation written by Christe and Martins [35]. The lower-lying ground state is obtained directly from their TBA, while for the other we used the idea of Fendley of twisting the TBA equation [36]. The numerical results are presented in tables 4.5 and 4.6.

In the case $Vir(3,7)$ treated in [34], it was possible only to have a comparison with TCS results, but it still looked pretty convincing. To summarize, we now have sufficient evidence

l	TCS	NLIE	TBA
0.1	-3.074916	-3.0749130189	-3.0749130190
0.3	-0.944161	-0.9441276204	-0.9441276204
0.5	-0.509764	-0.5096602194	-0.5096602194
0.8	-0.265436	-0.2651431026	-0.2651431026
1.0	-0.186038	-0.1855606546	-0.1855606546
1.5	-0.087300	-0.0861426792	-0.0861426792
2.0	-0.045910	-0.0437473815	-0.0437473815
2.5	-0.026746	-0.0232421927	-0.0232421927
3.0	-0.017868	-0.0126823057	-0.0126823057
4.0	-0.013546	-0.0039607326	-0.0039607326

Table 4.5: One of the two ground states of the Virasoro minimal model $Vir(3,5)$ perturbed by $\Phi_{(1,3)}$, corresponding to $\alpha = \frac{\pi}{3}$. The energy and the volume are normalized to the mass of the lowest excitation, which is the soliton of the unrestricted sine-Gordon model. The TCS data shown have the predicted bulk energy term subtracted.

l	TCS	NLIE	TBA
0.1	3.117844	3.1178476855	3.1178476853
0.3	0.985360	0.9853990810	0.9853990810
0.5	0.540427	0.5405470784	0.5405470784
0.8	0.282725	0.2830552991	0.2830552991
1.0	0.197143	0.1976769278	0.1976769278
1.5	0.089277	0.0905539780	0.0905539780
2.0	0.042960	0.0453290013	0.0453290013
2.5	0.019978	0.0238075022	0.0238075022
3.0	0.007209	0.0128843786	0.0128843786
4.0	-0.006592	0.0039866371	0.0039866371

Table 4.6: The other ground state of the Virasoro minimal model $Vir(3,5)$ perturbed by $\Phi_{(1,3)}$, corresponding to $\alpha = \frac{2\pi}{3}$. The energy and the volume are normalized to the mass of the lowest excitation, which is the soliton of the unrestricted sine-Gordon model. The TCS data shown have the predicted bulk energy term subtracted.

to believe that the α-twisted NLIE describes the correct scaling functions for ground states of minimal models perturbed by $\Phi_{(1,3)}$ *in unitary and nonunitary case.* However, the NLIE for sine-Gordon is known to work for excited states as well. But how do we get the excited state spectrum of the minimal models now?

4.8 α twist and minimal models: excited states

4.8.1 The choice of α

From now on we restrict ourselves to the case of neutral (i.e. $S = 0$) states. It is easy to see that even for states with a zero charge the relation between α and ω is highly nontrivial.

Now we proceed to show that choosing the value of ω as

$$\omega = \frac{k\pi}{p+1}$$

where k is integer, we can reproduce all the required values of α listed in equation (4.57). Observe that this expression for ω is different from (3.60), but totally equivalent, as will be clear soon. First of all, we substitute the value of p from (4.56) to obtain

$$\omega = \frac{k(s-r)\pi}{s} .$$

Since r and s are relative primes, the independent values of $\omega \mod \pi$ can be written as

$$\omega = \frac{l\pi}{s} , \ l = 0, \dots , s-1 .$$

For $S = 0$, we can rewrite the formula (3.42) as follows

$$\alpha = \frac{l\pi}{r} + \frac{2r-s}{2r}\pi \left(\left[\frac{1}{2} + \frac{l}{s} \right] - \left[\frac{1}{2} - \frac{l}{s} \right] \right) .$$

We are interested only in the value of $\alpha \mod \pi$, since using the parameter δ one can effectively shift α by π. This leaves us with the formula

$$\alpha = \frac{l\pi}{r} - \frac{s\pi}{2r} \left(\left[\frac{1}{2} + \frac{l}{s} \right] - \left[\frac{1}{2} - \frac{l}{s} \right] \right) .$$

The first possibility is that $l < \frac{s}{2}$, which simply gives us the values

$$\alpha = \frac{l\pi}{r}.$$

When s is even, we can have $l = \frac{s}{2}$, which gives us $\alpha = 0$. Finally, when $l > \frac{s}{2}$, we get the values

$$\alpha = \frac{(l-s)\pi}{r} .$$

It is easy to check that these formulae reproduce every value

$$\alpha = \frac{n\pi}{r} \mod \pi$$

at least once, as required by (4.57), using the fact that $s > r$ and that the values above form an uninterrupted sequence of s numbers (or when s is even, of $s-1$ numbers, the zero repeated) with equal distances $\frac{\pi}{r}$.

As we have already seen in the previous section, all the values

$$\alpha = \frac{k\pi}{r} \ , \ k = 1, \dots, r-1 \tag{4.59}$$

are necessary to reproduce correctly the $r-1$ ground states of the model $Vir(r,s) + \Phi_{(1,3)}$.

The twisted lattice Bethe Ansatz was analyzed by de Vega and Giacomini in [37]. On the lattice, passing from the sine-Gordon model to the perturbed Virasoro model amounts to going from the six-vertex model to a lattice RSOS model. In [37] it was shown that to obtain all the states of the RSOS model it is necessary to take all the twists

$$\omega = \frac{k\pi}{p+1} \ \ \text{mod} \ \ \pi$$

into account. The fact that not all these twists correspond to inequivalent values of α and so to different physical states is a consequence of the RSOS truncation.

To close this section we remark that the parameter α drops out of the second determination of Z in the attractive regime. This is important because as a consequence the IR asymptotics of the breather states does not depend on α and so the S-matrices involving breathers are unchanged. In fact, scattering amplitudes between solitons and breathers remain unchanged too, as can be seen from examining the argument that we used to derive them in section 4.6.4. This matches with the fact that the RSOS restriction from sine-Gordon theory to perturbed minimal models does not modify scattering amplitudes that involve two breathers or a breather and soliton [31].

4.8.2   The UV limit

There is in fact a very simple intuitive argument to show that the states we get from NLIE with an α twist are related to the minimal models in the UV limit. Let us first recall that the UV limit of the $\alpha = 0$ NLIE yields the vertex operators $V_{(n,m)}$ and their descendants (4.27, 4.28).

Let us look at the conformal dimensions. First note that because the value of α for a minimal model is never a multiple of π, one does not expect central sources in the UV limit but only right/movers or left movers. Indeed, in all the examples of sine-Gordon with central sources, the left-right symmetry (i.e. $Z(-\vartheta) = -Z(\vartheta)$ on the real axis) of the NLIE was crucial. This symmetry, however, only holds for $\alpha = 0$ or π. As a consequence we have

$$S^0 = 0, \qquad S = S^+ + S^- \ ,$$

and in addition $\mathcal{Q}_+(-\infty) = \mathcal{Q}_-(+\infty)$, which means that only *one-plateau systems* are allowed in the twisted case.

Using the formulas (4.26, 4.27) for the UV limit of the NLIE, one can see that introducing $\alpha \neq 0$ is equivalent to shifting the quantum number $n_\pm$ to $n_\pm + \frac{\alpha}{2\pi}$. One has to be careful that since the value of the central charge is shifted from 1 to the one of the minimal model, we have to take this shift into account when computing the conformal weight from the leading UV behaviour of the energy level (4.5). We put in (4.26) the value

$$\alpha = \frac{j\pi}{r}, \ j = 1, \dots, r-1 \ ,$$

as in (4.59), and the central charge

$$c = 1 - \frac{6(r-s)^2}{rs}$$

of the minimal model $Vir(r,s)$, as in section 4.7. By a computation similar to the one done in section 4.6 to obtain (4.27, 4.28, 4.30) one can obtain the following expression for conformal dimensions:

$$\Delta^\pm = \frac{(ls - l'_\pm r)^2 - (s-r)^2}{4rs} + N_\pm$$
$$l = S \tag{4.60}$$
$$l'_\pm = \pm \left(\delta - \frac{j}{r} + 2k_\pm - 2k_W^\pm \right) - 2\left(S - 2S^\pm \right).$$

The expression of $N_\pm$ is exactly the same that appears in (4.30). Moreover, from the formulae (4.26, 4.60) it is also clear that in general

$$2\left(\Delta^+ - \Delta^- \right) = 2S\frac{\alpha}{\pi} \mod 1$$

because only one plateau systems can take place, and so we see that general charged states will have fractional Lorentz spin. Actually, it is known that charged states in the models $Vir(r,s) + \Phi_{(1,3)}$ generally have fractional Lorentz spin [39].

Comparing the first line of (4.60) with (4.58) one observes that it can represent the conformal dimensions of an operator $\Phi_{(q,q')}$ only if some conditions are verified. The most general one is

$$\left(ls - l'r \right)^2 = \left(qs - q'r \right)^2 + 2rs \cdot \text{integer}, \qquad 1 \le q \le r-1, \, 1 \le q' \le s-1$$

(the l, l' are not integer numbers in general). Observe that it is an arithmetic (Diophantine) equation in q, q' and the unknown integer.

It is convenient to treat some specific cases, because, as for the sine-Gordon case, there is no proof about the general behaviour of $l'_\pm$ and $N_\pm$.

In the unitary $p = r$, $s = r + 1$ and neutral case $S = 0$ the resulting conformal weights take the form

$$\Delta^+ = \Delta^- = \frac{(2np + l)^2 - 1}{4p(p+1)} \ . \tag{4.61}$$

We see that this is the weight of the field $\Phi_{(l,l-2n)}$ in the minimal model $Vir(p, p+1)$, however, in order not to overflow the Kac table, the range of n must be restricted as

$$1 \le l - 2n \le p \ .$$

For charged states, a similar calculation can be performed.

By an inspection of the formula (4.26), for any state with $S = 0$, the property to have only one plateau implies that

$$\Delta^+ - \Delta^-$$

is integer or half-integer. In fact, choosing the quantization rule and the parameter δ in an appropriate way, one can ensure that this difference is integer (see [9, 28]). This means that the UV limit of any neutral state is either a field occurring in the ADE classification of modular invariants [38] or (in case we choose δ so that $\Delta^+ - \Delta^-$ is half-integer) it is a field from a fermionic version of the minimal model [20].

Until now it is not clear whether the weights actually stay inside the Kac table, for which in the unitary case one must require

$$1 < l - 2k + 4S^+ < p \ .$$

Due to the fact that the configuration of sources in the UV may be very non-trivially related to the one in the IR, this condition is very hard to check in general, but no concrete examples that we calculated have ever violated this bound.

4.9 Concrete examples of excited states

4.9.1 The $Vir(2, 2n+1) + \Phi(1,3)$ series

Let us start with examining the scaling Lee-Yang model $Vir(2,5) + \Phi_{(1,3)}$. There is only one independent value of the twist which we choose as

$$\alpha = \frac{\pi}{2} \, ,$$

since we have a single ground state, and as a result there are no kinks in the spectrum. We fix the value of α as above, so we still have a freedom of choosing δ. This can be done by matching to the UV dimensions: if for a certain state we choose the wrong value of δ, we find a conformal dimension that is not present in the Kac table of the model.

The excited states are multi-particle states of the first breather of the corresponding unrestricted sine-Gordon model, which has

$$p = \frac{2}{3}.$$

Now one can calculate the state containing one particle at rest. We find the numerical data presented in table 4.7.

It turns out that as we decrease l, the self-conjugate root starts moving to the right. It does not remain in the middle like in the $\alpha = 0$ case, which is to be expected since for nonzero α we have no left/right symmetry. However, the total momentum of the state still remains zero due to a contribution from the integral term in momentum equation (3.59). One can see that once again

l_B	TCS	NLIE
0.1	23.05277	n/a
0.5	4.679779	n/a
1.0	2.447376	n/a
1.5	1.748874	n/a
2.0	1.430883	n/a
2.6	1.238051	1.238012(#)
3.0	1.164321	1.164319
3.5	1.105220	1.105196
4.0	1.068256	1.068237
5.0	1.029356	1.029348

Table 4.7: The first excited state of the scaling Lee-Yang model. The energy and the volume are normalized to the mass of the lowest excitation, which is the first breather of the unrestricted sine-Gordon model. The TCS data shown have the predicted bulk energy term subtracted.

we have the phenomenon noticed in the case of the first breather of sine-Gordon theory, namely the appearance of the special root and its two accompanying holes, so the iteration breaks down again around $l = 2.5$. The (#) in the table 4.7 written after the NLIE result for $l = 2.6$ means that due to the fact that the singularities corresponding to the new holes and the special root are just about to cross the contour and upset the iteration scheme, the NLIE result becomes less precise. We will use this notation on later occasions too. In any case, the agreement still looks quite convincing.

Let us now look at the UV spectrum of the model. We know that the Lee-Yang model contains only two primary fields, the identity $\mathbb{I}$ and the field φ with left/right conformal weights

$$\Delta^+ = \Delta^- = -\frac{1}{5} \, .$$

In fact, the ground state of the massive model corresponds to φ in the UV limit. One can compute the UV limit of the first particle from the NLIE too, taking into account the appearance of the special root and the holes. It turns out that the special root and one of the holes moves to the left together with the self-conjugate root, while the other hole moves to the right. The result is

$$\Delta^+ = \Delta^- = 0 \; ,$$

i.e. the identity operator $\mathbb{I}$, which fits nicely with the TCS data (see also [15]).

Let us look now at moving breathers. If the self-conjugate root has Bethe quantum number $I = 1$, the corresponding state will have momentum quantum number 1, i.e.

$$P = \frac{2\pi}{R} \; ,$$

and in the UV $\Delta^+ - \Delta^- = 1$. One can note from the numerical data presented in table 4.8 that the special root does not appear here. The reason is that the self-conjugate root moves to the left and the real part of its position ϑ is given to leading order by

$$\sinh(\Re e \, \vartheta) \sim -\frac{2\pi I}{l_B} \; .$$

As a result, the contribution to the derivative of Z from the $l \sinh \vartheta$ term remains finite when $l \to 0$. In the previous example of the particle at rest the left-moving nature of the self-conjugate root when $I = 0$ does not prevent the occurrence of the breakdown in the iteration scheme: since its Bethe quantum number is zero, it does not move fast enough to the left in order to balance the negative contribution to derivative of Z coming from the self-conjugate root source. At the moment we have no way of predicting analytically whether or not there will be specials in the UV limit: we just use the numerical results to establish the configuration for the evaluation of UV weights, supplemented with a study of the self-consistency of the solution of the plateau equation (4.16). The UV dimensions for the moving breather turn out to correspond to the state $L_{-1}\varphi$.

l_B	TCS	NLIE
0.1	60.75048	60.74682
0.5	12.20618	12.20561
1.0	6.182516	6.182363
1.5	4.202938	4.202915
2.0	3.231734	3.231640
2.5	2.662186	2.662110
3.0	2.292273	2.292231
3.5	2.035552	2.035530
4.0	1.848892	1.848849
5.0	1.599792	1.599762

Table 4.8:   The one-particle states with Lorentz spin 1 of the scaling Lee-Yang model. The energy and the volume are normalized to the mass of the lowest excitation, which is the first breather of the unrestricted sine-Gordon model. The TCS data shown have the predicted bulk energy term subtracted.

One can similarly compute the UV dimensions for some other excited states. For example, the two-particle states with half-integer Bethe quantum numbers $I_1 > 0$, $I_2 < 0$ for the two self-conjugate roots are found to have

$$\Delta^+ = -\frac{1}{5} + I_1 + \frac{1}{2} \; , \; \Delta^- = -\frac{1}{5} - I_2 + \frac{1}{2} \; ,$$

in agreement with TCS data which show that they correspond in the UV to descendent states of φ. The first such state with quantum numbers

$$I_1 = \frac{1}{2} \ , \ I_2 = -\frac{1}{2}$$

corresponds in the UV to $L_{-1}\bar{L}_{-1}\varphi$ and is given numerically in table 4.9.

l	TCS	NLIE
0.1	123.583	123.5693
0.5	24.7806	24.77936
1.0	12.4870	12.48635
1.5	8.42926	8.428693
2.0	6.42931	6.429201
3.0	4.48444	4.484209
4.0	3.56367	3.563519
5.0	3.04899	3.048881

Table 4.9: The lowest lying zero-momentum two-particle state in the scaling Lee-Yang model as computed from the NLIE and compared with TCS.

The lowest lying three-particle state of zero momentum, with Bethe quantum numbers $(-1, 0, 1)$ corresponds to the left/right symmetric second descendent of the identity field, i.e. to the field $T\bar{T}$, where T denotes the energy-momentum tensor. This is very interesting, since from experience with NLIE UV calculations one would naively expect this to be a first descendent (descendent numbers are usually linked to the sum of Bethe quantum numbers of left/right moving particles and this state is the lowest possible descendent of the identity $\mathbb{I}$). However, the field $L_{-1}\bar{L}_{-1}\mathbb{I}$ is well-known to be a null field in any conformal field theory.

The above correspondences are again confirmed by comparing to TCS (see the wonderful figures in [15]). In general, one can establish the rule that states with odd number of particles must be quantized by integers ($\delta = 1$), while those containing even number of particles must be quantized by half-integers ($\delta = 0$) in order to reproduce correctly the spectrum of the scaling Lee-Yang model.

We conducted similar studies for the models $Vir(2, 7) + \Phi_{(1,3)}$ and $Vir(2, 9) + \Phi_{(1,3)}$ and found similarly good agreement with TCS data. For the first one-particle state of the model $Vir(2, 7) + \Phi_{(1,3)}$ we also checked our results against the TBA data in the numerical tables of [40] and found agreement with the TBA results.

Given the choice of α above, the correct rule of quantization in all of the models $Vir(2, 2n + 1) + \Phi_{(1,3)}$ is

$$\delta = M_{sc} \ \mathrm{mod} \ 2 \ ,$$

where M_{sc} is the number of self-conjugate roots in the source corresponding to the state. This is exactly the same rule as the one established for pure sine-Gordon theory in [9]. In the presence of the twist, such a rule of course has meaning only together with a definite convention for the choice of α.

4.9.2 One-breather states in the $Vir(3, 7)$ case

It is interesting to note that in the case of $Vir(3, n)$ models, all the neutral states must come in two copies, since they can be built on top of either of the two ground states. We take the example

of the $Vir(3, 7)$ model and the states corresponding to a breather at rest. We have

$$p = \frac{3}{4}$$

but now there are two inequivalent values for the twist

$$\alpha = \frac{\pi}{3} \ , \ \frac{2\pi}{3} \ .$$

When $\alpha = 0$, we can calculate the critical value of l to be $l_{critical} = 5.23$ using (4.54). In this case, the twist helps a bit, because it makes the self-conjugate root a left mover; it is intuitively clear that the bigger the twist, the more it lowers the eventual value of $l_{crtical}$, which is in accord with the numerical results of table 4.10. From the TCS data one can identify that breather #1 is really the one-particle state in the sector of ground state #1 ($\alpha = \pi/3$), while breather #2 is in the sector over ground state #2 ($\alpha = 2\pi/3$).

A direct calculation of the conformal weights gives the following results:$\Delta^+ = \Delta^- = \frac{3}{28}$for breather #1 and $\Delta^+ = \Delta^- = 0$for breather #2, which are in complete agreement with the TCS data. We also checked the two different states containing two breathers with Bethe quantum numbers$I_1 = \frac{1}{2}$, $I_2 = -\frac{1}{2}$,and found an equally excellent numerical agreement with TCS. Just like in the case of sine-Gordon and scaling Lee-Yang model, for these states one can continue the iteration of the NLIE down to any small value of l, although at the expense of a growing number of necessary iterations to achieve the prescribed precision.

	breather 1		breather 2	
l	TCS	NLIE	TCS	NLIE
0.1	32.21645	n/a	18.76030	n/a
0.5	6.671964	n/a	4.037716	n/a
1.0	3.662027	n/a	2.434501	2.434431(#)
1.5	2.769403	n/a	2.027227	2.027213
2.0	2.385451	n/a	1.884404	1.884388
2.5	2.190232	n/a	1.829459	1.829456
3.0	2.079959	n/a	1.809244	1.809248
3.5	2.012596	n/a	1.803873	1.803886
4.0	1.968808	1.968784(#)	1.804937	1.804953
4.5	1.938895	1.938889	1.808633	1.808658
5.0	1.917648	1.917635	1.813191	1.813224

Table 4.10:   The two one-breather states of the Virasoro minimal model $Vir(3, 7)$ perturbed by $\Phi_{(1,3)}$. The energy and the volume are normalized to the mass of the kink, which is the soliton of the unrestricted sine-Gordon model. Breather #1 has $\alpha = \frac{\pi}{3}$, while breather #2 corresponds to $\alpha = \frac{2\pi}{3}$. The TCS data shown have the predicted bulk energy term subtracted.

4.10   Conclusions

In this thesis it is studied how the nonlinear integral equation deduced from the light cone lattice model of [4] describes the excited states of the sine-Gordon/massive Thirring theory. The most important results are summarized as follows:

1. A derivation of the fundamental NLIE is presented from the light cone lattice which correctly takes into account the behaviour of the multivalued complex logarithm function.

2. By examining the infrared limits of the equation it has been shown that (1) it leads to the correct two-particle S-matrices for both scattering states and bounded states; (2) it is in agreement with the predictions of the TCS method if one chooses the correct quantization conditions for the source terms.

3. By computing the UV conformal weights from the NLIE we have shown that it is consistent with the UV spectrum of sG/mTh theory only if we choose the parameter δ (i.e. the quantization rule) as indicated in (4.31).

4. The predictions of the NLIE have been verified by comparing them to results coming from the TCS approach (for sG/mTh).

5. The framework required to deal with minimal models perturbed by $\Phi_{(1,3)}$ is built up. Many examples and numerical/analytical checks are given for the ground state in the unitary [32] and non unitary cases.

6. All the conformal dimensions can be reproduced (Kac table) with the convenient choice of the twist (4.59). The particular relation suggested in [43] is not enough to describe the whole spectrum.

7. The IR computations given in section 4.6.4 reproduce correctly the S-matrix of perturbed minimal models in the attractive regime (at list in the cases involving only solitons), because the attractive second determination drops the twist.

8. Numerical calculations of concrete examples give a strong evidence for the correctness of the energy levels derived from the twisted NLIE for excited states.

The understanding of "(twisted) sine-Gordon NLIE" and of the finite size behaviour of the continuum theory defined from the NLIE (3.54) is not quite complete. Indeed some open questions have not an answer, until now and also further interesting developments can take place:

1. Is the set of scaling functions provided by the NLIE complete i.e. can we find to every sG/mTh or minimal model state a solution of the NLIE describing its finite volume behaviour? This can be called a "counting problem". The main difficulty is that the structure of the solutions is highly dependent on the value of the coupling constant – to see that it is enough to consider e.g. the appearance of special sources.

2. The multi-kink states characteristic of the perturbed minimal models (except for the series $Vir(2, 2n + 1)$) have been omitted in the analysis so far performed. Although the general treatment of the IR spectrum in section 4.6.4 is valid for those states too, a detailed description is far more complicated than for states which contain only breathers and is left open to further studies.

3. There is also an unresolved technical difficulty, namely that the source configuration of the NLIE may change as we vary the volume parameter l. Typically what happens is that while the counting function Z is monotonic on the real axis for large volume, this may change as we lower the value of l and so-called special sources (and accompanying holes) may appear. We do not as yet have any consistent and tractable numerical iteration scheme to handle this situation, although the analytic UV calculations and intuitive arguments show that the appearance of these terms in the NLIE is consistent with all expectations coming from the known properties of perturbed CFT. In addition, in the range of l where we can iterate the NLIE without difficulty, our numerical results show perfect agreement with TCS. We want

to emphasize that these transitions are not physical: the counting function Z and the energy of the state are expected to vary analytically with the volume. It is just their description by the NLIE with requires a modification of source terms. As it was pointed out also in [8, 9], the whole issue is related to the choice of the branch of the logarithmic term in the NLIE (3.54).

4. The problem pointed out at the previous point is very similar to the behaviour of singularities encountered in the study of the analytic continuation of the TBA equation [18] and we can hope that establishing a closer link between the two approaches can help to clarify the situation. From the form of the source terms in the NLIE it seems likely that the excited state equations can be obtained by an analytic continuation procedure analogous to the one used in TBA [18] to obtain the excited state TBA equations. Certain features of the arrangement of the complex roots in the attractive regime and their behaviour at breather thresholds also point into this direction. This an interesting question to investigate because it can shed light on the organization of the space of states and can lead closer to solving the counting problem described above.

5. Even if on the lattice the Bethe vectors given in (2.37) completely describe the Hilbert space of the XXZ chain, the form of eigenvectors for continuum energy and momentum is completely unknown. This fact reflects the unresolved question of the form of energy and momentum eigenvectors for the minkowskian sine-Gordon theory (the Faddeev-Zamolodchikov algebra is only a phenomenological picture). Also the determination of correlation functions is in an early stage, but in recent publications [46] explicit expressions for the field $\left\langle e^{ia\varphi} \right\rangle$ and its descendent are given.

6. The extension of light-cone approach and NLIE to other QFT models is in progress. An interesting extension is the description of finite volume spectrum of Ziber-Mikhailov-Shabat model (imaginary Bullogh-Dodd). A first suggestion in this direction, even if is obtained in a completely different approach, recently appeared in the [44], for the ground state.

The second and fourth points are important because their investigation may lead closer to understanding the relation between the TBA and the NLIE approaches. It is quite likely that establishing a connection between the two methods would facilitate the development of both and may point to some common underlying structure.

As a final remark, I want to speak about an application of the NLIE to a chemical compound, i.e. "copper benzoate" $(\mathrm{Cu}(\mathrm{C_6D_5COO})_2 \cdot 3\mathrm{D_2O})$. Its specific heat has been computed in [45] using the vacuum untwisted ($\alpha = 0$) NLIE, where the finite size L is the inverse temperature $L = (k_B T)^{-1}$. This corresponds to do equilibrium thermodynamics of sine-Gordon model.

A curiosity: in that contest the NLIE is called Thermal Bethe Ansatz, emphasizing the well known relation between statistical mechanics and QFT. Exactly in a similar contest (Heisenberg ferromagnet model) was born the Bethe Ansatz [47].

Appendix A

Fourier transformation: some conventions

Given a bounded continuous function $f(x)$ defined on the whole real axis, its Fourier transform is defined as (all the integrals must be taken on the whole real axis):

$$\tilde{f}(k) = \int dx\, e^{-ikx\frac{1}{p+1}} f(x) \tag{A.1}$$

and the inverse Fourier transform is

$$f(x) = \frac{1}{p+1} \int \frac{dk}{2\pi} e^{ikx\frac{1}{p+1}} \tilde{f}(k). \tag{A.2}$$

The convolution of two functions, defined as follows, can be expressed in terms of the Fourier transforms of the two functions:

$$(f * g)_\theta = \int dx\, f(\theta - x)\, g(x) = \frac{1}{p+1} \int \frac{dk}{2\pi} e^{ik\theta\frac{1}{p+1}} \tilde{f}(k)\tilde{g}(k) \tag{A.3}$$

The following expression holds between the Fourier transforms of a function and its derivative:

$$\tilde{f}(k) = \frac{\tilde{f'}(k)}{ik}(p+1)$$

Appendix B

The function $\phi(\lambda, \nu)$

In this appendix all the important properties of the function ϕ will be clarified. Let

$$\phi(\vartheta, \nu) = i \log \frac{\sinh \dfrac{1}{p+1}(i\pi\nu + \vartheta)}{\sinh \dfrac{1}{p+1}(i\pi\nu - \vartheta)}, \qquad \phi(-\vartheta, \nu) = -\phi(\vartheta, \nu) \quad \forall \quad \vartheta \in \mathbb{C} \tag{B.1}$$

and continuity is required around the real axis. The interest is for $\nu = 1/2$, 1 and $p > 0$. The requirement of oddity implies, for real values of ϑ, that $\phi(0, \nu) = 0$. Oddity and continuity can be implemented only if the fundamental determination (FD) of the logarithm is assumed, in a strip containing the real axis:

$$-\pi < \Im m(\log_{FD} w) \le \pi.$$

This choice implies that ϕ is real on the real axis. The argument of the log has poles and zeros. They are essential singularities for the ϕ function. Their position is given by:

$$\begin{aligned} \Re e\, \vartheta &= 0 \\ \Im m\, \vartheta &= \pm\pi\, (k(p+1) - \nu), \qquad k \in \mathbb{Z}. \end{aligned} \tag{B.2}$$

The fundamental strip around the real axis (FD) is bounded by the first encountered singularity:

$$\vartheta \in \mathbb{R} \times\,]-\min\{\nu\pi,\, \pi\,(p+1-\nu)\},\, \min\{\nu\pi,\, \pi\,(p+1-\nu)\}[\,. \tag{B.3}$$

To extend the definition of (B.1) to the whole plane it is necessary to give a prescription for the position of the cuts (because of the logarithm, in a small closed trip around one of the singularities (B.2), the value of ϕ changes by 2π). This is done as in figure B.1.

The derivative of ϕ is the single value meromorphic function:

$$\phi'(\vartheta, \nu) = \frac{1}{p+1} \frac{2\sin \dfrac{2\nu\pi}{p+1}}{\cosh \dfrac{2\vartheta}{p+1} - \cos \dfrac{2\nu\pi}{p+1}}. \tag{B.4}$$

This shows that, on the real axis, ϕ is monotonically increasing if $0 < \dfrac{\nu\pi}{p+1} < \pi/2$ and decreasing if $\pi/2 < \dfrac{\nu\pi}{p+1} < \pi$. The asymptotic values, for ϑ in the fundamental strip, are:

$$\lim_{\vartheta \to \pm\infty} \phi(\vartheta, \nu) = \pm\pi(1 - \frac{2\nu}{p+1}). \tag{B.5}$$

(a)   (b)
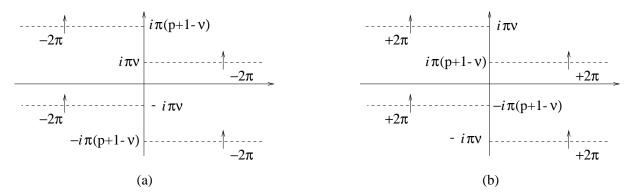
Figure B.1: Positions of singularities and cuts for the function ϕ. (a) in the case $\dfrac{\nu}{p+1} < 1/2$; (b) in the case $\dfrac{\nu}{p+1} > 1/2$. The little arrows indicate the jump in the values of the function.

Out of the fundamental strip, the prescription indicated in figure B.1 must be used.

The Fourier transformation of ϕ' can be obtained from the definition (A.1), using the theorem of residues:

$$\widetilde{\phi}'(k,\nu) = 2\pi \frac{\sinh \dfrac{\pi}{2} \left(\dfrac{p+1-2\nu}{p+1} \right) k}{\sinh \dfrac{\pi}{2} k} \tag{B.6}$$

This formula is the Fourier transform of $\phi'(\vartheta, \nu)$ only for ϑ in the fundamental strip (B.3), because out of this strip new singularities of (B.4) appear in the computation of Fourier transform.

Appendix C

A lemma for UV computations

In [8] the following lemma has been proved. Assume that $f(x)$ satisfies the non-linear integral equation

$$-i\log f(x) = \varphi(x) + 2\,\Im m \int \frac{dy}{i} G(x-y-i\epsilon)\log(1+f(x+i\epsilon))$$

where $\varphi(x)$ is real on the real axis and $G(x) = G(-x)$ is real too, with bounded integral and peaked around the origin. From this equation follows that $f(x)$ has unit modulus on the real axis. To avoid crossing of the branch cut of the logarithm, assume that

$$\text{if} \qquad f(x+i\epsilon) \in \mathbb{R} \qquad \text{then} \qquad f(x+i\epsilon) > -1. \tag{C.1}$$

Then the following expression holds:

$$2\,\Im m \int \frac{dx}{i}\varphi'(x+i\epsilon)\log(1+f(x+i\epsilon)) =$$
$$= -2\,\Re e \int_\Gamma \frac{du}{u}\log(1+u) - \frac{1}{2}\int dx\, G(x)\left(F^2(+\infty) - F^2(-\infty)\right) \tag{C.2}$$

where the curve Γ is any path in the complex plane that goes from $f_- = f(-\infty+i\epsilon)$ to $f_+ = f(+\infty+i\epsilon)$ avoiding the branch cut, i.e. respecting the condition (C.1) and

$$F(x) = 2\,\Im m\,\log(1+f(x+i\epsilon)).$$

In the 6-vertex case all the terms can be made manifest by the identification of G with that defined in (3.21), $f(x) = (-1)^\delta e^{iZ_\pm(x)}$ and $\varphi(x)$ with (4.25).

Consider the kink "+". The integral on the path Γ goes from the points

$$f_- = f(-\infty+i\epsilon) = (-1)^\delta e^{iZ_+(-\infty)} = e^{i\mathcal{Q}_+(-\infty)}$$
$$f_+ = f(+\infty+i\epsilon) = (-1)^\delta e^{iZ_+(+\infty+i\epsilon)} = 0$$

(the first one can be computed with (4.17)). Observe that $|f_-| = 1$ then the path Γ can be composed by an unit radius arc from f_- to the point 1 and a segment from 1 to 0. On the arc the integration variable has unit modulus then it is convenient to do the change of variables $u = e^{i\alpha}$. This simple computation gives

$$-2\,\Re e \int_{arc} \frac{du}{u}\log(1+u) = -\mathcal{Q}_+^2(-\infty).$$

The integration on the segment gives a well known dilogarithmic expression:

$$-2\,\Re e \int_1^0 \frac{du}{u} \log(1+u) = 2 \int_0^1 \frac{du}{u} \log(1+u) = \frac{\pi^2}{6}.$$

The quantities $F(\pm\infty)$, from their definition, give:

$$F(+\infty) = 0$$
$$F(-\infty) = 2\,\Im m\, \log(1 + (-1)^\delta e^{iZ_+(-\infty)}) = \mathcal{Q}_+(-\infty).$$

Remembering now that the integral of G appearing in (C.2) is expressed in (3.33) yields (the computation for the "$-$" kink is completely analogous):

$$2\,\Im m \int \frac{dx}{i} \varphi'_\pm(x+i\eta) \log\left(1 + (-1)^\delta e^{iZ_\pm(x+i\eta)}\right) =$$

$$= \pm\frac{\pi^2}{6} \mp \frac{\mathcal{Q}_\pm^2(\mp\infty)}{4} \frac{p+1}{p}$$

(C.3)

Bibliography

[1] A.B. Zamolodchikov, "Factorized S Matrices And Lattice Statistical Systems," in Khalat-nikov, I.M. (ed.): *Physics Reviews*, **vol. 2**, 1-40

[2] A.B. and Al.B. Zamolodchikov, *Ann. of Phys.* **120** (1979)

[3] R. Baxter, "Exactly solved models in statistical mechanics", Academic Press (London)

[4] C. Destri and H.J. de Vega, *Nucl. Phys.* **B290** (1987) 363

[5] L.D. Faddeev and L.A. Takhtadzhyan, *Russ. Math. Surv.* **34** (1979) 11

[6] H.J. de Vega, *Int. Jour. Mod. Phys.* **A4** (1989) 2371

[7] C. Destri and H.J. de Vega, *Nucl. Phys.* **B438** (1995) 413

[8] C. Destri and H.J. de Vega, *Nucl. Phys.* **B504** (1997) 621

[9] G. Feverati, F. Ravanini and G. Takács, *Nucl. Phys.* **B540** (1999) 543

[10] L. D. Faddeev in *Les Houches Summer Course Proceedings* (1995), hep-th 9605187

[11] C. Destri and H.J. de Vega, *J. Phys.* **A22** (1989) 1229

[12] P. Christe, M. Henkel, "Introduction to Conformal invariance and its Applications to Critical Phenomena", Springer (1993), Berlin

[13] M. Lüscher, *Comm. Math. Phys.* **104** (1986) 177

[14] M. Lüscher, *Comm. Math. Phys.* **105** (1986) 153

[15] V. P. Yurov and A. B. Zamolodchikov, *Int. J. Mod. Phys.* **A5** (1990) 3221

[16] Al. B. Zamolodchikov, *Nucl. Phys.* **B342** (1990) 695

[17] A. Klümper and P.A. Pearce, *J. Stat. Phys.* **64** (1991) 13
A. Klümper, M. Batchelor and P.A. Pearce, *J. Phys.* **A24** (1991) 3111

[18] P. Dorey and R. Tateo, *Nucl. Phys.* **B482** (1996) 639
P. Dorey and R. Tateo, *Nucl. Phys.* **B515** (1998) 575

[19] V. V. Bazhanov, S. L. Lukyanov and A. B. Zamolodchikov, *Nucl. Phys.* **B489** (1997) 487

[20] T. Klassen and E. Melzer, *Int. J. Mod. Phys*. **A8** (1993) 4131

[21] S. Coleman, *Phys. Rev.* **D11** (1975) 2088

[22] S. Mandelstam, *Phys. Rev.* **D11** (1975) 3026

[23] M. Karowsky, *Nucl .Phys.* **B300** (1988) 473

[24] J. L. Cardy, *Nucl. Phys.* **B270** (1986) 186

[25] Al. B. Zamolodchikov, *Int. J. Mod. Phys.* **A10** (1995) 1125

[26] T. Klassen and E. Melzer, *Nucl.Phys.* **B370** (1992) 511

[27] G. Feverati, F. Ravanini and G. Takács, *Phys. Lett.* **B430** (1998) 264

[28] G. Feverati, F. Ravanini and G. Takács, *Phys. Lett.* **B444** (1998) 442

[29] S. Pallua and P. Prester, *Phys. Rev.* **D59** (1999) 1256, hep-th 9902192

[30] Al. B. Zamolodchikov, *Nucl. Phys.* **B432** (1994) 427-456
     Al. B. Zamolodchikov, *Phys. Lett.* **B335** (1994) 436-443

[31] N. Reshetikhin and F. Smirnov, *Comm. Math. Phys.* **131** (1990) 157-181

[32] D. Fioravanti, A. Mariottini, E. Quattrini and F. Ravanini, *Phys. Lett.* **B390** (1997) 243

[33] T. R. Klassen and E. Melzer, *Nucl. Phys.* **B370** (1992) 511

[34] G. Feverati, F. Ravanini and G. Takács, hep-th/9909031, to be published by *Nucl. Phys.*

[35] P. Christe and M. J. Martins, *Mod. Phys. Lett.* **A5** (1990) 2189

[36] P. Fendley, *Nucl. Phys.* **B374** (1992) 667

[37] H. J. de Vega and H. J. Giacomini, *J. Phys.* **A22** (1989) 2759

[38] A. Cappelli, C. Itzykson, J.B. Zuber, *Nucl. Phys.* **B280** (1987) 445-465
     A. Cappelli, C. Itzykson and J.B. Zuber *Commun. Math. Phys.* **113** (1987) 1

[39] G. Felder and A. Leclair, *Int. J. Mod. Phys.* **A7** (1992) 239

[40] P. Dorey and R. Tateo, *Nucl. Phys.* **B515** (1998) 575

[41] P. Fendley, *Adv. Theor. Math. Phys.* **1** (1998) 210

[42] A. Mariottini, "Ansatz di Bethe Termodinamico ed Equazione di Destri-de Vega in Teorie
     di Campo Bidimensionali" (in Italian), *M. Sc. thesis – University of Bologna* (March 1996),
     available from http://www-th.bo.infn.it/hepth/papers.html

[43] P. Zinn-Justin, *J. Phys.* **A31** (1998) 6747

[44] P. Dorey and R.Tateo, hep-th 9910102

[45] F.H.L. Essler, "Sine-Gordon low-energy effective theory for Copper Benzoate", cond-mat
     9811309

[46] S. Lukyanov and A. Zamolodchikov, *Nucl.Phys.* **B493** (1997) 571
     V. Fateev, D. Fradkin, S. Lukyanov, A. Zamolodchikov and Al. Zamolodchikov, *Nucl. Phys.*
     B540 (1999) 587

[47] H. Bethe, *Z. Phys.* **71** (1931) 205